FTD-ID(RS)T-1042-78

FOREIGN TECHNOLOGY DIVISION

AD-A066213

SCIENTIFIC NOTES FROM THE CENTRAL
AERO-HYDRODYNAMIC INSTITUTE

(SELECTED ARTICLES)

Approved for public release;
distribution unlimited.

78 12 21 180

FTD- ID(RS)T-1042-78

UNEDITED MACHINE TRANSLATION

FTD-ID(RS)T-1042-78 14 August 1978

MICROFICHE NR: FTD-78-C-001099

SCIENTIFIC NOTES FROM THE CENTRAL AERO-HYDRODYNAMIC INSTITUTE (SELECTED ARTICLES)

English pages: 267

Source: Uchenyye Zapiski TsAGI, Vol. 1, No. 3, 1970, pp. 1-114.

Country of origin: USSR
This document is a machine translation.
Requester: FTD/TQTA
Approved for public release; distribution unlimited.

PREPARED BY

TRANSLATION DIVISION
FOREIGN TECHNOLOGY DIVISION
WP-AFB, OHIO.

Table of Contents

U. S. BOARD ON GEOGRAPHIC NAMES TRANSLITERATION SYSTEM

Block	Italic	Transliteration	Block	Italic	Transliteration
А а	*А а*	A, a	Р р	*Р р*	R, r
Б б	*Б б*	B, b	С с	*С с*	S, s
В в	*В в*	V, v	Т т	*Т т*	T, t
Г г	*Г г*	G, g	У у	*У у*	U, u
Д д	*Д д*	D, d	Ф ф	*Ф ф*	F, f
Е е	*Е е*	Ye, ye; E, e*	Х х	*Х х*	Kh, kh
Ж ж	*Ж ж*	Zh, zh	Ц ц	*Ц ц*	Ts, ts
З з	*З з*	Z, z	Ч ч	*Ч ч*	Ch, ch
И и	*И и*	I, i	Ш ш	*Ш ш*	Sh, sh
Й й	*Й й*	Y, y	Щ щ	*Щ щ*	Shch, shch
К к	*К к*	K, k	Ъ ъ	*Ъ ъ*	"
Л л	*Л л*	L, l	Ы ы	*Ы ы*	Y, y
М м	*М м*	M, m	Ь ь	*Ь ь*	'
Н н	*Н н*	N, n	Э э	*Э э*	E, e
О о	*О о*	O, o	Ю ю	*Ю ю*	Yu, yu
П п	*П п*	P, p	Я я	*Я я*	Ya, ya

*<u>ye</u> initially, after vowels, and after ъ, ь; <u>e</u> elsewhere.
When written as ё in Russian, transliterate as yё or ё.

RUSSIAN AND ENGLISH TRIGONOMETRIC FUNCTIONS

Russian	English	Russian	English	Russian	English
sin	sin	sh	sinh	arc sh	sinh^{-1}
cos	cos	ch	cosh	arc ch	cosh^{-1}
tg	tan	th	tanh	arc th	tanh^{-1}
ctg	cot	cth	coth	arc cth	coth^{-1}
sec	sec	sch	sech	arc sch	sech^{-1}
cosec	csc	csch	csch	arc csch	csch^{-1}

Russian	English
rot	curl
lg	log

Page 1.

Maximum flows of viscous fluid with stationary separation zones with $Re\to\infty$.

G. I. Taganov.

Are examined the maximum flows of the viscous incompressible fluid for which strive with an infinite increase in Reynolds number the flows with stationary separation zones after flat/plane symmetrical bodies. Are obtained quantitative results in the case of circulation flow within separation zone.

The qualitative study of the field of the possible flows of viscous fluid with stationary separation zones with large Reynolds numbers Re, when flow in the thin layers of mixing and friction can be described by the equations of Prandtl, carried out in work [1], it is supplemented below some quantitative asymptotic results with $Re\to\infty$ for the case of the nondegenerate flow within separation zone with circulation nucleus. Is conducted the analysis of the global picture of flow about flat/plane body (transverse size/dimension of body d) with the unlimitedly growing with Re→∞ extent of separation zone l_s and is more precisely formulated the local picture of flow near body, described in [1]. The analysis of the local picture of flow near body and in in the region of connection makes it possible to obtain asymptotic formula for the drag coefficient of symmetrical flat/plane body of Re→∞ and the presence of dissipator

The qualitative investigation of dependence $c_x = f(\mathrm{Re})$ for the flat/plane plate, establish/installed perpendicularly to flow and by that streamlined with stationary separation zone, it leads to the interesting paradox: beginning with certain, sufficiently large number $\mathrm{Re} = \frac{u_\infty d}{\nu}$, resistance of the plate, establish/installed in a direction perpendicular to flow, becomes lesser than resistance of the same plate, establish/installed at zero angle of attack and streamlined without flow breakaway with the same Reynolds number. This paradox is the consequence of the obtained in work asymptotic law of resistance of the cylindrical bodies, which have the symmetrical form of section, streamlined with stationary separation zones when $\mathrm{Re}_d \to \infty$: $c_x \sim \mathrm{Re}_d^{-1}$.

Page 2.

Are given the results of calculations regarding the form of the duct/contour of the separation zone, which corresponds to the limiting condition of flow with $Re \to \infty$ about the symmetrical flat/plane body of final extent (maximally weak dissipator - point D, when $c_x = 0, \Delta = \bar{u}_2^2 - \bar{u}_1^2 = 0$ [1]). It turned out that the duct/contour of the separation zone in this case was close to ellipse, but it does not coincide with it, its major axis is directed along flow, while minor axis comprises approximately 60o/o of major axis.

The form of the duct/contour of separation zone during maximum flow ($Re \to \infty$, $\Delta = 0$) is compared with the form of the duct/contour of the separation zone, obtained as a result of the numerical solution of the equations of Nav'ye - Stokes for the case of the flow around round cylinder with Re=500 [2]. It proves to be that the unexpected for the authors of work [2] increase in the thickness ratio of the duct/contour of separation zone with Re=500 completely regularly testifies to the approach/approximation of the picture of flow with Re=500 to the maximum picture of flow with $Re \to \infty$ and $\Delta = 0$.

In conclusion are analyzed the reasons for inapplicability previously proposed models of flow [3] - [7] for describing the maximum flow of viscous fluid with stationary separation zone with $Re \to \infty$. Turns attention to the resemblance of some properties of maximum flow ($Re \to \infty$ and $\Delta = 0$) and of Zhukovskiy circulation flow: they both pertain to the class of plane flows with theoretically infinite kinetic energy of the disturbed motion, but with the zero value of the drag coefficient during steady motion.

1. Global picture of maximum viscous flows with stationary separation zone with Re→∞.

Since, as shown in work [1], the extent of separation zone l_k unlimitedly grow/rises with Re→∞ and the values of the parameter Δ>0, which characterizes the effectiveness of dissipator ($\Delta=\bar{u}_k^2-\bar{u}_r^2,\ \bar{u}_k=\frac{u_k}{u_\infty};\ \bar{u}_r=\frac{u_r}{u_\infty}$, where u_k, u_r - with respect to the velocity in points on the external and internal borders of the viscous layer of the mixing, which separate/liberates external potential and internal vortex/eddy inviscid flows, while u_∞ - is the velocity of the undisturbed flow), becomes unsuitable the use of a size/dimension of body d as reference length. It is more convenient in this case during the study of the global picture of flow to take as reference length the extent of separation zone l_k and to pass to dimensionless coordinates $\bar{x}=\frac{x}{l_k},\ \bar{y}=\frac{y}{l_k}$. It is easy to see that the case of the degenerate flow within separation zone ($\bar{u}_r=0,\ \Delta=1$), occurring with Re→∞ and the presence of maximally powerful dissipator [1] within the separation zone when external flow can be described with the aid of the model Gilbarg-Efros it will be depicted in plane $\bar{x}\ \bar{y}$ as axis intercept $\bar{x}$, arrange/located between the point $\bar{x}=0$ (body) and the point $\bar{x}=1$ (region of connection) (Fig. 1).

FOOTNOTE *. In accordance with work [1] to maximally powerful dissipator corresponds the degenerate flow within separation zone without circulation of core. ENDFOOTNOTE.

Page 3.

During a fall in the effectiveness of dissipator (case 0<A<1) within separation zone appears the circulation flow with constant eddy/vortex. Static pressure in separation zone is direct after body and directly before the region of connection it is raised to the value equal to to stagnation pressure for line of demarcation of the current of internal vortex/eddy inviscid flow $\bar{p}=\frac{2(p-p_\infty)}{\rho u_\infty^2}=1-\Delta$. Consequently, in the vicinity of points (0, 0) and (1, 0) to plane $\bar{x}$ $\bar{y}$ external irrotational flow must provide precisely this static pressure, i.e., velocity in these points must be equal to $\frac{u}{u_\infty}=\sqrt{\Delta}$. This requirement can be carried out only in such a case, when the duct/contour of the separation zone has at points (0, 0) and (1, 0) the zero angle of sharpening, and also different from zero [nonvanishing] thickness ratios $\bar{y}_m$ (Fig. 2), i.e., the transverse size/dimension of separation zone must be the value of the order of the extent of separation zone along flow.

In the case when Δ=0 (maximally weak dissipator), with the unlimited increase in the extent of separation zone l, with Re number the requirement of the zero angle of sharpening at points (0, 0) and (1, 0), as is evident from preceding/previous, drops off flow in the vicinity of body and region of connection it approaches rest [1]. The duct/contour of the separation zone with final angle of throat at points (0, 0) and (1, 0) takes in this case (A=0) the form, presented in Fig. 3.

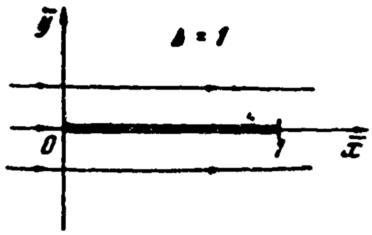

Fig. 1.

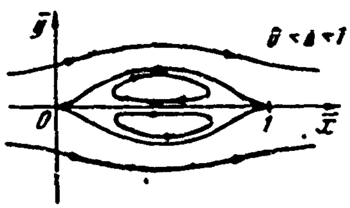

Fig. 2.

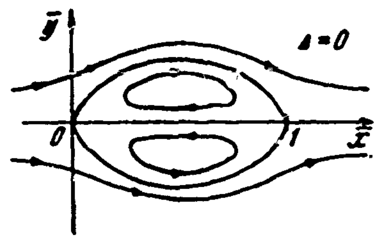

Fig. 3.

Legend.

Page 4.

2. Local picture of flow near body and in the region of connection with $0 \leq \Delta < 1$.

The presence of the zero angle of sharpening of the duct/contour of separation zone at points (0, 0) and (1, 0) leads to the fact that internal flow with constant eddy/vortex is close to stagnant in sufficient extended in the direction of $\bar{x}$-axis the sections, which adjoin points (0, 0) and (1, 0). The examination of internal flow with constant eddy/vortex in the vicinity of the point of inflection of wedge with aperture angle β leads to following relationship/ratio for value $\frac{\partial u_\tau}{\partial \bar{x}}$ at point of inflection [1].

$$\frac{\partial u_\tau}{\partial \bar{x}} = -\operatorname{tg}\beta \frac{1}{2}\Omega. \quad (2.1)$$

FOOTNOTE [1]. This escape/ensues from the qualitative analysis of the flow at point of inflection, carried out by V. S. Sadovskiy (description of flow is given into in § 4). ENDFOOTNOTE.

Consequently, at $\beta=0$ and finite value Ω $\frac{\partial u_\tau}{\partial \bar{x}} \to 0$ with $\bar{x}=0$ and $\bar{x}=1$, and from the equation of Bernoulli follows that and $\frac{\partial^2 \bar{p}}{\partial \bar{x}^2}=0$ at these points. Thus, after body and before the region of connection occur sections with the almost constant static pressure: $\bar{p}=1-\Delta$.

If we now return to the use as reference length of a size/dimension of body d, then easily is detected the local agreement of the picture of flow near body in the case in question with the local picture of flow about the body, streamlined when disengaged flow lines are present,, which descend from body surface (flow of Kirchhoff).

The important property of flows with free boundaries is the fact that the local picture of external irrotational flow near body weakly depends on flow conditions far from body, including on the velocity of the undisturbed flow, and it is determined by the form of body, by the position of the points of the descent of jets on body and by velocity on disengaged flow lines, which adjoin the body. This property is constant/invariably confirmed by precise numerical calculations of flows with free boundaries according to the patterns of Ryabushinskiy and Gilbarg-Efros over a wide range of a change in the number of cavitation $Q=\frac{p_\infty-p_0}{\frac{\rho u_\infty^2}{2}}$ (i.e. during a considerable change in the configuration of global flow, in particular, during a considerable change in the thickness ratio of cavern), and also with the sufficiently close location of the rigid borders of channel to the streamlined body. Hence escape/ensues the important consequence: the drag coefficient of body, in reference to velocity on the free boundaries, which adjoin the body, does not depend on velocity of incident flow and it is equal to the drag coefficient of body c_{xK}, streamlined according to Kirchhoff's pattern, when velocity on free boundaries is equal to the velocity of the undisturbed flow and number Q=0:

$$c_x' = \frac{2X}{\rho u_1^2 d} = c_{xK} = c_x(0). \qquad (2.2)$$

Page 5.

Now it is easy to pass to the usual drag coefficient of the body, in reference to the velocity of the undisturbed flow:

$$c_x = c_x' \frac{u_1^2}{u_\infty^2}. \qquad (2.3)$$

it is final, with use (2.2), we obtain:

$$c_x = c_{x\kappa}\frac{u_0^2}{u_\infty^2} - c_x(0)(1+Q). \qquad (2.4)$$

Formula (2.4) have long utilized during calculations of cavity flows and it is constant/invariably confirmed by the experiment (for example, see [8], [9]). For flat/plane plate $c_{x\kappa} = \frac{2\pi}{\pi+4} \approx 0,88,$ for a circular cylinder depending on the position of separation point accepted value c_x is changed from 0.5 to 0.55. The first numeral is better confirmed by experiment [9].

The coincidence of the local picture of external irrotational flow about body with separation zone in the presence of a dissipator within zone, which ensures the assigned magnitude of the parameter Δ, and of the local picture of flow with disengaged flow lines makes it possible to obtain the value of the pressure drag coefficient c_{x1}, of the acting on body in the general case circulation flow within separation zone.

Since $\frac{u_0'}{u_\infty} = \sqrt{\Delta},$ where u_0' - velocity in point (0, 0) of plane $\tilde{x}\ \tilde{y}$, then of (2.4) we have:

$$c_{x1} = c_{x\kappa}\,\Delta. \qquad (2.5)$$

However, this is only part of the drag coefficient of system body + dissipator. It is necessary to determine another the force, which acts on dissipator [1].

Let us turn to the determination of the conditions, necessary for the existence of flow as a whole, i.e., the conditions, by which is possible the coupling of the internal flow with constant eddy/vortex, described by the equation of Poisson, with the external irrotational flow, described by the equation of Laplace when body and region of connection is present. Here again proves to be essential coincidence of the local pictures of flow near body and in the region of connection after separation zone with local pictures in the appropriate zones of flow with free boundaries.

For symmetrical relative to X-axis of the flow of Ryabushinskiy, formed by two plates, perpendicular to the direction of the incident flow, Demechko [10] it demonstrated the theorem, according to which the flow of Ryabushinskiy exists only in the case of the plates of identical size/dimension.

Under the assumption about the independence of the local picture of flow about plate from flow conditions far from plate, i.e., under the same assumption, under which was obtained formula (2.4), theorem of Demechko can be demonstrated by following path. Resistance of system of two plates of different length, rigidly connected and streamlined according to the pattern of Ryabushinsky (zero flow line coincides with duct/contour ABCD in Fig. 8), according to oylera - d' Alembert's paradox must be equal to zero:

$$X_{AB}+X_{CD}=0. \quad (2.6)$$

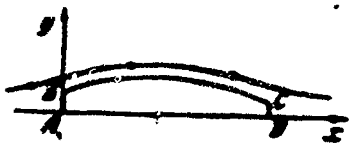

Fig. 4.

Page 6.

However, to plate $\overline{AB}$, is applied the resisting force, equal according to formula (2.4):

$$X_{\overline{AB}}=\overline{AB}\frac{\rho w_\infty^2}{2}c_{x\kappa}(Q+1), \tag{2.7}$$

and to plate $\overline{CD}$ - the force

$$X_{\overline{CD}}=-\overline{CD}\frac{\rho w_\infty^2}{2}c_{x\kappa}(Q+1). \tag{2.8}$$

Since values Q and $c_{x\kappa}$ are identical for both plates, then for execution (2.6) it is necessary, in order to

$$\overline{AB}=\overline{CD}. \tag{2.9}$$

The generalization of theorem Demchik to the case of inviscid flow with constant eddy/vortex within duct/contour ABCD and the final jump of Bernoulli's constant on border BC (case 0<A<1) is conducted analogously, but with the use additionally of agreement of the local pictures of flow, i.e., in the same assumptions, by which is obtained formula (2.5):

$$X_{1\overline{AB}}=\overline{AB}\frac{\rho w_\infty^2}{2}c_{x\kappa}\Delta;$$

$$X_{1\overline{CD}}=-\overline{CD}\frac{\rho w_\infty^2}{2}c_{x\kappa}\Delta.$$

Since c_{xx} and A are identical for both plates, of (2.6) it follows:

$$\overline{AB}=\overline{CD}.$$

Thus, internal flow with constants like the wind in the generalized pattern of Ryabushinskiy can be conjugate/combined with external irrotational flow in the presence of the final jump of Bernoulli's constant on the line of coupling and, strictly speaking, when $\frac{\overline{AB}+\overline{CD}}{2\overline{AD}}\to 0$ only at the identical length of those limit the flow of plates.

It is certain, the pattern of Ryabushinskiy is inapplicable to the description of flow in the region of connection after separation zone. For describing the flow in this region, approaches the model, proposed in work [1], which uses a pattern Gilbarg-Efros with recurrent jet. Two Dimensional parameters determine the local picture of flow in the region of the connection: the thickness of recurrent jet, equal to $2\delta_{+}^{**}$, where δ_{+}^{**} - thickness of the acquisition of momentum/impulse/pulse in the viscous boundary layer of circulation flow (characteristic linear dimension), and velocity on disengaged flow lines.

Page 7.

It is possible to expect that the thickness of recurrent jet in the flow Gilbarg-Efros it must comprise the completely defined portion of the length of plate, just as the size/dimension of closing plate in the flow of Ryabushinsky it is connected with the size/dimension of front/leading plate for the possibility of the realization of flow as a whole. In fact the force X_{cn}, from which closing plate in the flow of Ryabushinskiy acts on flow, it is provided in the flow Gilbarg-Efros by the reaction of the recurrent jet, which appears during a change in the direction of the motion of liquid, which forms jet, on 180°. Actually the thickness of recurrent jet when $p_k = p_\infty$ is 0.22 d [9]; the reaction of jet, equal to a change in the momentum of liquid during the rotation of jet in opposite direction, comprises $2\rho u_\infty \cdot 0{,}22 \cdot d \cdot u_\infty = 0{,}88 \frac{\rho u_\infty^2}{2} d$, i.e. in accuracy/precision it is equal to the force from which closing plate in the flow of Ryabushinsky when $p_k = p_\infty$ acts on flow.

Consequently, for the realization of flow in the whole thickness of recurrent jet in the region of connection it must be completely determined, that ensures the reaction of jet, equal in magnitude to the pressure drag, which acts on body.

Since are now known the parameters of recurrent jet, can be determined the thrust, applied to the dissipator which is in an ideal-liquid model, examined in work [1], by the flow of the momentum/impulse/pulse of recurrent jet. If dissipator is arrange/located on the section where $\bar{p}=1-\Delta$, then for satisfaction of periodicity condition in the viscous boundary layer of the circulation flow of dissipator it must provide the absorption of entire momentum/impulse/pulse of recurrent jet, i.e., the amount of thrust, applied to dissipator must comprise half from the value of the reaction of jet in region of connection or, on the basis that presented it is higher, the half of the amount of the resisting force of the pressure, applied to the body:

$$c_T = \frac{c_{x1}}{2}, \qquad (2.10)$$

where $c_T = \frac{2T}{\rho u_\infty^2 d}$ - thrust coefficient, applied to dissipator. Then taking into account (2.5) we obtain the drag coefficient of system boat + dissipator in the case of the nondegenerate flow with circulation nucleus in the separation zone:

$$c_x = c_{x1} - c_T = \frac{1}{2} c_{x1} = \frac{1}{2} c_{xK} \Delta \qquad (2.11)$$

or, accordingly (2.10),

$$c_x = c_T. \qquad (2.12)$$

In the case of the degenerate flow in separation zone $\Delta=1$, if body is the plate in which $c_{xK} = \frac{2\pi}{\pi+4}$, formula (2.11) gives the result, which coincides with that obtained in work [1] for a system plate + ideal dissipator: $c_x = \frac{\pi}{\pi+4}$.

Page 8.

During the derivation of asymptotic formula (2.11) was not considered the effect of displacement, connected with the deviation of the flow lines external irrotational flow in the region of connection of the thickness, equal to the displacement thickness of the exterior of the viscous layer of mixing, although a precise ideal- liquid model of stalled flow, described in work [1], is included this effect in examination. Without being stopped here on the procedure which can be proposed for the account of the effect of displacement in the case of maximum flow with Re→∞, let us explain the mechanism of transmission to the body of pressure drag, which appears due to displacement and added to value (2.11) in flow with separation zone.

In the case of the flow around rigid airfoil/profile, as is known, this occurs due to the decrease of pressure on the rear portion of the airfoil/profile. If we visualize the nonseparated flow of the rigid duct/contour ABCD (see Fig. 8), then due to the effect of displacement, the force of pressure, acting on closing plate, decreases. Apparently, analogous with this required value of the reaction of jet in the region of the joining of jet in the flow of Gilbarg-Efros also decreases, and this causes, other conditions being equal, the decrease of the thrust/rod, which acts on dissipator, and therefore an increase in resistance of system the body + dissipator.

§ 3. Paradox of viscous flows with the large Re numbers.

Let us explain now how will change of an increase in Re number the drag coefficient at the symmetrical flat/plane body of size/dimension d with the dividing plate, arrange/located along the axis of symmetry within separation zone.

Let the dividing plate have the assigned/prescribed length l, of the order of the size/dimension of body d and the assigned/prescribed distance between the dividing plate and the body also of order d. Thus, the dissipator is the entire rubbing surface of the dividing plate and the part of rubbing surface of body, which adjoins the separation zone. Let us examine first the artificial case: let friction on the back side of body be equal to zero (all moving surface), and the dissipation of energy of recurrent jet is realize/accomplished on the dividing plate whose position relative to body is changed with a change in Re number so that it is always located in the region where the velocity of circulation flow is maximum. Since the maximum speed of circulation flow is of the order of the velocity of the undisturbed flow, the coefficient of friction drag of the dividing plate c_T will change $\sim Re^{-\frac{1}{2}}$. Consequently, and the part of the drag coefficient of system body + the dividing plate (without the account of the frictional resistance of end connections of the body) will change according to the law $\sim Re^{-\frac{1}{2}}$, since accordingly (2.11) this part of the drag coefficient of the system of order c_T.

However, in the real case the position of the dividing plate relative to body, as this is stipulated above, fix/recorded comprises the value of order d. Therefore with an increase in the extent of separation zone with Re→ both velocity of circulation flow and recurrent jet velocity in the location of the dividing plate they will vanish, since flow will approach maximum, appropriate Δ=0 (see Fig. 8). It means coefficient c_T it will vanish faster than according to the law $\sim Re^{-\frac{1}{2}}$ (preceding/previous case) and, consequently, also the total coefficient of friction drag of end connections of the body, which vanishes faster than $Re^{-\frac{1}{2}}$, due to the tendency of the local characteristic velocity (u° toward zero) will vanish faster than $Re^{-\frac{1}{2}}$.

Page 9.

At very rapid incidence/drop and the low values of drag coefficient, connected with friction in the viscous boundary layer of circulation flow, it is not possible to already disregard the value of viscous dissipation in an entire range of circulation flow with constant eddy/vortex and in an entire range of external irrotational flow. It is easy to show that the work, necessary for maintaining the steady potential flow around separation zone and flat/plane circulation flow with constant eddy/vortex in the maximum flow (see Fig. 8), it is provided, if the law of resistance takes the form

$$c_x = A\,\mathrm{Re}_d^{-1}, \qquad (3.1)$$

where A - the number, which depends only on the configuration of separation zone. For the configuration of the flow, presented in Fig. 5, A=85 π.

In fact, the viscous dissipation E in external zone of flow and in the range of circulation flow with constant eddy/vortex, not depending on size/dimension l_b, proportional $\mu\left(\frac{u_\infty}{l_b}\right)^2 l_b^2 \sim \mu u_\infty^2$, must be provided by the work of the resisting force of body, proportional $\rho u_\infty^3 c_x d$, i.e. $\mu u_\infty^2 \sim \rho u_\infty^3 c_x d$, whence it follows (3.1).

If the drag coefficient of body with separation zone when $\mathrm{Re}_d \to \infty$ falls faster than according to the law $c_x \sim \mathrm{Re}_d^{-\frac{1}{2}}$, valid during the nonseparated flow of fine/thin airfoil/profiles and, in particular, during continuous flow around the plate, establish/installed at zero angle of attack, then it occurs the interesting paradox: beginning with certain sufficient large Re number with further increase in Re number resistance of the plate, establish/installed perpendicularly to flow, it becomes lesser than resistance of the same plate, establish/installed at zero angle of attack and streamlined without flow breakaway with the same Re number.

§ 4. Determination of the form of the duct/contour of separation zone in maximum plane flow with $Re \to \infty$ and $\Delta = 0$.

Mathematically more idle time is the task of determining the form of the duct/contour of the separation zone of maximum flow with in presence of the jump of Bernoulli's constant on the border of duct/contour, i.e., the case $\Delta = 0$ (see Fig. 3). If one considers that this case answers the limiting condition of the flow of viscous fluid about the real symmetrical body of final extent (with the dividing plate of finite length or without it) whose coefficient vanishes with $Re \to \infty$, then the examination of this case represents the greatest interest.

Was at first made the attempt to roughly evaluate the form of duct/contour, finding flow with constant eddy/vortex from the solution of the equation of Poisson within the assigned/prescribed duct/contour and external irrotational flow about the same duct/contour, attaining by the variation of the geometric parameters of duct/contour during precise satisfaction of boundary conditions only in some points of the duct/contour of a minimum root-mean-square difference in the velocities of external and internal flow along the length the duct/contour, possessing two axes of symmetry.

Page 20.

The calculations, N. P. Sinitsynoy's carried out, showed that if we search for the solution of problem in the class of elliptical duct/contours, then the root-mean-square difference in the velocities along the length duct/contour (characterizing the value of error during satisfaction to boundary condition) during the variation of the relation of the semi-axes of ellipse b/a in the range from 0.1 to 1.0 has the acute/sharp minimum with b/a=0.64. The value of root-mean-square difference in the velocities comprises in this case about 7o/o of velocity of the undisturbed flow. From this, as is evident, sufficient rough estimate it followed that the duct/contour of the separation zone was close, but it does not coincide with the ellipse whose major axis is directed along flow, while minor axis comprises approximately 0.64 from major axis.

The method of the joint solution of internal and exterior problem, proposed by V. S. Sadovskiy, makes it possible to determine duct/contour with high accuracy/precision. Fig. 5 in coordinates $\bar{x}=\frac{x}{l_b}$ and $\bar{y}=\frac{y}{l_b}$ depicts the duct/contour, calculated by V. S. Sadovskiy on BTsVM · digital computer] (are plotted/applied also to the flow line of internal flow when $\psi=-0{,}01;\ -0{,}02;\ -0{,}03;\ \psi$ it is referred to the value of eddy/vortex Ω_0 and the square of the half of the length of zone).

Table gives the reduced coordinates of duct/contour.

$\bar{x}$	$\bar{y}$	$\bar{x}$	$\bar{y}$	$\bar{x}$	$\bar{y}$	$\bar{x}$	$\bar{y}$
0	0	0,025	0,0610	0,150	0,192	0.350	0,282
0,0005	0,0030	0 035	0,0770	0,165	0,202	0.375	0,287
0,001	0,0053	0,045	0,0913	0,180	0,212	0.400	0,292
0,002	0,0092	0,055	0,104	0,195	0,221	0,425	0,295
0,0035	0,0142	0,065	0.116	0,210	0,229	0,450	0,298
0,005	0.0187	0,075	0,127	0,225	0,237	0.475	0.299
0.0075	0,0254	0,090	0,143	0,250	0,248	0,500	0.2995
0,010	0,0315	0,105	0,157	0,275	0.258		
0,015	0,0424	0.120	0,170	0,300	0,267		
0,020	0,0621	0.135	0,181	0,325	0,275		

As is evident, the thickness ratio of the duct/contour of separation zone $2y_{max}$ = 0.599, i.e., is close to estimation; the form of duct/contour is close to elliptical in the range of the maximum of thickness, but it differs from the elliptical with approach to the edges of duct/contour to the side of the larger sharpening of duct/contour.

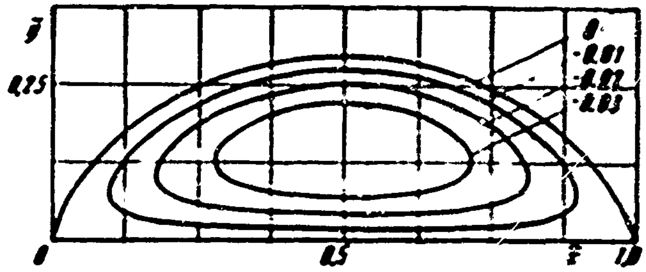

Fig. 5.

Page 11.

Is of interest the comparison of the form of the duct/contour of maximum flow with Re→∞ and A=0 with the duct/contour of the separation zone, obtained from the numerical solution of the task of the flow around the flat/plane symmetrical body, described by the equations of Nav'ye - Stokes, with the moderate Re numbers. Until recently with the aid of the numerical methods of the solution of the equations of Nav'ye - Stokes, it was possible with sufficient accuracy/precision to obtain the flow around flat/plane symmetrical bodies to Re number on the order of 100. Recently Jones and Khanratti [2] was obtained the numerical solution of the equations of Nav'ye - Stokes for a circular cylinder with Re=500 with the application/use of a sufficiently small mesh (14000 points of mesh) and with the expenditure of long time (19 hour to on IBM360, model 75). They obtained with Re=500 the unexpectedly thick separation zone whose form sharply differs from the elongated along flow separation zones, obtained with the smaller Re numbers both in their inherent calculations and other authors's works, and also in known experiments [11]. In Fig. 6 in coordinates $\bar{x}=\frac{x}{l_b}$ and $\bar{y}=\frac{y}{l_b}$ the duct/contour of the separation zone, obtained in work [2] with Re=500, is compared with the duct/contour of the separation zone of maximum flow with Re→∞ and A=0. (During the use of data of the work [2] for the duct/contour of the separation zone, was accepted the flow line $\psi=0$, while distance between centers of circular cylinder and by the position of the maximum of the thickness of separation zone was taken as equal to $\frac{l_b}{2}$). The comparison of duct/contours testifies to the approach/approximation of the picture of stalled flow already with Re=500 to the picture of maximum flow with Re→∞ and A=0.

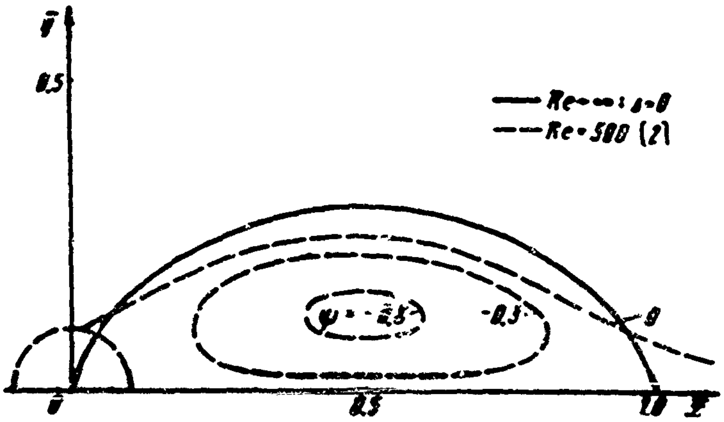

Fig. 6.

Page 12.

§ 5. On previously proposed models for description of maximum flow with Re→∞.

The importance of obtaining maximum steady flow with separation zone for the study of flow with the moderate Re numbers, in particular, with the aid of the method of asymptotic expansions, was noted repeatedly (for example, see [12]). Task was complicated by impossibility to utilize during the construction of the theoretical model of maximum flow experimental given or data of the numerical solution of the equations of nav'ye - Stokes, since they were limited to number Re<100 (in experiments - due to the instability of the stationary form of motion).

The first attempts at the construction of the theoretical model of maximum flow are related to the 30's. In the works of Squire [3], Imaya [4], [5] as the maximum form of viscous flow with Re→∞, it was examined the flow of Kirchhoff with free boundaries and the quiescent liquid in separation zone. According to this model of Re→∞, the drag coefficient of flat/plane plate approached final limit 2π/π+4, the extent of separation zone unlimitedly grow/rose, the thickness of separation zone increased with distance from plate according to the law $y \sim x^{\frac{1}{2}}$. On the basis of the finiteness of resistance in maximum flow, Imaya [5] was obtained the linear dependence of the length of the separation zone on Reynolds number, which is confirmed by data of experiment and numerical calculations to Re number on the order of 100. However, the vulnerable place of this model, not removed and during a last/latter on time attempt at the theoretical substantiation of the correctness of this model [1] is the fact that the postulated flow within separation zone does not satisfy equations of motion under real boundary conditions in separation zone after plate.

FOOTNOTE [1]. V. V. Sichev. On the steady laminar flow of liquid after dull body with the large Re number. Report on VIII symposium in the contemporary problems of the mechanics of fluids and gases. Tarda, Poland, 18-23 September of 1967.

The short presentation of some results work gives in [13].

ENDFOOTNOTE.

As shown in work [1], for the execution of equations of motion within separation zone with the postulated picture of flow (case of the degenerate flow without circulation nucleus $A \approx 1$) are necessary special boundary conditions (maximally powerful dissipator) are absent from the real task of the flow around body, and consequently, this model is inapplicable for describing the limiting condition of viscous flow about the body of final extent with $Re \to \infty$.

In 1956 by bachelor [6] was proposed the theoretical model of maximum flow, in which was considered for the first time the dependence of flow as a whole on the boundary conditions within separation zone, governing the intensity of circulation flow in separation zone. (Relationship/ratio between the extent of the actionless and movable sections of the duct/contour of separation zone is one of the parameters, determining the magnitude of eddy/vortex at the arbitrary form of the duct/contour of separation zone). According to bachelor's theoretical model, in maximum flow with $Re \to \infty$ the extent of separation zone remains final, $c_x \to 0$, the jump of Bernoulli's constant on the border of separation zone is final, the duct/contour of the separation zone in region of connection has the zero angle of sharpening. However, the attempts to obtain quantitative results within the framework of this model ran into nonremovable computational difficulties. On the basis of data given in § of 2 present articles, it is possible to conclude that these difficulties are fundamental. From these data it follows that with the finite quantity of the jump of Bernoulli's constant on the border of separation zone (A>0) with the union of flow with constant eddy/vortex within zone with external irrotational flow is necessary the final (comparable with size/dimension of d of body) thickness of recurrent jet in the range of connection, which is incompatible with requirement $c_i = 0$.

Page 13.

Model, proposition in work [7] (see [13]), it is in essence extrapolation to the large Re numbers of authors's known experimental results, for which it was possible to tighten stationary flow conditions with the aid of the dividing plate after circular cylinder to number Re≈170 (without the dividing plate stationary flow conditions was disrupted with Re≈40). According to this model in maximum flow about the body of final extent with Re→∞, the flow in separation zone remains viscous, the extent of zone unlimitedly increases, the thickness of separation zone comprises the value of the order of the transverse size/dimension of body, the coefficient of static pressure on the back side of body is retained constant, $\bar{p} \approx -0.45$. In order to observe the sequence during the extrapolation of the experimental data, obtained with the small Re numbers, to the large Re numbers, should extrapolate experimental conditions. The fact is that the length of the dividing plate in experiments with small Re always constituted a value of the order of the extent of separation zone and several times exceeded the transverse size/dimension of body. If we visualize that with an increase in Re number and an increase in the extent of separation zone the length of the dividing plate also increases, remaining always the value of order l_k, then with $Re \to \infty$ we come to the picture of maximum flow, which corresponds to the case $0<\Delta<1$, presented in Fig. 2. The dividing plate by the length of order l_k is sufficiently powerful dissipator which ensures the finite quantity of the drag coefficient of system body + the dividing plate, and consequently, according to the data § of 2 present articles, and the finite quantity of the positive coefficient of static pressure on the back side of body.

Thus, some properties, described by the model, proposed in work [7], they retain its value with $Re \to \infty$, true, as we see for other conditions, for a body with the infinitely extended dividing plate. However, as a whole this model is inapplicable for description of maximum flow even under these changed conditions: data § 1 attest to the fact that the thickness of separation zone with 0<A<1 comprises the value of order l_n and not order d, as this follows from model [7], and flow within the range of circulation flow must be considered with Re → under these conditions as inviscid.

In conclusion let us focus attention on the resemblance of some properties of maximum flow to stationary separation zone about flat/plane symmetrical and final body with Re→∞ constructed according to the model of work [1], and of circr tion flow about the flat/plane duct/contour, streamlined with the unrestricted flow (flow of Joukowski). As is known, the flow of Joukowski from final circulation around flat/plane duct/contour possesses theoretically infinite kinetic energy of the disturbed action of liquid with drag coefficient equal to zero in the steady motion (for example, see [14]). The obtained maximum flow with stationary separation zone, as we see that it possesses analogous properties. Otherwise the formation of steady flow occurs for infinite time after the start of body. During entire this time the motion of liquid is unsteady and the driving/moving body (with different from zero resistance in unsteady motion) spends the necessary for the creation of flow work. It seems that the resemblance of the properties indicated of these flows not random, since both they belong to one class - class of the separating flat/plane steady flows whose properties considerably differ from the properties of the flows of nonseparable.

Page 14.

The author thanks V. S. Sadovskiy, who granted the data of numerical calculations, and also N. P. Siniitsyna for aid in the carrying out of calculations.

REFERENCES

1. G. I. Taganov. To the theory of stationary separation zones. Izv. of the AS USSR, MZhG, 1968, No 5.

2. Sen J. S., Hanratty T. J. Numerical solution for the flow around a cylinder at Reynolds numbers of 40, 200 and 500, J. Fluid Mech. 1969, v. 35, p. 369.

3. Squire H. B. Phil. Mag., 1934, 17, 1150.

4. Imai I. Discontinuous potential flow, as the limiting form of the viscous flow for vanishing viscosity. J. Phis. Soc. Japan, 1953, v. 8, p. 399.

5. Imai I. Theory of bluff bodies. University of Maryland. Tech. Note, 1957.

6. Batchelor G. K. A proposal concerning laminar waces beпind bluff bodies at large Reynolds number. J. Fluid Mech., 1956, v. 1, pt. 3.

7. Acrivos A., Snowden D. D., Grove A. S. Petersen E. E. The steady separated flow past a circular cylinder at large Reynolds numbers. J. Fluid Mech., 1965, v. 21, p. 737.

8. G. Birkhoff. Gidrodinamik, M., publ. foreign lit., 1954.

9. M. I. Gurevich. Theory of the jets of ideal fluid. Fizmatgiz, 1961.

10. Demtchenko B. Nne méthode de calcul des surfaces de glissement avec quelques application. Comptes Rendus du 3-ime Congrese International de Méchanique Appl., Stockholm, 1930.

11. Grove A. S., Shair F. H., Petersen E. E., Acrivos A. An experimental investigation of the steady separated flow past a circular cylinder J Fluid Mech, 1964, v 19, pt. 1, p 60.

12. Van Dyke M. Perturbation methods in fluid mechanics, 1964, Acad Press.

13. Acrivos A, Leal L. G., Snowden D D., Pan F. Further experiments on steady separated flows past bluff objects J Fluid Mech, v 34, part 1, October, 1968.

14. Batchelor G K. An introduction to fluid dynamics. Cambridge University Press 1967

The manuscript entered 10/VII 1969.

Page 85.

Hypersonic self-similar flow around cone, [redacted]moving along power law.

S. K. Betyayev.

For the slowly accelerated body or for the oscillatory with small frequency hypersonic flow is valid the piston analogy of Hays. In work based on the example of hypersonic axisymmetric flow past round cone (and of wedge), driving/moving with variable speed, is examined the substantially unsteady flow when the gas velocity, induced with the acceleration of body, considerable, and piston analogy is inapplicable. It is characteristic that the hypersonic flow in question contains between hyperbolic ranges the elliptical zone of the isotropic propagation of weak disturbance/perturbations with entropy special feature/peculiarity.

Problem is solved by the method of external and internal asymptotic expansions. Numerical results within the framework of the hypersonic theory of the slight disturbances are obtained by method of characteristics.

Developed theory of the self-similar action of method of calculation of the dependence of the coefficient of wave impedance c_x on time for the cone of the finite dimensions. It is shown, that during the exponential acceleration of cone c_x can increase the maximum two times.

§ 1. Formulation of the problem.

The quiescent with t<0 (t - time) cone or wedge at the moment of time t=0 begins to move in ideal perfect gas according to the law $x_0 = -bt^n$, where b - positive dimensional constant, x_0 - longitudinal coordinate of the apex/vertex of body. Flow will be self-similar, if we disregard pressure the undisturbed gas [1].

FOOTNOTE [1]. Taking into account pressure the undisturbed gas, the flow will be self-similar only with $t \gg t_0$, if body accelerates, and with $t<t_a$, if the motion of body decelerates. $t_a=\left(\frac{a_0}{b}\right)^{\frac{1}{n-1}}$ - characteristic time, a_0 - speed of sound in the undisturbed gas. With n=1 is feasible the account of pressure the undisturbed gas.

BIBLIOGRAPHY.

This flow occurs in the vicinity of the sharp apex/vertex of the arbitrary flat/plane or axially symmetrical body, which accelerates over power law depending on time.

Let us relate the density of gas to the density of the undisturbed gas, the comprising speeds along the axes x' and y', connected with the apex/vertex of the body (axle/axis x' coincides with the direction of the incident flow, axle/axis y' is perpendicular to it), to the rate of the action of body $|u_0|=n\,bt^{n-1}$, and pressure - to the density of the undisturbed gas, multiplied by u^2_0.

Page 16.

Then the equations of motion, continuity and inflow of heat can be written in the form

$$
\left.\begin{aligned}
&(u-\alpha)u_\alpha+(v-\beta)u_\beta+m(u-1)+\frac{1}{\rho}p_\alpha=0;\\
&(u-\alpha)v_\alpha+(v-\beta)v_\beta+mv+\frac{1}{\rho}p_\beta=0;\\
&(u-\alpha)\rho_\alpha+(v-\beta)\rho_\beta+\rho u_\alpha+\rho v_\beta+\nu\rho\frac{v}{\beta}=0;\\
&(u-\alpha)S_\alpha+(v-\beta)S_\beta+2mS=0.
\end{aligned}\right\} \quad (1.1)
$$

Here p, ρ, u, v - dimensionless pressure, density and the comprising rates along the axes x' and y'; $\nu=0$ for plane flow, $\nu=1$ - for axisymmetric;

$$S=p\rho^{-\gamma};\quad \alpha=\frac{x'}{bt^n};\quad \beta=\frac{y'}{bt^n};\quad m=\frac{n-1}{n}\leqslant 1$$

(γ - adiabatic index).

c - dimensionless velocity of propagation of shock wave, $\beta=\beta_1(\alpha)$ - the form of shock wave, δ - semiapex angle of cone or wedge. Boundary conditions will be conditions on the shock wave:

$$
\left.\begin{aligned}
&u(\alpha,\beta_1)=1-\frac{2c\sin\sigma}{\gamma+1};\quad v(\alpha,\beta_1)=\frac{2c\cos\sigma}{\gamma+1};\\
&p(\alpha,\beta_1)=\frac{2c^2}{\gamma+1};\quad \rho(\alpha,\beta_1)=\frac{\gamma+1}{\gamma-1};\\
&c=\beta_1\cos\sigma+(1-\alpha)\sin\sigma;\ \operatorname{tg}\sigma=\beta_1',
\end{aligned}\right\} \quad (1.2)
$$

and condition not the body:

$$v(\alpha,\beta_0)=u(\alpha,\beta_0)\operatorname{tg}\delta;\quad \beta_0=\alpha\operatorname{tg}\delta.$$

Value c is equal to distance from point (1.0) of tangent to shock wave at point (α, β_1).

With a=0 is feasible the account of pressure the undisturbed gas; in linear setting this task was examined, for example, in works [1], [2].

Before transfer/converting to the study of hypersonic flow, let us examine some properties of flow in the general case. In flow there is an elliptical range, where

$$\Delta^2 = (u-\alpha)^2 + (v-\beta)^2 < \gamma \frac{p}{\rho} - a^2.$$

On the boundary of this range, is arrange/located characteristic for self-similar flows entropy special feature/peculiarity. Since the slope tangent of trajectory [1] in plane $\alpha\beta$ to axle/axis α is equal to $v-\beta/u-\alpha$, first singular point is arrange/located on body and has coordinates $\alpha_0=u$, $\beta_0=v$, then singular point is arrange/located on body and has coordinates $\alpha_0=u$, $\beta_0=v$, which correspond to the position of the "marked" particle of gas of the particle, arrange/located with t≤0 in the beginning of coordinates.

FOOTNOTE [1]. Trajectories in plane $\alpha\beta$ let us call the characteristics according to which are spread entropy disturbance/perturbations. ENDFOOTNOTE.

Page 17.

The effect of the apex/vertex of body on the flow of gas is localized. The domain of effect is separated from the range, immune to to the effect of apex/vertex, by removable discontinuity. In the flat/plane case in the range where does not manifest itself the effect of the apex/vertexes, unknown function will depend on one coordinate y=ρcosθ-εsinθ, flow will be the same as after the flat piston, which are expanded according to the law y=const [3], [4]. In the axisymmetric case the solution of problem in the range, immune to to the effect of the apex of the cone, while explicit form is unknown, by its it is necessary to find any numerical method (for example, by method of characteristics) or with the aid of expansion in series in the vicinity of point ε=∞, where the difference with the flat/plane case disappears.

Just as in the stationary case, if angle θ, of more critical, shock wave is disconnected from the apex/vertex of body in vicinity of which is arrange/located elliptical range.

For the solution of problem by us will be required another equations in the coordinates one of which coincides with body surface, and another is perpendicular to it. $x=\beta\sin\delta+\alpha\cos\delta$, $y=\beta\cos\delta-\alpha\sin\delta$.

System of equations (1.1) in coordinates x, y takes the form

$$\left.\begin{aligned}
&(u-x)u_x+(v-y)v_y+m(u-\cos\delta)+\frac{1}{\rho}p_x=0;\\
&(u-x)v_x+(v-y)v_y+m(v+\sin\delta)+\frac{1}{\rho}p_y=0;\\
&(u-x)\rho_x+(v-y)\rho_y+\rho u_x+\rho v_y+v\rho\frac{u\sin\delta+v\cos\delta}{x\sin\delta+y\cos\delta}=0;\\
&(u-x)S_x+(v-y)S_y+2mS=0.
\end{aligned}\right\} \quad (1.3)$$

Conditions on the shock wave $[y=y_1(x)]$ and on body $(y=0)$ accept the following form:

$$\left.\begin{aligned}
&u(x,y_1)=\cos\delta-\frac{2c}{\gamma+1}\frac{y_1'}{\sqrt{1+y_1'^2}};\quad \rho(x,y_1)=\frac{\gamma+1}{\gamma-1};\\
&v(x,y_1)=-\sin\delta+\frac{2c}{\gamma+1}\frac{1}{\sqrt{1+y_1'^2}};\ p(x,y_1)=\frac{2c^2}{\gamma+1};\\
&c=\frac{y_1+\sin\delta-(x-\cos\delta)y_1'}{\sqrt{1+y'^2}};
\end{aligned}\right\} \quad (1.4)$$

$$v(x,0)=0. \quad (1.5)$$

If angle δ is smaller than critical, then shock wave is connected to body, and to apex/vertex will adjoin hyperbolic range. In the vicinity of apex/vertex, is established stationary conical flow, all dimensionless quantities depend on ratio α/β. If $m=0$, then dependence is valid up to the maximum characteristic after which are arrange/located transonic and further elliptical of zone. The elliptical zone, included between hyperbolic ranges, has various forms for the accelerated (m>0), retarded (m<0) and uniform to (m=0) action (Fig. 1a, b, c).

Page 18.

Entropy special feature/peculiarity at point x_m is shown on Fig. 1 by asterisk, maximum characteristics - by dotted lines. For accelerated flow the speed of sound nct body after point x_0 is equal to zero; therefore information about flow for it does not penetrate. The line of removable discontinuity, which is maximum characteristic, passes through the singular point (see Fig. 1a). In the case of increasing motion of wedge x_0=const. For retarded action the speed of sound of body after "marked" particle is infinitely great, disturbance/perturbations are spread immediately but entire surface, the line of removable discontinuity and the line of parabolicity asymptotically approach a body with $e\to\infty$ (see Fig. 1b).

The whimsical form of the domain of the effect of apex/vertex and the presence of entropy special feature/peculiarity lead to the specific mathematical difficulties during the numerical integration of the equations of self-similar action. Under the conditions of task, enter three parameters: δ, and M and γ. After using the methods of external and internal asymptotic expansions [5], let us examine the theory of slight disturbances ($\delta \ll 1$), the theory of thin shock layer $\left(\varepsilon = \frac{\gamma - 1}{\gamma + 1} \ll 1\right)$ and Newton's theory ($M = \infty$).

§ 2. Theory of the slight disturbances.

Let us pass to the examination of hypersonic flow. Let the angle δ be sufficiently small, shock wave connected to body. After assuming $\delta \ll 1$, $\beta > 0$, in accordance with the theory of slight disturbances [6] let us present the solution of system (1.1) in the form

$$\left.\begin{aligned} u = 1 + O(\delta^2); \quad v = \delta V(x, \eta) + O(\delta^3); \\ p = \delta^2 P(x, \eta) + O(\delta^3); \\ \rho = R(x, \eta) + O(\delta); \quad \eta = \frac{\beta}{\delta}. \end{aligned}\right\} \quad (2.1)$$

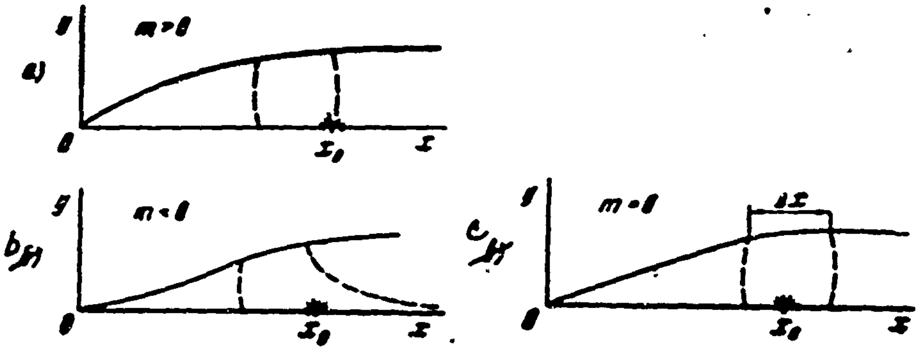

Fig. 1.

Page 19.

Substituting these values in equations (1.1) and disregarding low second-order quantities, we will obtain following system of equations for determining the functions V, P and R:

$$
\left.\begin{aligned}
&(1-\varepsilon)V_{\varepsilon}+(V-\eta)V_{\eta}+mV+\frac{1}{R}P_{\eta}=0,\\
&(1-\varepsilon)R_{\varepsilon}+(V-\eta)R_{\eta}+RV_{\eta}+\frac{\nu RV}{\eta}=0;\\
&(1-\varepsilon)P_{\varepsilon}+(V-\eta)P_{\eta}+2mP+\gamma P\left(V_{\eta}+\nu\frac{V}{\eta}\right)=0.
\end{aligned}\right| \qquad (2.2)
$$

Boundary conditions (1.2) and condition on body are converted to the form

$$\left.\begin{aligned} V(s,\eta_1)=\frac{2c}{\gamma+1};\quad R(s,\eta_1)=\frac{\gamma+1}{\gamma-1};\quad P(s,\eta_1)=\frac{2c^2}{\gamma+1};\\ c=\eta_1(s)+(1-s)\eta_1'(s);\quad V(s,s)=1. \end{aligned}\right\} \quad (2.3)$$

The domain of the effect of the apex/vertex of body stretches to line $s=1$. On this line the unknown solution corresponds to the solution of the problem of the self-similar motion of flat/plane or cylindrical piston.

1. System of equations (2.2) is everywhere hyperbolical. This fact makes it possible to utilize for the solution of problem or for finding of the initial data, necessary for the numerical integration of system, a method expansion in series. Let us examine first approximate solution of two-dimensional problem in range $m \ll 1$. Let us present function in the form of a series according to degrees of m, after being restricted to two terms of the expansion:

$$\left.\begin{aligned} V=1+mV_1+O(m^2);\quad P=\frac{\gamma+1}{2}+mP_1+O(m^2);\\ R=\frac{\gamma+1}{\gamma-1}+mR_1+O(m^2);\quad \eta_1=\frac{\gamma+1}{2}s+ma_1(s)+O(m^2). \end{aligned}\right\} \quad (2.4)$$

The unknown solution is represented in the form of the converging series:

$$\left.\begin{aligned}
&P_1(\varepsilon,\eta)=(\gamma+1)k\ln\prod_{i=1}^{\infty}k^{-\frac{1}{k}}(\varepsilon-\eta+k_1)(1-\varepsilon)^{\frac{1-k}{k}}\left[\left(k_2^i\frac{1-\eta+k_1}{1-\varepsilon}+\right.\right.\\
&\left.\left.+k_3\frac{k_2^i-1}{k_2-1}-1\right)\left(-k_2^i\frac{1-\eta-k_1}{1-\varepsilon}+k_3\frac{k_2^i-1}{k_2-1}-1+2k_2^i\right)\right]^{k_4^i};\\
&a_1(\varepsilon)=\frac{1-\varepsilon}{2}\int_0^{\varepsilon}P_1\left(\varepsilon,\frac{\gamma+1}{2}\varepsilon\right)\frac{d_\varepsilon}{(1-\varepsilon)^2};\quad k(\gamma)=\left(\frac{1}{2}\frac{\gamma}{\gamma-1}\right)^{\frac{1}{2}};\\
&k_1=(\gamma-1)k;\quad k_2=\frac{2k-1}{2k+1};\quad k_3=\frac{\gamma+1}{2}-\frac{3-\gamma}{2}k_1;\\
&k_4=\frac{1-k}{1+k}.
\end{aligned}\right\}\quad(2.5)$$

Page 20.

In the case $\gamma=2$, series break themselves:

$$P_1=3\ln(1+\varepsilon-\eta);\quad a_1(\varepsilon)=3\frac{2-\varepsilon}{2}\ln\frac{2-\varepsilon}{2}-3\frac{1-\varepsilon}{2}\ln(1-\varepsilon).$$

At low values ε, expansion (2.4) gives asymptotically exact solution. Therefore an error in the expansion should be estimated with $\varepsilon=1$. We have:

$$P_1(1,\eta)=\frac{\gamma+1}{2}\ln\left[k_2^{\frac{1-k^2}{k^2}}\left(1+\frac{1-\eta}{k_1}\right)^{k+1}\left(1-\frac{1-\eta}{k_1}\right)^{1-k}\right]a_1(1)=$$
$$=\frac{1}{2}P_1\left(1,\frac{\gamma+1}{2}\right).$$

Values $P_1(1,\eta)$ and $a_1(1)$ coincide with the appropriate solution linearized by parameter ε of the one-dimensional task of the expansion of flat piston the accuracy/precision of solution of which is satisfactory for sufficiently low values of |n|. So, with $n > n_1 = [\gamma - 1/2a_1(1)]$ (n=0.435; 0.441; 0.461; 1.95 respectively for γ=4/3, 7/5, 5/3 and ∞) $\eta_1(1) < 1$, and solution loses physical sense; with n<-0.5, as is known, the solution of problem not at all has physical sense [7].

2. Let us examine solution of axisymmetric problem in range $\varepsilon > 1$. At a great distance from apex/vertex ($\varepsilon \to \infty$) the flow of gas will be the same as after flat piston. Approximate solution can be obtained, after expanding the unknown functions in the vicinity of the infinite point in a series according to negative degrees η. We will be restricted to the simplest case of the uniform motion of cone.

$$\left.\begin{aligned} V &= 1 + \eta^{-i} V_i(\eta - \varepsilon); \quad P = \frac{\gamma+1}{2} + \eta^{-i} P_i(\eta - \varepsilon); \\ R &= \frac{\gamma+1}{\gamma-1} + \eta^{-i} R_i(\eta - \varepsilon); \quad \eta_1 - \varepsilon = \frac{\gamma+1}{2} + \eta_1^{-i} a_i. \end{aligned}\right\} \quad (2.6)$$

The sign of summation over index i(i=1, 2, 3, ...) is lowered. After substituting expansion (2.6) into equations (2.2) and under boundary conditions (2.3) and after selecting terms with identical degree η we will obtain the system of ordinary differential equations for determining functions V_i, R_i and P_i with the appropriate boundary conditions. From this system of equations and boundary conditions which for brevity are not here extracted, functions V_1, R_1, P_1, and constants s_1 are also determined consecutively. For the first three terms of expansion (2.6) we have:

$$a_1 = -\gamma\frac{\gamma+1}{8}\frac{\gamma-1}{2\gamma-1};\quad a_2 = -\frac{(\gamma+1)(\gamma-1)^2}{48}\frac{17\gamma^3+25\gamma^2-15\gamma+1}{(7\gamma-5)(2\gamma-1)^2};$$

$$P = \frac{\gamma+1}{2}\left\{1-\gamma\frac{\gamma-1}{2\gamma-1}\eta^{-1}+\left[\gamma\frac{\gamma-1}{2}\frac{13\gamma^3-28\gamma^2+25\gamma-6}{(7\gamma-5)(2\gamma-1)^2}-\right.\right.$$
$$\left.\left.-\gamma\frac{\gamma-1}{2\gamma-1}(\eta-a)+\frac{3\gamma-1}{\gamma-1}\frac{\gamma^2-4\gamma+1}{(7\gamma-5)(2\gamma-1)}(\eta-a)^2\right]\eta^{-2}\right\}.$$

Page 21.

The accuracy/precision of method can be rate/estimated in terms of the values of functions with $a=1$. So, when $\gamma=1.405$ $\eta_1(1)$ is equal to 1.2025 in the first approximation, 1.121 - in the second and 1.081 - in the third; value P(1.1) is respectively equal to 1.2025, 0.825 and 1.038 [precise value $\eta_1(1)$ is equal to 1.098, the precise value P(1.1) - 1.085].

The same method of approximate solution of axisymmetric task in the range, immune to to the effect of apex/vertex, can be used, also, with $s=0$; however, calculations in this case prove to be more laborious, since the task of the irregular motion of flat piston, generally speaking, does not have quadrature solution. For estimating pressure distribution in range $a>1$ in engineering calculations, it is possible to assume

$$P(a, a) \approx P_{01} + \frac{P_{00}-P_{01}}{a}. \qquad (2.7)$$

Here P_{a1} - pressure on flat piston, P_{a2} - on cylindrical. Analogously it is possible to determine dependence $\eta_s(a)$, etc.

3. For further target/purposes of conveniently utilizing Mises's coordinates a and ψ (ψ - function of current). From equations (2.2) we find

$$\left.\begin{aligned} &V_\psi + \frac{(1-a)^{2+\nu}}{R^2\eta^\nu} R_a = -\nu\left(\frac{1-a}{\eta}\right)^2 \frac{V}{R};\\ &(1-a)\,V_a + \frac{\eta^\nu}{(1-a)^{1+\nu}} P_\psi = -aV;\\ &P = (1-a)^{2a} R^\gamma f(\psi);\quad \frac{d\eta}{da} = \frac{V-\eta}{1-a} + \frac{(1-a)^{2+\nu}}{R\eta^\nu}\Psi'(a), \end{aligned}\right\} \quad (2.8)$$

where $f(\psi)$ - certain unknown function of its argument, $\psi = \Psi(a)$ - arbitrary line in plane ψ, a. On body surface $\psi = 0$, and on shock wave $\psi = \psi_1(a)$. Then boundary conditions (2.3) accept the following form:

$$V(a, \psi_1) = \frac{2c}{\gamma+1};\quad P(a, \psi_1) = \frac{2c^2}{\gamma+1};\quad R(a, \psi_1) = \frac{\gamma+1}{\gamma-1}; \quad (2.9)$$

$$\left.\begin{aligned} &\eta^{1+\nu}(a, \psi_1) = (1+\nu)(1-a)^{1+\nu}\psi_1;\quad c = \frac{(1-a)^{2+\nu}}{\eta^\nu}\frac{d\psi_1}{da};\\ &V(a, 0) = 1;\quad \eta(a, 0) = a \end{aligned}\right\} \quad (2.10)$$

Condition for $\eta(\varepsilon, \psi_1)$ is the consequence of the last/latter equation of system (2.9) and of conditions on shock wave.

In the vicinity of the apex/vertex of body, let us present solution in the form of a series according to degrees ε:

$$\left.\begin{array}{l} V = V_0(\lambda) + \varepsilon V_1(\lambda) + \ldots; \quad P = P_0(\lambda) + \varepsilon P_1(\lambda) + \ldots; \\ R = R_0(\lambda) + \varepsilon R_1(\lambda) + \ldots; \quad \eta = \varepsilon \eta_0(\lambda) + \varepsilon^2 \eta_1(\varepsilon) + \ldots; \quad \lambda = \psi \varepsilon^{-1} \end{array}\right\} \quad (2.11)$$

After substituting expansion (2.11) into equations (2.8) and after gathering terms with identical degree ε, it is possible to obtain system of equations for the consecutive determination of the terms of series (2.11). It proves to be that the system of equations for the first terms of expansion V_0, R_0, P_0 and η_0 describes (in the variables of Lagrange) flow after the flat/plane or cylindrical piston, driving/moving with constant velocity.

Page 22.

As is known from the hypersonic theory of the slight disturbances, the same flow is realized during the stationary hypersonic flow around cone or wedge.

For a wedge it is easy to find subsequent members of expansion (2.11):

$$\left.\begin{array}{c}P_0=\frac{\gamma+1}{2};\ P_1=m\frac{\gamma+1}{2}\frac{2-\gamma}{2\gamma-1};\ \eta_0=1+\frac{\gamma-1}{\gamma+1}\lambda;\\ \eta_1=\frac{\gamma-1}{\gamma+1}\lambda\left[\frac{3m}{2\gamma-1}\left(\frac{\lambda}{\gamma+1}-1\right)-1\right].\end{array}\right\}\quad(2.12)$$

Far from the apex/vertex of wedge, solution (2.12) can lead to larger error than solution (2.5).

Expansion (2.11) describes asymptotic behavior of functions in the vicinity of apex/vertex, it was used for determining the initial data, necessary for the calculation of flow by method of characteristics.

4. System (2.8) has two families of real characteristics:

$$d\varphi=\pm R\alpha\gamma\frac{d\alpha}{(1-\alpha)^{2+\nu}};\quad a=\sqrt{\gamma\frac{P}{R}},\qquad(2.13)$$

along which are fulfilled differential conditions

$$dV\pm\frac{dP}{Ra}=-\left[mV\pm a\left(\frac{2m}{\gamma}+\nu\frac{V}{\eta}\right)\right]\frac{d\alpha}{1-\alpha}.$$

Line $\alpha=1$ is person for characteristics; with $\alpha\to1$ the tangent of angle of the slope/inclination of characteristics to axle/axis unlimitedly grow/rises, on the line $\alpha=1$ of the characteristic of both families, they pour.

In range $\alpha<1$, the problem was solved by ETsVM (digital computer) by method of characteristics. As initial data were accepted the first terms of expansion (2.11). In the axisymmetric case the system of equations for determining these members was solved by Runge-Kutta's method with the constant space, equal to $\lambda_1/32$. Line $\alpha=\alpha_0$, which carries data, it was selected from the condition so that the solution on line $\alpha=2\alpha_0$, obtained by method of characteristics, would differ from the solution, corresponding to the first terms of series (2.11), it is less than to 1%. The number of points in layer was retained constant and it was equal to 33. The calculation flow chart for four points in layer is shown on Fig. 2. By dotted line is shown the characteristic, passing through the point, arrange/located to halfway direct/straight, that connects point on shock wave from adjacent the layer.

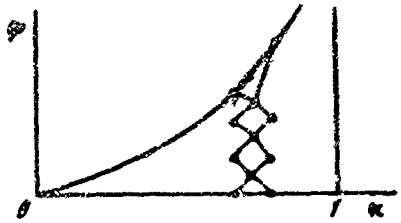

Fig. 2.

Page 23.

With numerical count it was necessary to solve the elementary problems of the calculation of field point, point on body and points on shock wave [8]. The calculation of field point was performed with one recalculation, remaining elementary problems were solved with two recalculations. With $\alpha \to 1$ $\eta_1 \to \infty$, therefore the problem was solved to values α=0.95-0.98.

Fig. 3, gives dependence pressure on wedge and density on α, and also the form of shock wave $\eta_1(\alpha)$ - a for the different values of parameter n; Fig. 4, shows the same dependences for an axisymmetric task. Calculations were performed for a value γ=1.405. The solution, obtained by method of characteristics, was mated with exact solution with φ=1. It is assumed that the error in the determination of pressure does not exceed 2o/o, but in determination $\eta_1(\alpha)$- 1o/o. The comparison of the numerical solution of task with n=0 with quadrature showed that for that selected in Fig. 3 and 4 scales an error in the numerical count was negligible up to line φ=0.99.

As can be seen from those given to Fig. 3 and 4 curve/graphs, shock wave in the flat/plane case convex with n>1 and concave with n<1. With n=0.7 the curves P(α, φ) and $\eta_1 - \alpha$ sharply grow/rise near line φ=1 $(\eta_1(1) = 2.76,\ P(1,1) = 3.02)$. For the high values of parameter n, dependence P(φ, α) has a maximum near weak discontinuity/interruption (φ=1), while for sufficiently low values of n - minimum. Gas density with increase α approaches infinity for accelerated flow (n>1) and for zero - for that retarded (n<1). Case $\alpha \to \infty$ (n=1) corresponds to the task of the motion of cone or wedge exponentially depending on time.

Qualitatively the same nature have dependences in the axisymmetric case. With n<2/3 solution of two-dimensional problem, there are, therefore, there is no solutions of axisymmetric problem, since with $\alpha \to \infty$ the flow of gas the same as after flat piston.

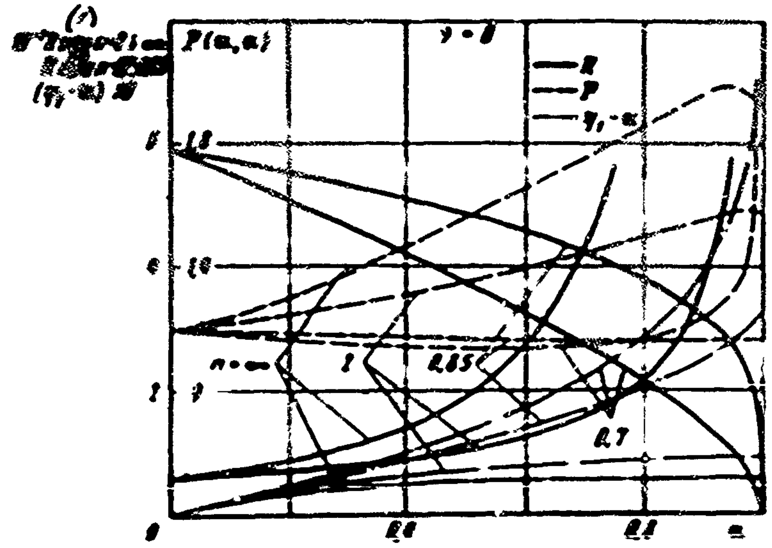

Fig. 3.

Key: (1). with.

Page 28.

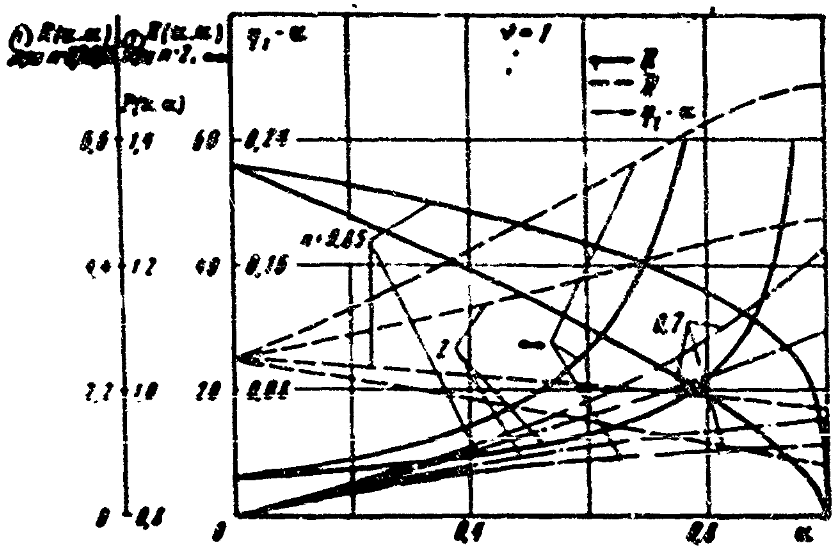

Fig. 4.

Key: (1). with.

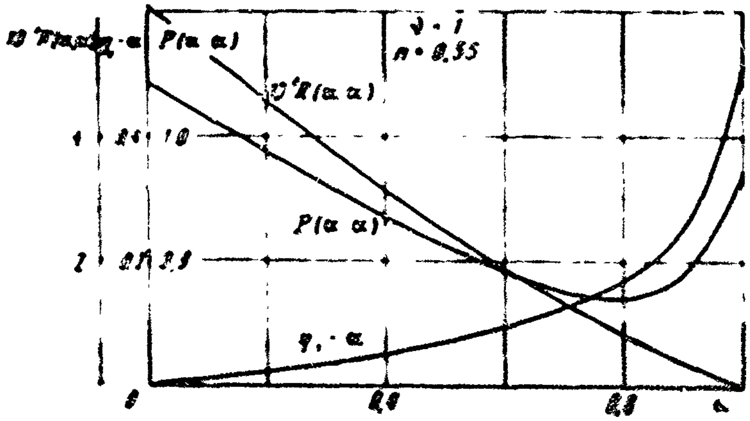

Fig. 5.

However, with $1/2<n\leqslant 2/3$ there is solution of the problem of the self-similar penetration of slender cone into the half-space of the harassed gas, since in this case it suffices to obtain solution in range $\alpha\leqslant 1$, after accepting plane $r=bt^n$ ($\alpha=1$) beyond solid boundary. That correspond to solution with $n=0.55$ is shown on Fig. 5.

Let us note that the task on the accelerated penetration of wedge the half-space, filled by quiescent gas, is equivalent to the task on the hypersonic flow around the delta-like wing of rhombiform cross section with alternating/variable (exponential) sweepback.

The second terms of external expansions for speed u have a gap on special line. In actuality this gap must not occur. Consequently, in the vicinity of special line the external expansion, which confines entire elliptical field into straight line, incorrectly describes the picture of flow. In this range it is necessary to utilize internal asymptotic expansion. With this width of elliptical zone on shock wave Δx (see Fig. 1c) in the case of the uniform motion of the wedge of order δ with small δ and $\varepsilon^{1/2}$ with small ε

Internal expansion represents by itself the linear addition to the solution of the problem of the expansion of one-dimensional piston, which satisfies the conditions of union with external expansion with the unlimited increase of longitudinal internal variable to both sides from special line or on the lines of removable discontinuity.

However, for determination in the first approximation, of total action characteristic - the coefficient of the wave impedance (see Section 4) - it suffices to find pressure on body surface within the framework of external expansion, since gap on the special line of higher order, than the principal term of expansion.

§ 3. Theory of thin shock layer.

According to the theory of thin shock layer the solution of problem let us present in the form

$$\left.\begin{aligned} u &= \cos\theta + O(\varepsilon);\quad v = \varepsilon V(x,\tau) + O(\varepsilon^2);\\ p &= P(x,\tau) + O(\varepsilon);\\ \rho &= \frac{R(x,\tau)}{\varepsilon} + O(1);\quad y = \varepsilon\tau;\quad \varepsilon = \frac{\gamma-1}{\gamma+1} \ll 1 \end{aligned}\right\} \quad (3.1)$$

Substituting those values under system (1.3) and conditions

(1.4) and disregarding smalls of the second order, we will obtain the following system of equations and boundary conditions for determining the functions P, R, V:

$$\left.\begin{aligned} P_\eta = -mR\sin\delta;\quad (\cos\delta - x)R + (V-\eta)R_\eta + RV_\eta + \nu R\frac{\cos\delta}{x} = 0;\\ (\cos\delta - x)P_x + (V-\eta)P_\eta + P\left(2m + V_\eta + \nu\frac{\cos\delta}{x}\right) = 0; \end{aligned}\right| \quad (3.2)$$

$$\left.\begin{aligned} V(x,\ \eta_1) = \eta_1 - (x - \cos\delta)\eta_1' - \sin\delta;\\ P(x,\ \eta_1) = \sin^2\delta R(x,\ \eta_1) - 1;\\ V(x,\ 0) = 0. \end{aligned}\right| \quad (3.3)$$

Page 26.

Problem is solved in the quadratures:

$$
\begin{aligned}
&P - \sin^2\delta\left[1+\frac{m}{\cos\delta}\frac{(\cos\delta-x)^{1+\nu}}{x^{\nu}}(\psi_1-\psi)\right]^{\frac{1}{\varkappa}m} = \\
&= \left|\left(1-\frac{x}{\cos\delta}\right)f(\psi)\right|^{2m}\frac{\sin^2\delta}{p}; \\
&V=\sin\delta\int_0^{\psi}\left\{\frac{m}{\cos\delta}\frac{(\cos\delta-x)^{1+\nu}}{x^{\nu}}\times\right. \\
&\times\left[\frac{(\cos\delta-x)^{1+\nu}x^{-\nu}\left(1+\frac{\nu\cos\delta}{x}\right)(\psi_1-\psi)}{m(\cos\delta-x)^{1+\nu}x^{-\nu}(\psi_1-\psi)+\cos\delta}-2\right]- \\
&\left.-\nu\left(\frac{\cos\delta-x}{x}\right)^2\right\}\frac{d\psi}{R}; \\
&\eta=\operatorname{tg}\delta\frac{(\cos\delta-x)^{1+\nu}}{x^{\nu}}\int_0^{\psi}\frac{d\psi}{R}; \\
&f(\psi)=\begin{cases} 1+[(1+\nu)\psi]^{\frac{1}{1+\nu}} & \text{(1) при } x\leqslant\cos\delta; \\ [1+(1+\nu)\psi]^{\frac{1}{1+\nu}}-1 & \text{(1) при } x\geqslant\cos\delta; \end{cases} \\
&\psi_1=\begin{cases} \frac{1}{1+\nu}\left(\frac{x}{\cos\delta-x}\right)^{1+\nu} & \text{(1) при } x<\cos\delta; \\ \cos\delta\frac{(x-0{,}5\cos\delta)^{\nu}}{(\cos\delta-x)^{1+\nu}} & \text{(1) при } x\geqslant\cos\delta. \end{cases}
\end{aligned}
\qquad (3.4)
$$

Key: (1). with.

In the theory of this layer the special line, which demarcates two different solutions, is line x=cosδ. In the range, immune to to the effect of apex/vertex, the density not body R(x, 0) is equal to - with m>0; 0 with m<0 and 1 with m=0. In the case m=0, the pressure is constant: P=sin²δ. This fact suggests to examine another external expansion which let us call/name Newton's theory. Let there be

$$\left.\begin{aligned} &u = \cos\delta + O(\varepsilon);\ v = \varepsilon V(x,\eta) + O(\varepsilon^2);\ p = \sin^2\delta + \varepsilon P(x,\eta) + O(\varepsilon^2);\\ &\rho = \frac{1}{\varepsilon} + R(x,\eta) + O(\varepsilon);\ y = \varepsilon\eta;\ \varepsilon \ll 1;\ 0 < m < 1;\ q = \frac{m}{\varepsilon}. \end{aligned}\right\} \quad (3.5)$$

The solution of problem takes the form

$$V = -\nu\frac{\cos\delta}{x}\eta_1;\quad \eta_1 = \begin{cases} \dfrac{x\,\mathrm{tg}\,\delta}{1+\nu} & \text{(1) при } x \leqslant \cos\delta;\\ \sin\left(1 - \dfrac{\nu}{2}\dfrac{\cos\delta}{x}\right) & \text{(1) при } x \geqslant \cos\delta; \end{cases} \quad (3.6)$$

$$P = \sin^2\delta + q(\eta_1 - \eta)\sin\delta - 2\nu\sin\delta\frac{\cos\delta}{x}\eta_1 + \nu\cos^2\delta\frac{\eta_1^2 - \eta^2}{x^2};$$

$$\rho - R\sin\delta = \begin{cases} (1-\nu)\sin^2\delta + 2q\sin^2\delta\ln\dfrac{\cos\delta - x + (2x)^{\frac{\nu}{1+\nu}}(\eta\,\mathrm{ctg}\,\delta)^{\frac{1}{1+\nu}}}{\cos\delta}\\ \qquad \text{(1) при } x \leqslant \cos\delta;\\ \sin^2\delta - \dfrac{2\nu x\eta\sin^2\delta}{2x\eta + (x-\cos\delta)^2\,\mathrm{tg}\,\delta} +\\ + 2q\sin^2\delta\ln\left[\dfrac{\eta}{\sin\delta}\left(\dfrac{2x}{x - \cos\delta + \sqrt{(x-\cos\delta)^2 + 2x\eta\,\mathrm{ctg}\,\delta}}\right)^{\nu}\right]\\ \qquad \text{при } x \geqslant \cos\delta. \end{cases}$$

Key: (1). with.

Page 27.

Special line is also line η=cosδ. Singular point for flow lines η=cosδ, y=0 is node/unit. When $\nu=0$ - single node/unit, when $\nu=1$ - all the curves, except line second, they enter in singular point in the direction $\eta=0$.

Table gives the orders of basic values in the theories of slight disturbances (I), of thin shock layer (II) and of Newton (III).

Fig. 6, gives for a comparison the distribution of pressure p(x, x) on cone with $\delta=0.3$, $\gamma=1.405$, $n=\infty$ and Q.85, designed by the method of external asymptotic expansions in terms of theories I, II and III. According to the theory of the slight disturbances in the range, immune to to the effect of apex/vertex, the pressure was calculated from formula (2.7). With $\eta=0.85$ curved III is designed formally on formulas (3.5), (3.6). By dotted line is shown the asymptotic value of pressure with $x\to\infty$.

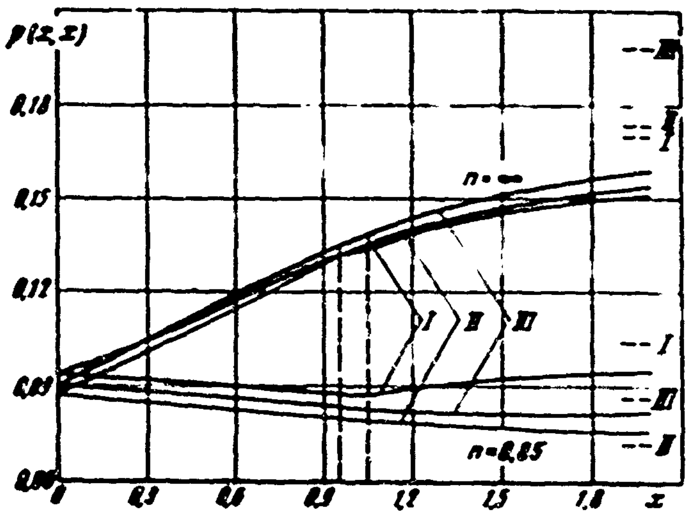

Fig. 6.

Table

	y	u	v	p	ρ
I	$\sim\delta$	1	$\sim\delta$	$\sim\delta^2$	~ 1
II	$\sim\varepsilon$	$\cos\delta$	$\sim\varepsilon$	~ 1	$\sim\varepsilon^{-1}$
III	$\sim\varepsilon$	$\cos\delta$	$\sim\varepsilon$	$\sin^2\delta$	ε^{-1}

Page 28.

It is evident that even at such high values δ and the limiting values of parameter n in the case of increasing motion the curves I and II give satisfactory coincidence, while in the case of retarded motion the difference in the determination of pressure from the theory of thin layer and theory of the slight disturbances are more than in the case of increasing motion. In the case $\nu=1$, Newton's theory gives only qualitative result, since at the high values of n it is barely suitable.

§ 4. Motion of the cone of the finite dimensions.

Flow past cone of the finite dimensions will not be self-similar. However, during the hypersonic motion of cone in perfect gas, the effect of end effect on pressure distribution according to its lateral surface will manifest itself only into that time interval when elliptical zone passes the section/shear of cone. Therefore during the use of external asymptotic expansion, which confines the range of ellipticity into straight line, end effect can be disregarded. Then the coefficient of wave impedance, in reference to the area of the basis (without the account of base pressure) of cone or wedge of length l_0

$$c_x = \left(\frac{2\delta r^{\circ} \cos\theta}{l_0}\right)^{\nu+1} \sin^2\theta \int_0^{\frac{l_0}{\delta r^{\circ}\cos\theta}} \frac{p(x,0)}{\sin^2\theta} x^{\nu}\, dx \qquad (4.1)$$

Let us calculate integral (4.1), after using, for example, quadrature solution from the theory of thin shock layer. According to formulas (3.4), the distribution of dimensionless pressure according to lateral body surface $p(x, Q)$ is determined by the following expression:

$$\frac{p(x,0)}{\sin^2\delta}=\begin{cases}1+\frac{m}{\nu+1}\frac{x}{\cos\delta} & \text{при (1) } x\leqslant\cos\delta;\\ 1+m\left(1-\frac{\nu}{2}\frac{\cos\delta}{x}\right) & \text{при (1) } x>\cos\delta.\end{cases} \quad (4.2)$$

Key: (1). with.

The special line proceed will hit to section/shear at the moment of time $t_1=\left(\frac{L_0}{b\cos^2\delta}\right)^{1/\nu}$. With $t>t_1$ entire/all lateral surface will be arrange/located in the domain of the effect of the apex/vertex of body. Comparing solution (4.2) into formula (4.1) and by integrating, we will obtain:

$$c_x=2\sin^2\delta\begin{cases}1+m\left[1-\frac{z}{2}-\nu z\left(\frac{1}{2}-\frac{z}{8}\right)\right] & \text{при (1) } t\leqslant t_1,\\ 1+\frac{m}{2+\nu}z^{-1} & \text{при (1) } t\geqslant t_1,\end{cases} \quad (4.3)$$

Key: (1). with.

where $z=\frac{bt^{\nu}\cos^2\delta}{L_0}$

As follows from expression (4.3), dependence c_x on time monotonic. With $t\to\infty$ $c_x\to 2\sin^2\delta$. With $t\to 0$ $c_x\to 2(1+m)\sin^2\delta$, reaching minimum value for retarded motion and maximum - for that accelerated.

at the moment of the time when the domain of the effect of apex/vertex encompasses entire lateral surface of body, addition to value c_x because of unsteady condition effect decreases in absolute value two times for a wedge and three times for a cone. Limiting value c_x is reached during the acceleration of body exponentially (n=1) and at zero time two times exceeds appropriate conservative value.

Page 29.

Qualitatively the same results are obtained during the application/use of Newton's theory to the calculation of the coefficient of wave impedance c_x° of final cone or wedge. Dependences $c_x^\circ(z)$ and $c_x(z)$ in the case $\nu=1$ ($\gamma=1.405$) are compared in Fig. 7. In the case of the exponential acceleration of cone c_x° at zero time, exceeds corresponding conservative value 2.68 times (in the case of the exponential acceleration of wedge - 1.86 times).

The author is grateful to A. I. Golubinskiy for useful conversations on the theme of this work.

REFERENCES

1. A. Sakurai. The flow due to impulsive motion of a wedge and

its similarity to the diffraction of shock waves. J of the Physical Soc. of Japan, 1955, V 10, No 3.

2. A. Sakurai. The flow due to impulsive motion of a wedge, II. J of the Physical Soc. of Japan, 1956, V 11, No 9.

3. N. L. Krasheninnikova. On unsteady motion of the gas, displaced by piston. Izv. of the AS USSR, OTN, 1955, No 8.

4. N. N. Kochin, N.S. . Mel6nikova. On unsteady motion of the gas, displaced by piston, without the account of counterpressure. PMM, Vol. XXII, iss. 4, 1958.

5. M. Van Dyke. Perturbation methods in fluid mechanics. M., (peace/world", 1967.

6. U. D. Kheyz, R. F. Probstin Theory of hypersonic flows, M., publ. foreign lit., 1962.

7. L. Lees, T. Kubota. Inviscid hypersonic flow over blunt-nosed slender bodies JAS, 1957, 23, No 3.

8. O. N. Katskova et al. Experiment in the calculation of the plane and axisymmetric supersonic flows of gas by method of

characteristics. M., the CC of the AS USSR, 1961.

The manuscript entered 23/V 1969.

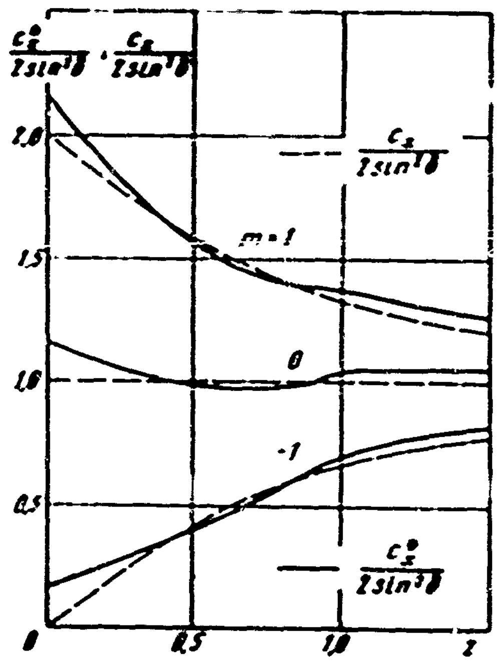

Fig 7

Page 30.

THE NATURE OF TURBULENT MOTION.

V. N. Zhigulev.

In work is voiced the view according to which the chain/network of the equations of Friedman and Keller does not actually contain the mechanism of the emergence of turbulence.

is proposed the examination of stability condition "on the average" as necessary condition for explaining the mechanism of the generation of correlations.

§ 1. Setting

The chain/network of the equations of Friedman and Keller for the incompressible fluid takes the form:

$$\left.\begin{array}{c}\frac{\partial V_1}{\partial q_{11}}=0;\ \frac{\partial V_a}{\partial t_1}+V_1\frac{\partial V_a}{\partial q_{11}}+\frac{\partial W^{(2)}_{a1}}{\partial q_{11}}+\frac{\partial p}{\partial q_{1a}}=\nu\Delta_1 V_a;\\ \sum_{1\leqslant l\leqslant s} \delta_{n_l}\left[\left(\frac{\partial}{\partial t_l}+V_1(t_l\bar{q}_l)\frac{\partial}{\partial q_{l1}}\right)W^{(s)}_{m\ldots}\, f_{a_l}\ldots+\right.\\ +W^{(s)}_{m}\ f^{l-1}_{a_{l-1}}1f^{l+1}_{a_{l+1}}\ \frac{\partial V_{f_1}}{\partial q_{l1}}-W^{(s-1)}_{m}\ f^{l-1}_{a_{l-1}}f^{l+1}_{a_{l+1}}\ \times\\ \times\frac{\partial W^{(2)}_{a f_1}(t_l\bar{q}_l,t_l\bar{q}_l)}{\partial q_{l1}}+\frac{\partial}{\partial q_{l1}}W^{(s+1)}_{m\ldots}\,f^{l}_{a_l,1}(\ldots,t_l\bar{q}_l)+\\ \left.+\frac{\partial}{\partial q_l f_{a_l}}\ W^{(s)}_{m+1}\ f^{l-1}_{a_{l-1}}f^{l}_2 f^{l+1}_{a_{l+1}}-\nu\Delta_l W^{(s)}_{m\ldots}\, f^{l}_{a_l}\right]=0;\\ \frac{\partial}{\partial q_{l1}}W^{(s)}_{m\ldots}\,f^{s-1}_{a_{s-1}1}=0\ \ (\text{for } n_s=1)\\ (s=2,3,4,\ldots),\end{array}\right|\quad(1.1)$$

where V_a - averaged velocity vector component; p - averaged pressure, referred in the value of density ρ.

Values $W^{(s)}_{m}f^1_{a_1}f^2_{a_2}\ldots f^s_{a_s}=W^{(s)}_{m\ldots}\,f_{a_l}\ldots$ are the averaged product of the pulsation of the velocity vector and pulsations of pressure (referred to density). Product consists of s of the factors, from which m is the pulsations of pressure (corresponding index $n_l=2$) and (s-m) - by the pulsations of velocity (index $n_l=1$); the l factor it is calculated at space-time point $t_l q_l$ $1\leqslant l\leqslant s$.

Page 31.

Aggregate index $f^l_{a_l}$ in the case $n_l=1$ indicates the component of pulsating speed, and in the case $n_l=2$ simply it is related to the pulsation of pressure. The totality of values $W^{mn}_{m}\ldots f_{\alpha_1}\ldots$ with fixed/recorded n, m and α_1 in tensor (n-m) of rank; values possess the following property of symmetry:

$$W^{mn}_{m}\ f_{\alpha_1}\ f_{\alpha_2}\ (\ldots, f_1\bar{q}_1, \ldots f_2\bar{q}_2 \ldots) =$$
$$= W^{mn}_{m}\ldots f_{\alpha_2}\ f_{\alpha_1}\ldots(\ldots f_2\bar{q}_2 \ldots f_1\bar{q}_1 \ldots). \qquad (1.2)$$

i.e. the values in question coincide, if during the exchange of complex indices to produce in simultaneous the exchange of the corresponding four-dimensional arguments.

Value $\alpha_i = 1$, if $n_i = 1$, and $\alpha_i = 0$, if $n_i = 2$; $\Delta_i = \frac{\partial^2}{\partial q_{i\gamma} \partial q_{i\gamma}}$; on the twice encountered index γ in any term is assumed addition from 1 to 3.

The chain/network of equations (1.1) is obtained from Navier-Stokes equations [1].

FOOTNOTE [1]. To consider the system of the solutions of Navier-Stokes equations the specific statistical ensemble at present as yet is impossible. ENDFOOTNOTE.

It is assumed that it describes turbulent action of the incompressible fluid.

It is necessary to say that obtaining the method of Friedman and

Keller the chain/network of equations (1.1) from the Navier-Stokes equations is contradictory since, as can easily be seen that the chain/network of equations (1.1) formally includes all the solutions of Navier-Stokes equations (on basis of which it it is constructed) as special case when all the correlation functions are equal to zero. On the other hand, is assumed the existence also of such solutions, when correlations are different from zero. Physically this contradiction occurs because is a priori unclear, which unsteady solutions of Navier-Stokes equations comprise the random part of the turbulent hydrodynamic field and in which measure correlation functions can be considered arbitrarily assigned with the formation of initial and boundary-value problem for equations (1.1). To us it seems that this is the basic question which must be placed before the method of Friedman and Keller [1].

Together with this in real time, there is another, free from the contradiction indicated posing of the question concerning the statistical theory of turbulence.

In works [2] - [4] on the basis of the equations of Bogolyubov, is initiated the investigation of the new statistical ensemble, which differs in that the probability of its states it is simultaneous at different macroscopic points are not, generally speaking, in the form of the products of the probabilities of states in each of the points in question. In other words, the studied ensemble is characterized by the absence of the property of statistical independence.

Page 32.

Very important render/showed the fact that the studied ensemble in the case of the hydrodynamic motions of perfect gas, besides the independent characteristics average density, the averaged-mass speeds and medium energies (temperature), composing the basis of usual aerodynamic description, is determined additionally, generally speaking, by the infinite set of the independent correlation functions, for which are superimposed only general integral conditions about coordination. Thus, correlation - these are new fundamental and independent motion characteristics.

The investigation of different special cases led to the fact that the hydrodynamic equations for the totality of the determining values formally coincided with the appropriate equations of Friedman and Keller.

Thus, it turned out that for correlation functions one should look as at independent, given by initial and limit data.

In accordance with this is proposed the following model of turbulence T: turbulent motion of the incompressible fluid are determined by the totality independent[a] values V_α, p, $W^{(s)}_{\alpha_1 \ldots \beta_1 \ldots}$ ($s=2, 3, 4, \ldots$; $m=0, 1, 2, \ldots, s$), which satisfy the chain/network of equations (1.1); values $W^{(s)}_{\alpha \ldots \beta_1 \ldots}$ possess the property of symmetry (1.2) and satisfy general integral conditions of the type

$$\int W^{(s)}_{\alpha \ldots \beta_1 \ldots} d\vec{q}_s dt_s = 0 \qquad (1.3)$$

(where the integration comman for whole four-dimensional space - time).

§ 2. Theorem on breaking of chain/network (1.1) in the case of homogeneous turbulence.

Let us approach toward the analysis of the introduced above model T.

Homogeneous turbulence usually is called this form of the turbulent motion when average values V_α and p are constant in flow, while correlations $W^{(s)}_{\alpha \ldots \beta_1 \ldots}$ depend on the coordinate of physical space only by means of differences $\vec{q}_i - \vec{q}_1$ ($i=2, \ldots, s$).

In the case of homogeneous turbulence, the chain/network of equations (1.1) takes the form:

$$\left.\begin{aligned}&\sum_{1\le i\le s} a_{\alpha_i}\Big[\frac{\partial}{\partial t_i} W^{(s)}_{\alpha\dots j^i_{\alpha_i}\dots} + \frac{\partial}{\partial q_{j1}} W^{(s+1)}_{\alpha\dots j^s_{\alpha_s}} + \\ &+\frac{\partial}{\partial q_{ij^i_{\alpha_i}}} W^{(s)}_{\alpha+1\dots j^{i-1}_{\alpha_{i-1}} j^i_{1} j^{i+1}_{\alpha_{i+1}}\dots} - \nu\Delta_i W^{(s)}_{\alpha\dots j^i_{\alpha_i}\dots}\Big] = 0;\\ &\frac{\partial}{\partial q_{i1}} W^{(s)}_{\alpha\dots j^{s-1}_{\alpha_{s-1}} 1} = 0 \ (\text{azz } \alpha_s = 1).\end{aligned}\right\}\quad (2.1)$$

It is interesting to note that in the case of homogeneous turbulence of equation for pulsations V'_α and p^0 they will be in accuracy/precision Navier-Stokes equations, if we examine turbulence in the coordinates, connected with averaged-mass motion ($V_\alpha = 0$).

Page 33.

Equations (2.1) they allow/assume the following class of exact solutions, which is reduced to the finite number of indicial equations (theorem about breaking).

Let at initial moment ($t_i = t_0, i = 1, 2, \dots, s$) all the correlation functions, beginning with $s>s_0$, they turn into zero; then occurs exact solution, when these correlations are always equal to zero and chain/network (1.1) is converted into the system of the finite number of equations for functions $W^{(s)}_{\alpha\dots j^i_{\alpha_i}\dots}$ ($s \leq s_0$).

Let us note that the case, examined by Karman and Hovarth

($W^{R}_{L_s} \neq 0$), also they belong to recently the noted class of the exact solutions of equations for turbulence. In order of this to be convinced that that among $W^{(n)}_{\alpha} \ldots l^{l}_{s_1}$ $(s<s_0)$ are different from zero only those correlations which correspond m=0 (i.e. there are no correlations with pressure); then chain/network takes the form:

$$\sum_{1 \leq l \leq s} \left[\frac{\partial}{\partial t_l} W^{(n)}_{L \ldots l_s} + \frac{\partial}{\partial q_{l1}} W^{(n+1)}_{L \ldots l_{s1}} - \nu \Delta_l W^{(n)}_{L \ldots l_s} \right] = 0 \qquad (2.2)$$

$$(s<s_0;\ W^{(n+1)}_{L \ldots l_{s,1}} = 0).$$

Introducing new variables $t_1 = t,\ t_l = t + \tau_l$ ($l=2, \ldots, s$), we see that system (2.2) is simplified:

$$\frac{\partial}{\partial t} W^{(n)}_{L \ldots l_s} + \sum_{1 \leq l \leq s} \left[\frac{\partial}{\partial q_{l1}} W^{(n+1)}_{L \ldots l_{s1}} - \nu \Delta_l W^{(n)}_{L \ldots l_s} \right] = 0 \qquad (2.3)$$

$$(s<s_0;\ W^{(n+1)}_{L \ldots l_{s,1}} = 0).$$

In the system of equations (2.3) values τ_l they enter as parameters and, in particular, it it is possible to examine with all $\tau_l = 0$: obvious that in this last/latter class is located the solution, examined by pocket and Howarth.

Directly from the theorem about breaking it follows that homogeneous turbulence is classed according to the character of initial data [1].

REMARKS [1]. Let us note that the analogous result about broken of chain/network was obtained previously P. S. Vassesensky in the examination of homogeneous turbulence from the positions of the kinetics of perfect gas. IZBPCOTBOBB.

§ 3. On the stability condition of turbulent flow.

Let us examine the set of boundary conditions, which must be fulfilled during the solution of the chain/network of equations for turbulent motion in the case of the flow around body of stationary turbulent flow. For speed V, this

- speed in oncoming flow (is assign/prescribed $\bar{V}_\infty$);

- the condition of adhesion on body $\bar{V}|_{S_1=0}$ (S_1 - the surface of the streamlined body).

Page 34.

Let us formulate new conditions for $W^{(n)}_{m\ldots j_{n_1}\ldots}$. For this, let us assume that the wall of body sufficiently smooth, so that the pulsations of velocity vector on it are also equal to zero. The consequence of this will be the condition

$$W^{(n)}_{m\ldots j_{n_1}\ldots}=0, \qquad (3.1)$$

if one of three-dimensional/space arguments $\bar{q}_l$, that corresponds to any pulsation of velocity ($n_l=1$), takes the values, which correspond to body surface S_1.

Further, taking into account the experimental data about the fact that in the developed turbulent flow usually pulsation level is much higher than the level of initial turbulence [1], seems reasonable to require condition about the weakening of the correlations when one of arguments $\vec{q}_1$ is accepted values that correspond to the incident flow, i.e., to count for this zone

$$W^{1}_{m-l_{n_1}} \to 0. \quad (3.2)$$

FOOTNOTE [1]. Here there are in form cases of the emergence of turbulence unlike the tasks where turbulence is assigned in the incident flow or in initial data as, for example, this was into § 2. ENDFOOTNOTE.

But since conditions (3.1) and (3.2) are uniform, one of the solutions of problem will be, obviously, $W^{(1)}_{m-l_{n_1}}=0$ everywhere in flow, i.e., laminar flow, if, of course, this solution exists. Therefore in the range of values of the parameters, which determine flow and for the classes of the bodies where simultaneously there exist and laminar and turbulent flow, the solution of the formulated above problem for the chain/network of equations (1.1) for turbulent motion is not only. In the case of the flow around flat/plane plate at zero angle of attack, the solution, which corresponds to laminar flow, exists always, while experiment it shows that most frequently is realized (for sufficiently long plates) the precisely turbulent flow.

This occurs, so it seems to us that the system of equations (1.1) does not contain in actuality the mechanism of the formation/education of turbulence, but is only certain conditions, by which must satisfy turbulent action.

To the success of classical kinetic theory of gases it contributed, by the way, first that there were concrete/specific/actual subjects of investigations (atoms, molecules), while if in flow occurred chemical reactions, then were conditions for formation of these objects and a mechanism of the momentum diffusion and energy of beam of particles. Using this analogy, it is possible to say that chain/network (1.1) indisputably contains the mechanisms of the destruction of correlations; however, does not contain the mechanism of their generation.

On the basis of the aforesaid, finding the mechanism of the generation of correlations is the important problem of the construction of the theory of turbulence.

To us it seems that the examination of the stability of turbulent motion on times and on the length scales, which correspond to turbulent motion as a whole, is necessary for explaining the unknown mechanism.

Stability condition is by itself trivial, without it is not in practice realize/accomplished the solution in question, however, apparently in the theory of turbulence, it plays the significant role, since the emergence of turbulence, as this is well known, it is connected with the instability of viscous actions.

Page 35.

Even the fugitive analysis of the stability condition of turbulent flow or stability "on the average" shows that in it is contained something significant. It is real/actual, under conditions where the laminar solution is unstable, stability condition is compulsory will be to lead to the appearance of turbulent solutions, since, as we saw above, laminar solutions satisfy the chain/network of equations (1.1), and therefore the usual stability theory of laminar flows is a special case of overall stability theory "on the average".

Similarly the condition of stability "on the average" leads to the determination of turbulent state T_1. Immediately gets up a question concerning the uniqueness of state T_1. To us it seems that state T_1 is not only and with sufficiently large Reynolds numbers there is a spectrum of states T_i. If this them, then easily can be explained the dependence of the emergence of turbulent conditions/modes on values of initial turbulence. With sufficiently large Reynolds numbers, not far from stable even laminar state is arrange/located turbulent state T_i and the greater the level of initial pulsations, the earlier the flow from the "potential pit", which corresponds to laminar flow, it will pass into the "potential pit" of close turbulent state. By this method can be, obviously, explained experimental fact about hysteresis of turbulent flow. It is possible that during the developed turbulent action the mechanical system can occupy with the specific probability all states T_i and then the theory of developed turbulence - this statistics of states T_i. In this case becomes clear that wide frequency spectrum which is excited in the developed turbulent flow.

REFERENCES.

1. L. Keller, A. Friedman. Pros. 1-St. Int. Congress Appl. Mech., 1924, Delft.

2. V. N. Zhigulev. To the theory of the ordered statistical systems. DAN of the USSR, Vol. 161, No. 5, 1965.

3. V. N. Zhigulev. On the equations of the turbulent motion of

gas. DAN of the USSR, Vol. 165, No. 3, 1965.

4. V. N. Zhigulev. Some problems of nonequilibrium statistical mechanics and their communication/connection with questions of the statistical theory of turbulence. Transactions of TsAGI [' - Central Institute of Aerohydrodynamics im. N. Ye Zhukovskiy, iss. 1135, 1969.

The manuscript entered 29/IV 1969.

Page 36.

INTERFERENCE OF WING AND OF JET IN THE CARRYING FLOW.

V. B. Arnol'dov, N. G. Gordon, A. A. Savinov.

Are led the results of the experimental investigation of jet effect, which ensue at angle of 90° to lower surface of wing, on the aerodynamic characteristics of the isolated/insulated wings far from screen and near from it. On the basis of calculations and results of the experimental study of interaction of the jets of the various forms of initial section with the wings of different relative size/dimensions and planforms, is given the analysis of the reasons, which cause change in the effective thrust/rod of jets with an increase in the velocity of incident flow and a decrease of the distance of wing of screen. It is shown, that far from screen the external flow around jet plays the dominant role in a change in aerodynamic wing characteristics with an increase in the velocity of oncoming flow, while near from screen essential favorable effect exerts the vortex/eddy shaft, which appears on the surface of screen.

The interference of wing and jet, which ensues at certain angle to its lower surface, leads, as is known, to formation/education on the wing of the negative lift which decreases the value of the effective thrust/rod of jet. Simultaneously undergo considerable change and other aerodynamic wing characteristics. These changes in the aerodynamic characteristics are obtained by especially essential in a decrease of the distance of wing of screen and an increase in the velocity of incident flow. Thrust losses of jet, which appear in the absence of the incident flow, caused by the viscous forces. Jet in this case, involving into action surrounding air, creates disturbed flow about wing. Because of this on pressure side of wing, appear the evacuation/rarefactions, which decrease the effective thrust/rod of jet. Far from screen these losses are small. A considerable increase in the losses during the decrease of the distance of wing with jet of screen is connected with the formation/education of the fan jet, which possesses considerably larger ejecting ability, and the approach/approximation of wing to this perturbation source [1] - [3].

An increase in the losses of lift and a change in other aerodynamic wing characteristics with jet with an increase in the velocity of incident flow is connected, in the first place, with the disturbance/perturbations, which appear during the flow around jet, and, in the second place, it is possible, with certain change of its sucking properties in entrainment flow.

On Fig. 1 shown experimental distribution of the pressure which appears on flat surface during the flow around the rigid cylinder and real jet, normal to this surface, and calculated distributio of pressure, obtained during the replacement of jet by the system of the arranged/located on its axle/axis flows on the assumption that the interference of wing and jet is caused only by sucking action of jet [4].

Page 37.

Comparison shows that pressure distribution in the vicinity of real jet according to the character of the location of the zones of the increased and reduced pressure is qualitative analogous with pressure distribution around rigid cylinder and it is opposite to the calculated distributios of pressure.

However, the amounts of the supplementary lift which appear from real jet and rigid cylinder, substantially differ from each other. These differences are obtained by especially considerable in the range of comparatively low values of the given relation to velocity of incident flow to jet velocity $\left(\frac{V_\infty}{V_c}\sqrt{\frac{\rho_\infty}{\rho_c}}=\bar{V}_\infty\sqrt{\bar{\rho}_\infty}\right)$. Real jet, being bent and being expanded, acquires in the carrying flow the complex three-dimensional/space form, very distant from cylinder [5]. It is characteristic that most considerable change of the size/dimensions of jet in the carrying flow (unlike jet in the flooded space) occurs on its initial section and can cause essential disturbance/perturbations on the wing surface.

Fig. 2, gives some results of the approximate computations which were carried out for the case of ideal fluid for purpose of qualitative evaluation of lift increment (in the portions of the thrust/rod of jet), induced on flat surface by cylinder and the expanded solid body, imitating size/dimensions and the form of jet. Calculations show that the expanded body, which has the elliptic form of cross section with the relation of semi-axes 1:4 and the transverse size/dimension b, undertaken on the experimental data [5], is caused in comparison with cylinder a many times larger in value force, especially in the range of comparatively low values of the given relation to velocity of incident flow to jet velocity.

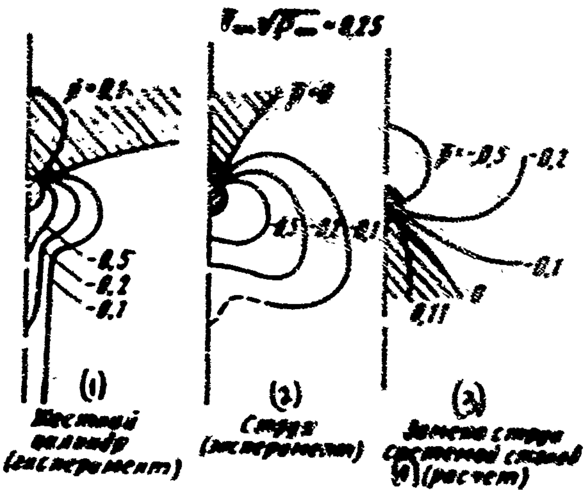

Fig. 1.

Key: (1). Rigid cylinder (experiment). (2). Jet (experiment). (3). Replacement of jet by system of flows (calculation).

Page 38.

This bears out the fact that the form of jet and its change with an increase in the velocity of incident flow play important role in the presence of the interference of wing and jet. Moreover, the analysis of these data shows that at the small values of the given velocity ratio the basic disturbances on wing are created by the section of the jet of large extent, which possesses lift effectiveness similar to certain low-aspect-ratio wing, arranged/located at high angle of attack with respect to the surface of main wing. With an increase in the curvature of jet, the lift effectiveness of its distant sections decrease as a result of the decrease of their angle of attack, and increasing value begin to play the disturbance/perturbations, caused by the flow around the initial section of jet as bluff body, close in form to cylinder directly on the wing surface. therefore, for example, the decrease of the initial an e of jet inclination to wing plane leads to the essential decrease of thrust losses of all range of a change in the given velocity ratio, and at its very high values, when, it would seem, jet is most distant on its form from cylinder, pressure field, induced by circular jet, as shown in work [6], already it differs little not only qualitatively, but also it is quantitative from pressure field in the vicinity of rigid cylinder.

Experimental investigations were carried out on the models of the rectangular wings with elongation λ=2 at angle of attack α=0. Was investigated the interference of wings with the jets, which had in initial section the form of circle (circular jet) and of the ellipse (elliptical jet) whose major axis could be arrange/located perpendicularly and in parallel to the velocity vector of the incident flow. Subsequently for convenience, let us call elliptical jet depending on the position of its major axis an elliptical jet across flow and elliptical jet along flow.

Far from screen on wing, which has sufficiently high size/dimensions in comparison with the size/dimensions of initial jet cross-sectional area $\left(\bar{F}_c = \frac{F_c}{S_{kp}} = 0.00164\right)$, most significant thrust losses gives elliptical across flow jet, while the jets of circular and elliptical along flow form give close in magnitude of losses (Fig. 2). Fig. 3. shows also the effect of the form of initial jet cross-sectional area on an increase in the pitching moment of wing.

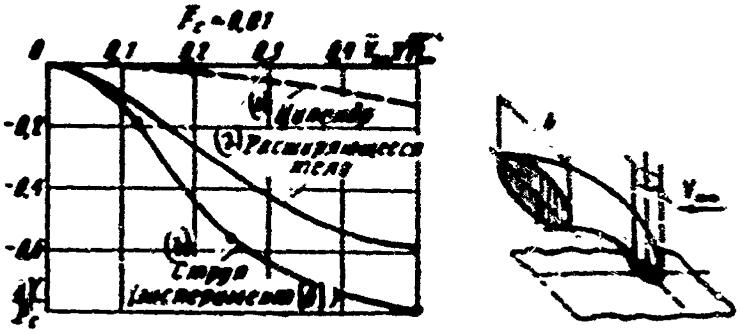

Fig. 2.

Key: (1). Cylinder. (2). Expanded body. (3). Jet (experiment).

Page 39.

The elliptical across flow jet (relation of semi-axes is equal to 1:10) it is bluff in initial sections, but bent, i.e., in in itself bluff obstruction, arrange/located on the wing surface. Even at comparatively small velocities of incident flow basic disturbance/perturbations on the wing are created by its initial section in the form of the vast zones of the elevated pressure before the jet and of evacuation/rarefaction after jet. The spectra of silk threads on the wing surface show that before the jet occurs braking flow and characteristic boundary-layer separation, although after jet is formed vast breakaway zone (Fig. 4).

Elliptical along flow jet is well streamlined on initial section (narrow trace, the absence of the visible zone of the backwater before the jet). But this jet intensely is expanded in transverse direction and is least bent. Experiments in the flooded space show that by the characteristic feature of the propagation of elliptical jet is its very nonuniform expansion on large and to the minor axes of ellipse. Along minor axis is obtained approximately six times more intense expansion, than on large. during the flow around jet of the carrying flow occurs the supplementary strain of the form of its sections. On the frontal surface of jet, appears the overpressure, while on lateral surfaces and from behind - evacuation/rarefaction.

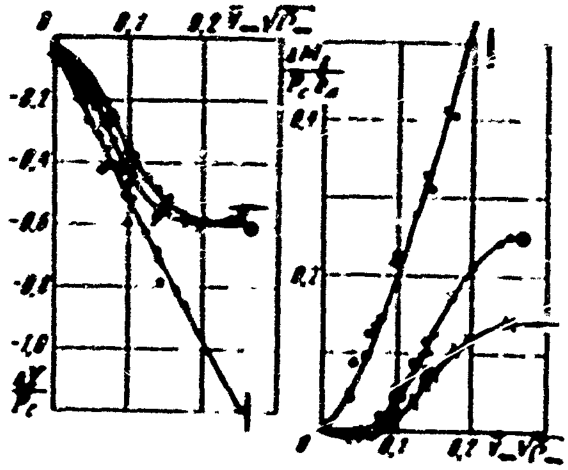

Fig. 3.

Fig. 4.

Page 40.

Therefore most significant expansion occurs in the direction, perpendicular to the direction of velocity of incident flow, and elliptical along flow jet at certain removal/distance from the wing surface acquires the form which introduces considerable disturbance/perturbations into flow. Basic disturbance/perturbations on the wing surface are created precisely by these sections of jet. They are exhibited predominantly in the formation/education of rarefaction zones about jet and bear significantly more uniform character, than disturbance/perturbations from elliptical across flow jet.

Turning again to the results of the tests rectangular wing with the jets of various forms, which ensue at angle of 90° to its lower surface (see Fig. 3), it should be noted that they correspond to the representation of the role of different sections of jet in the formation/education of losses with an increase in the velocity of incident flow. Imparting to the initial section of the jet of streamlined shape does not lead to the decrease of thrust losses in the inspected comparatively narrow range of a change in the given velocity ratio. The jets of circular and elliptical along flow form are caused close in the magnitude of losses of thrust/rod. Consequently, in these conditions/modes is important not so much the form of initial jet cross-sectional area, as complete three-dimensional/space form of the jet which is formed in the carrying flow. while it is obtained by close of both jets, judging from the fact, that at a distance of five bores from the wing surface they give already approximately identical trace on the mesh of silk threads (Fig. 5).

The effect of the form of initial jet cross-sectional area (or the mutual location several jets) on aerodynamic wing characteristics depends substantially on relation to the area of initial jet cross-sectional area to wing area.

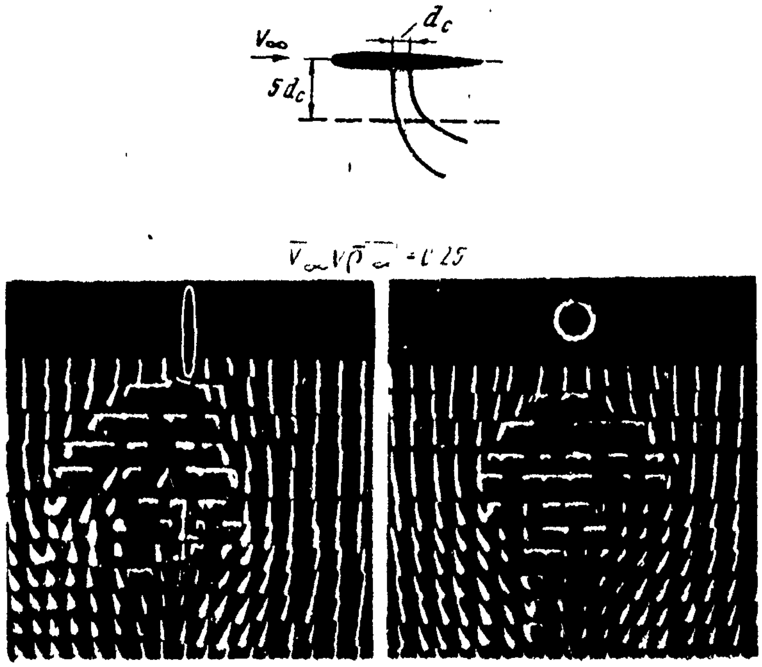

Fig. 5.

Page 41.

Thrust losses on the rectangular wing of small size/dimensions with the jets of elliptical across flow and circular shape $(F_c = 0{,}01)$ first increase with an increase in the giver velocity ratio, and then, after achieving the greatest value, they decrease also finally $\frac{\Delta Y}{P_c}$ it reverses the sign (Fig. 6). In this case, the increment of pitching moment reaches the significant magnitudes. Elliptical jet along flow on a small wing, as on large, are caused thrust losses which increase with the increase of the given velocity ratio.

A sharp qualitative change in the aerodynamic wing characteristics with to the jets of circular and elliptical across flow form, that occurs during the relative size decrease of wing, is connected with the fact that on a small rectangular wing the part of the zone of the essential disturbance/perturbations, caused by jets, proves to be out of the limits of wing. At certain value of the given ratio of the velocities when appear positive lift increments the prevailing value acquires the zone of the elevated pressure before the jet, while the rarefaction zone, which appears beyond jet, is located partially out of wing. the measurements of the distribution of pressures on the surface of the wing (for example, [6]) show that with an increase in the velocity of incident flow gradually is developed the zone of the backwater before the jet during the simultaneous decrease of size/dimensions and the shift downstream of rarefaction zone. Possibly, to the same manifests itself jet effect on the flow around suction side of wing.

during the size decrease of wing with elliptical along flow jet, these phenomena do not have the vital importance because of the special feature/peculiarities of the disturbance/perturbations, which appear during the flow around this jet, which it was discussed above.

Elliptical across flow jet (or the location of jets in a series across flow) has on a small rectangular wing essential advantages as compared with elliptical along flow jet (or arrangement of jets in a series along flow).

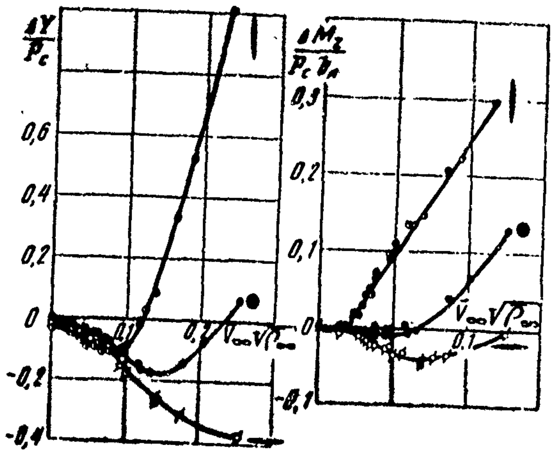

Fig. 5.

Page 42.

The considerably larger increment of pitching moment, obtained on wing with this jet, it allows in certain assigned/prescribed center-of-gravity location to displace elliptical across flow jet nearer to trailing wing edge and to obtain for this count supplementary advantages in comparison with elliptical along flow jet with sufficiently large values of the given velocity ratio.

A change in the form of jet or the layouts of jets on wing allows on the rectangular wings, which have close to real relation to the area of nozzle to wing area ($\bar{F}_c \approx 0{,}01$), not only it is substantial to decrease the thrust losses, but also to completely considerably increase the effective thrust/rod of jet. This will agree with the results of the investigation of the diverse variants of the location of nine jets on the rectangular wing, given in work [7].

The possibilities of using the zone of elevated pressure for decreasing the thrust losses on the wings of the limited size/dimensions depend on wing planform and the position of jets on wing. Thus, for instance, as a result of the special feature/peculiarities of the geometry of delta wing the positive action of the backwater, which appears before the jet, is not utilized, and the effect of diffluences prevails, determining a change in the total aerodynamic characteristics. Therefore on delta wing with relatively the front/leading position of jets elliptical across flow jet causes considerably larger thrust losses, than the jet of circular and elliptical along flow form. For the same reasons the shift of circular jet to leading wing edge causes an essential increase in the thrust losses at the high values of the given velocity ratio.

Thus, far from the earth/ground the external flow around jet is the important factor which determines a change in the aerodynamic wing characteristics with an increase in the velocity of incident flow. a change in the forms of jet or location of jets on wing makes it possible to decrease the harmful interference of wing and jet in the carrying flow.

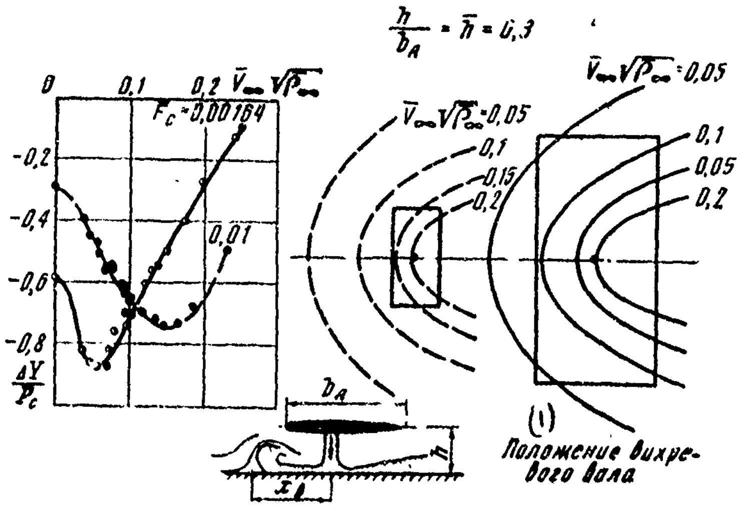

Fig. 7.

Key: (1). Position of vortex/eddy shaft.

Page 43.

The nearness of the earth/ground considerably complicates the picture of interaction of the jet of wing and is exerted a substantial influence on aerodynamic wing characteristics with jet. From the diversity of the factors, which determine the interference of wing and jet near the earth/ground, it is expedient to isolate three basic phenomena which consecutively can occur with an increase in the velocity of incident flow.

First, the formation/education of the accurate [fan] jet, which possesses considerably larger ejecting ability, than free jet, and the approach/approximation of wing to this perturbation source, the causing increase in the thrust losses. This effect is basic at velocity of incident flow, equal to zero, and it plays the significant role at comparatively low values of the given velocity ratio.

In the second place, the formation/education of the vortex/eddy shaft, which arises during braking of fan jet by the incident flow. The shift of shaft with an increase in the velocity of incident flow is brought, beginning with certain value of the given velocity ratio, to decrease in thrust losses, since before the shaft during its flow appears the zone of elevated pressure, while the sucking action of fan jet decreases as a result of its size decrease. If we compare the position of vortex/eddy shaft with change in losses of thrust/rod with an increase in the given velocity ratio, then it is not difficult to establish that the decrease in thrust losses begins when gain or less considerable portion of wing proves to be in the zone of the backwater before the shaft (Fig. 7). It is logical that with a decrease of the relative size/dimensions of wing or increase F_c the positive effect of vortex/eddy shaft is exhibited less considerably. This effect depends also on wing planform, the position of jet on wing and the angle of deflection of jet.

And finally thirdly, the usual proximity effect of the earth/ground, which becomes basic effect at sufficiently high velocity of incident flow, when the jet bends so, that the vortex/eddy shaft does not appear. As an example it is possible to give the results of the tests of the rectangular wing with elliptical across flow jet (Fig. 8).

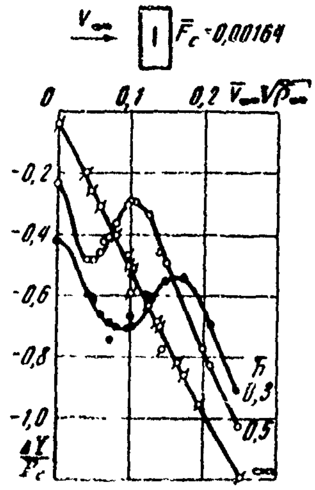

Fig. 8.

Page 44.

In the range of the low values of the given velocity ratio, are observed the same special feature/peculiarities of the course of dependence $\frac{\Delta Y}{P_c}(V_\infty \sqrt{\rho_\infty})$, as in the examined previously examples (losses first increase, they reach maximum and then they decrease). With further increase in the given ratio of the velocities reaches the minimum of thrust losses, connected with the liquidation of vortex/eddy shaft on the earth's surface. The value of the given velocity ratio, by which occurs the liquidation of vortex/eddy shaft, increases during the decrease of the relative distance of wing of the earth/ground.

Thus, the substantial change in the aerodynamic wing characteristics with jet near the earth/ground, which occurs with an increase in the velocity of incident flow, is connected with emergence, shift and finally by the liquidation of vortex/eddy shaft. The favorable effect of shaft can be used for decreasing the harmful interference of wing and jet near the earth/ground.

REFERENCES.

1. W. Seibold. untersuchungen uber die von Eubstrahlen an Senkrechtstarten erzeugten Sekundarkrafte. Jahrbuch 1962 der WGLR, 1963.

2. L. A. Wyatt. Static tests on ground-effect on planform fitted with a centrally-located round lifting jet. ARCCR, No. 749, 1962.

3. O. V. Yakovlevskiy, A. N. Sekundov. Study of interaction of jet with the closely spaced screens. Izv. of the AS USSR, ser. "Mechanics and Machine construction." No. 1, 1964.

4. G. I. Taganov. To the theory of the sucking action of jet in the cross flow. Transactions of TsAGI, iss. 1172, 1969.

5. I. B. Palatnik, D. I. Temirbayev. Laws governing the propagation of axisymmetric air jet in the carrying uniform flow. Problems of thermal-power engineering and applied of thermophysics, iss. 4, 1967.

6 Bradbury L. J. S., Wood M. N. Pressure distribution around a circular jet exhausting normally from a plane wall into an airstream. ARC CP, № 822, 1965.

7. Williams J., Wood M. N. Aerodynamic interference effects with jet-lift V/STOL aircraft under static and forwardspeed conditions ZFW, Hf № 7, 1967.

The manuscript entered 4/VII 1969.

Page 45.

DETERMINATION OF THE AMPLITUDE OF THE OSCILLATIONS OF AXISYMMETRIC SPACE VEHICLE WITH UNGUIDED LANDING IN THE ATMOSPHERE.

V. V. Voyeikov, V. A. Yaroshevskiy.

Are examined the special feature/peculiarities unguided motion of space vehicle about the center of mass with descent in the atmosphere. Primary attention is devoted to the determination of the possible amplitudes of oscillations and transverse overloads on landing trajectory at the low values of initial angular velocity. are given the formulas and the curve/graphs, which make it possible to determine the parameters indicated.

Is examined the task of the determination of the amplitude of the oscillations of the unguided space vehicle, entering in the atmosphere of planet. It is assumed that the vehicle is axially symmetrical body, angle of attack α is defined as angle between vectors of speed and the longitudinal axis of vehicle.

Work [1] shows, that the character of the motion of the unguided space vehicle about the center of mass is determined by the dimensionless parameter

$$\mu=\frac{2|\bar{N}_0|}{I\lambda V_0|\sin\theta_0|},$$

where $\bar{N}_0$ - initial moment of momentum in atmosphereless space; λ - the logarithmic gradient of atmospheric density $(\rho=\rho_0 e^{-\lambda H})$; I - axial moment inertia; V_0 and θ_0 - rate of entry and the angle of entry into the atmosphere.

At high values μ, the motion of vehicle is quasi-periodic in an entire trajectory, eliminating perhaps the section of small extent in the vicinity of the boundary of the atmosphere (in the case of plane motion - a section of transition from rotary motion to oscillatory). Therefore with μ>>1 the amplitude of the oscillations of vehicle on angle of attack α_m can be determined with the aid of asymptotic method or the method of averaging [2] - [5]. At the moderate values μ, commensurable with one, asymptotic method is applicable only in the sufficiently dense layers of the atmosphere. With small μ(μ<<1) low initial rotational energy of vehicle does not in practice affect its motion in the dense layers of the atmosphere. The determining parameter becomes the angle of attack of vehicle on the boundary of the atmosphere α_0, which, as a rule, is random variable. Therefore task acquires probabilistic character.

Page 46.

In the present work are given the results, which make it possible to determine a series of the parameters, which represent practical interest, in the case of small μ.

It is known that the axially symmetrical body in void completes motion of the type of regular precession. Let us determine initial boundary conditions of the atmosphere through angles ϕ_1, ϕ_2 and ϕ_3 (Fig. 1), the characterizing cone precessions and moment of momentum $\bar{K}_0$; ϕ_1 - angle between vectors of the speed of vehicle and the vector of initial moment of momentum (by axle/axis of cone) ϕ_2 - nutation angle (half-angle of the solution/opening of cone); ϕ_3 - precession angle of vehicle (position of the axle/axis of vehicle on the cone of the precession).

In sufficiently dense layers of the atmosphere where the oscillations in angle of attack are small, a change of the amplitude of oscillations is determined with the aid of asymptotic method [2] - [.] from the formula

$$\alpha_m = \frac{C\exp\left[\int\limits_{t_0}^{t}\left(\frac{m_z^{\bar{\omega}_z} qSl^2}{2IV} - \frac{c_y^{\alpha} qS}{2mV}\right)dt\right]}{\sqrt[4]{-\frac{m_z^{\alpha} qSl}{I}}}, \qquad (1)$$

where $m_z^{\bar{\omega}_z}$ - derivative of the coefficient of the damping moment in dimensionless angular velocity $\bar{\omega}_z = \frac{\omega_z l}{V}$; c_y^{α} and m_z^{α} - the derivatives of the lift coefficient and pitching moment in angle of attack α (all derivatives are calculated for α=0); S, l, m - characteristic area, length and the mass of vehicle; V - velocity; $q=\rho V^2/2$ - velocity head; C - constant.

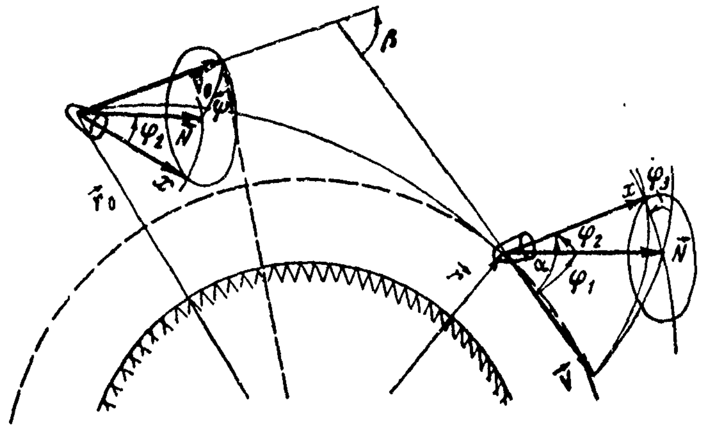

Fig. 1.

Page 47.

In the case of the large μ, when asymptotic method is applicable in an entire trajectory of descent [1], constant can be expressed directly through angles ϕ_1 and ϕ_2 and $|\bar{N}_0|$:

$$C = \begin{cases} C_1\left(\sin\frac{\varphi_1}{2} + \sin\frac{\varphi_2}{2}\right) & \text{при (1)} \quad \varphi_1 + \varphi_2 < \pi, \\ C_1\left(\cos\frac{\varphi_1}{2} + \cos\frac{\varphi_2}{2}\right) & \text{при (1)} \quad \varphi_1 + \varphi_2 > \pi, \end{cases} \qquad (2)$$

Key: (1). with.

where

$$C_1 = \sqrt{\frac{2\omega_{0\,э}}{\sin\varphi_2}} = \sqrt{\frac{|\bar{N}_0|}{I}}$$

($\omega_{0э}$ - an initial equatorial angular velocity).

In particular, for the plane motion when $\phi_1=\phi_2=\pi/2$,

$$C=2\sqrt{\omega_0}. \quad (3)$$

If parameter μ is low, then picture significantly changes. Let us examine for an example the plane motion when in atmosphereless space vehicle rotates in trajectory plane with constant angular velocity ω_0. Asymptotic method is inapplicable on the section of transition from rotary motion to oscillatory - in the vicinity of the boundary of the atmosphere. In this interval of motion, it is possible to consider that the velocity and the flight path angle virtually coincide with rate of entry V_0 and the angle of entrance θ_0) and to disregard damping effect (terms, proportional $m_z^{\omega_z}$ and c_y^{α}). Then equation of motion

$$\frac{d^2\alpha}{dt^2}=\frac{m_z(\alpha)qS}{I} \quad (4)$$

taking into account dependence $\rho=\rho_0 e^{-\lambda H}$ via substitution $x=\sqrt{-\frac{2m_z^{\alpha}\rho Sl}{I\lambda^2\sin^2\theta_0}}$ can be converted to the following form:

$$\frac{d^2\alpha}{dx^2}+\frac{1}{x}\frac{d\alpha}{dx}+h(\alpha)=0, \quad (5)$$

where $h(\alpha)=\frac{m_z(\alpha)}{m_z^{\alpha}}$ - the standardized/normalized moment characteristic $dh/d\alpha(0)=1$ (similar equation for the linear case was examined in work [6]).

Initial conditions can be fixed for the low value x_0 (low values ρ):

109

$$\alpha(x_0)=\alpha_0;\quad \frac{d\alpha}{dx}(x_0)=\frac{2\omega_0}{\lambda V_0|\sin\theta_0|}\,\frac{1}{x_0}=\frac{\mu}{x_0}.$$

With large x when the amplitude of the oscillations becomes small, it is possible to count that $b(\alpha)\approx\alpha$ and to present the solution of equation (5) through Bessel functions:

$$\alpha = C_1 I_0(x) + C_2 Y_0(x), \tag{6}$$

which have the following asymptotic representation:

$$I_0(x)=\sqrt{\frac{2}{\pi x}}\cos\left(x-\frac{\pi}{4}\right)\left[1+0\left(\frac{1}{x}\right)\right];$$

$$Y_0(x)=\sqrt{\frac{2}{\pi x}}\sin\left(x-\frac{\pi}{4}\right)\left[1+0\left(\frac{1}{x}\right)\right].$$

Page 48.

Hence it follows that amplitude of the angle of attack α_m with large x can be presented in the following form:

$$\alpha_m \approx \frac{\chi}{\sqrt[4]{2}\sqrt{x}}, \tag{7}$$

where χ a constant which depends on the initial conditions (α_0 and μ).

With a fixed μ function χ depending on α_0 (sufficient to examine range $-\pi<\alpha_0<\pi$) has with certain $\alpha_0=\alpha_{0*}$ the infinite peak, which corresponds to suspension of vehicle in the position of unstable equilibrium during transition from rotary motion to oscillatory. Since the initial value α_0 is more or less arbitrary, to conveniently present function χ depending on $\Delta\alpha_0=\alpha_0-\alpha_{0*}$.

Results of calculation according to equation (5) for purpose of the determination of function $\chi(\mu, \Delta\alpha_0)$ for the sinusoidal moment characteristic $h(\alpha)=\sin\alpha$ (sphere with eccentricity) are given to Fig. 2. With large μ function $\chi(\Delta\alpha_0)$ weakly depends on $\Delta\alpha_0$ (with the exception/elimination of vicinity $\Delta\alpha_0\approx0$). On the other hand, with $\mu\leq0.55$ the curves $\chi(\mu, \Delta\alpha_0)$ barely depend on value μ, especially in the most interesting range of low values $\Delta\alpha_0$.

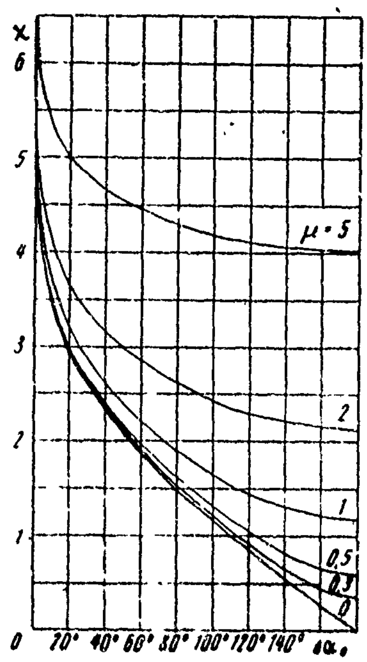

Fig. 2.

Page 49.

Consequently, with small μ there is no need for carrying out calculation for each value μ, and it suffices to be restricted to the one-parameter calculation of function $\chi(\Delta\alpha_0)$ at limit value $\mu=0(|\bar{v}_0|=0)$.

Comparing formulas (1) and (7) in the vicinity of the boundary of the atmosphere, it is not difficult to be convinced of their equivalency with an accuracy to the exponential term in (1) whose effect still is not exhibited in the vicinity of the boundary of the atmosphere, if we assume in (1)

$$C=\chi(\mu, \Delta\alpha_0)\sqrt{\frac{\lambda V_0|\sin\theta_0|}{2}}. \quad (8)$$

From formulas (3) and (8) it follows that with large μ

$$\chi\approx 2\sqrt{\mu}. \quad (9)$$

Let us examine in more detail the case $\mu=0$, replacing function $\chi(\mu, \Delta\alpha_0)$ on $\chi(\alpha_0)$, where $\alpha_0=\pi-\Delta\alpha_0$. Function $\chi(\alpha_0)$ depends on the form of the moment characteristic of function $h(\alpha)$.

The results of calculations for several types of moment characteristic are given to Fig. 3. As one would expect that the decrease of righting moment

in vicinity of $\alpha_0=180°$ leads to an increase of the maximum probable amplitudes, proportional to values χ in vicinity $\alpha_0=0$. It is real/actual, in these cases the conditions/mode of hovering lasts longer and vehicle is run up/turned to low angles of attack with large velocity heads, which leads to more intense oscillations.

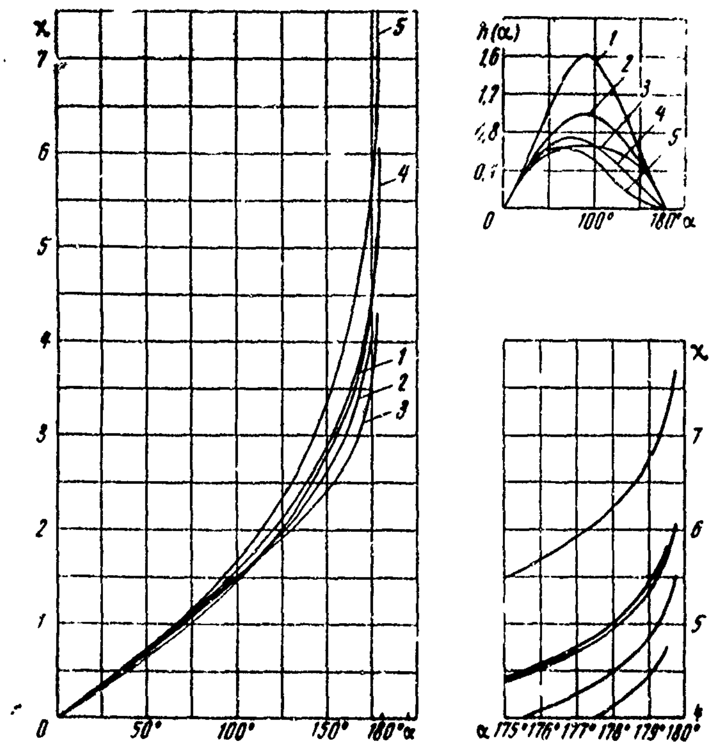

Fig. 3.

Page 90.

An increase "completeness" $[\int_0^\pi h(\alpha)\,d\alpha]$ of ascent characteristic also leads to the increase of the maximum probable amplitudes of oscillations.

Thus, with $\mu \ll 1$ it suffices to find the distribution of probable values α_0 on the boundary of the atmosphere. This derivation is valid both for a plane and for the spatial motion of vehicle about the center of mass. Since the action of vehicle in the extreme case with $\omega_{x0}=0$ is plane, the spatial motion of vehicle with $\mu \to 0$ becomes close to plane in the sense that the ratio of minimum solid angle of attack to maximum, undertaken for one oscillatory period, vanishes.

Let us examine the diverse variants of the distribution of the initial angles of attack axisymmetrical vehicle on the boundary of the atmosphere.

1. Plane motion: $\omega_{x0}=0,\ \varphi_1=\varphi_2=\frac{\pi}{2},\ \varphi_3=\alpha_0.$ In this case the values α_0 are equiprobable to:

$$p(\alpha_0)=\frac{1}{\pi},\quad P(\alpha_0<\alpha)=\frac{\alpha}{\pi}. \qquad (10)$$

2. All directions of initial moment of momentum in space are equiprobable. In this case not one of the 1 directions of vehicle in space it is preferred, if there is no correlation between values Φ_1 and Φ_2. It is hence not difficult to obtain:

$$p(\alpha_0)\quad \frac{1}{2}\sin\alpha_0,\quad P(\alpha_0<\alpha)=\frac{1-\cos\alpha}{2}. \qquad (11)$$

3. Let at torque/moment, which precedes isolation/evolution of descent vehicle from spacecraft, ship be stabilized on velocity vector and possesses very small or zero it is stabilized on velocity vector it possesses very small or zero angular velocity. After

isolation/evolution the axis of the symmetry of vehicle completes regular precession relative to axle/axis N; the position of this axle/axis can be described by angles ϕ_2 and ψ (see Fig. 1). Angle ψ can be considered equiprobable random variable in the range 0-2π (it suffices to be restricted to interval 0-π), it is determined by the angle between planes $(\bar{N}, \bar{V})$ and $(\bar{r}, \bar{V})$, where $\bar{r}$ - a vector of local vertical line.

For determination of angle ϕ_1 at the moment of entry into the atmosphere, it is possible to utilize the relationship/ratio

$$\cos\varphi_1 = \cos\beta\cos\varphi_2 + \sin\beta\sin\varphi_2\cos\psi, \quad (12)$$

where β - an angle between vectors of speed at the moment of isolation/evolution and at the moment of entry into the atmosphere (see Fig. 1).

Angle of attack the descent vehicle on boundary of the atmosphere α_0 is determined by formula

$$\cos\alpha_0 = \cos\varphi_1\cos\varphi_2 - \sin\varphi_1\sin\varphi_2\cos\varphi_3. \quad (13)$$

Knowing distributions $p(\phi_2)$ and $p(\psi) = \frac{1}{\pi}$, it is possible to find distribution $p(\phi_1)$. If $\varphi_2 = \frac{\pi}{2}(\omega_{x0} = 0)$, then ϕ_1=arccos(sinβcosψ)

$$p(\varphi_1)=\frac{1}{\pi}\frac{\sin\varphi_1}{\sqrt{\sin^2\beta-\cos^2\varphi_1}} \quad \text{при (1)} \quad |\cos\varphi_1|<|\sin\beta|;$$
$$p(\varphi_1)=0 \quad \text{при (1)} \quad |\cos\varphi_1|>|\sin\beta|. \qquad (14)$$

Key: (1). with.

Page 51.

Hence, taking into acccunt that $p(\phi_3)=1/2\pi$, $\cos\alpha_0=\sin\phi_1\cos\phi_3$, and calculating function distribution according to the distribution of arguments [7], we will obtain:

$$p(\alpha_0)=\frac{2}{\pi^2}K\left(\left|\frac{\sin\beta}{\sin\alpha_0}\right|\right) \quad \text{(1) при} \quad \left|\frac{\sin\beta}{\sin\alpha_0}\right|<1;$$
$$p(\alpha_0)=\frac{2}{\pi^2}\left|\frac{\sin\alpha_0}{\sin\beta}\right|K\left(\left|\frac{\sin\alpha_0}{\sin\beta}\right|\right) \quad \text{(1) при} \quad \left|\frac{\sin\beta}{\sin\alpha_0}\right|>1. \qquad (15)$$

Key: (1). with.

Here K(k) - complete elliptical integral of the first kind. It is interesting to note that with $\alpha_0=\beta$ and $\varphi_0=\pi-\beta$ the density of distribution $p(\alpha_0)$ goes to infinity. If $\omega_{x0}\neq 0$, it is necessary to consider distribution $p(\phi_2)$.

Let us assume that the initial angular velccity appears as a result of the effect of perturbaticn momentum/impulse/pulse $\bar{N}=(N_x N_y N_z)$ at the moment of isolation/evolution, so that $\omega_{x0}=\frac{N_x}{I_x}$, $\omega_{y0}=\frac{N_y}{I}$, $\omega_{z0}=\frac{N_z}{I}$, and the value of each pulse component is distributed according to normal law with dispersions σ_x^2 and $\sigma_y^2=\sigma_z^2=\sigma^2$.

Then

$$p(N_x)=\frac{1}{\sigma_x}\sqrt{\frac{2}{\pi}}e^{-\frac{N_x^2}{2\sigma_x^2}};$$
$$p(N_э)=\frac{N_э}{\sigma^2}e^{-\frac{N_э^2}{2\sigma^2}}, \qquad (16)$$

where $N_э=\sqrt{N_y^2+N_z^2}$ - equatorial momentum/impulse/pulse.

Since $\frac{N_э}{N_x}=\operatorname{tg}\varphi_2$, $\overset{(1)}{\text{ТО}}$ $p(\varphi_2)=p\left(\operatorname{arctg}\frac{N_э}{N_x}\right)$.

Key: (1). then.

Calculating function distribution according to the distributions of arguments, we will obtain:

$$p(\varphi_2)=-\frac{d}{d\varphi_2}\left(\frac{1}{\sqrt{1+\left(\frac{\sigma_x}{\sigma}\operatorname{tg}\varphi_2\right)^2}}\right),$$
$$P(\varphi_2<\varphi)=1-\frac{1}{\sqrt{1+\left(\frac{\sigma_x}{\sigma}\operatorname{tg}\varphi\right)^2}}. \qquad (17)$$

Since with the aid of relationship/ratios (12) and (13) it is possible to express the value α_0 in terms of the value of the angles φ_2, ψ and φ_3 whose distributions are known, it is possible to calculate the distributions of probabilities p (α_0) and the integral probabilities P ($\alpha_0<\alpha$) for the different values of the angle β and of parameter $\Omega=\frac{\sigma_x}{\sigma}$. The results of numerical calculations are given to

Fig. 8-7. Let us note that with an increase in the parameter Ω, beginning from zero, the peak of function p (α_0) with $\alpha_0=\pi-\beta$ disappears, but another peak with $\alpha_0=\beta$ grow/rises.

Page 52.

With $\beta>\pi/2$ values p (α_0) in vicinity $\alpha_0=\pi$ grow/rise at first, which indicates an increase in the probability of appearing the conditions/modes of hovering, while with further increase Ω, all values α_0 are confined to angle β, distribution p (α_0) degenerates into delta function δ ($\alpha_0-\beta$) and values p (α_0) with $\alpha_0\neq\beta$, including in vicinity $\alpha_0=\pi$, they vanish. It is necessary to note that with that fix/recorded Ω

$$p(\alpha_0,\beta)=p(\pi-\alpha_0,\ \pi-\beta),$$
$$P(\alpha,\beta)=1-P(\pi-\alpha,\ \pi-\beta),$$

therefore are given the results only fo $\beta>\pi/2$.

Let us determine the amplitude of the oscillations of angle of attack α_m and maximum transverse overload $n_{n\,max}$ with the aid of formulas (1) and (8). Being limited to the case $\mu\to0$, we will obtain:

$$\alpha_m\approx\frac{\sqrt{\frac{\lambda V_0|\sin\theta_0|}{2}}}{\sqrt[4]{-\frac{m_z^\alpha qSl}{I}}}\chi(\alpha_0)\exp\int_{t_0}^{t}\left(\frac{m_z^{\bar\omega_z}qSl^2}{2IV}-\frac{c_y^\alpha qS}{2mV}\right)dt. \quad (18)$$

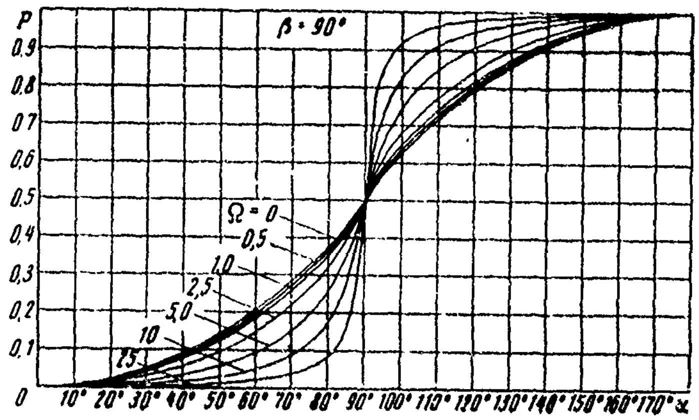

Fig. 4.

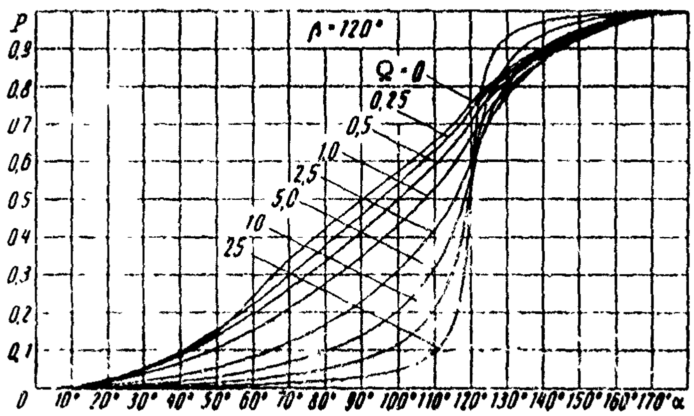

Fig. 5.

Page 53.

If we make an assumption $|\sin\theta| \ll n_r$, then last/latter factor is simplified:

$$\alpha_m \approx \sqrt[4]{\frac{I\lambda^2 \sin^2\theta_0}{-2m_z^\alpha \rho S l}}\,\chi(\alpha_0)\left(\frac{V}{V_0}\right)^{\frac{1}{2}\left(\frac{c_y^\alpha}{c_x} - \frac{m_z^{\bar{\omega}_z}}{c_x i_9} - 1\right)}, \qquad (19)$$

where $I_1 = \frac{I}{ml^2}$.

Having a dependence of density on velocity, it is possible to determine the law of amplitude change along the trajectory of descent.

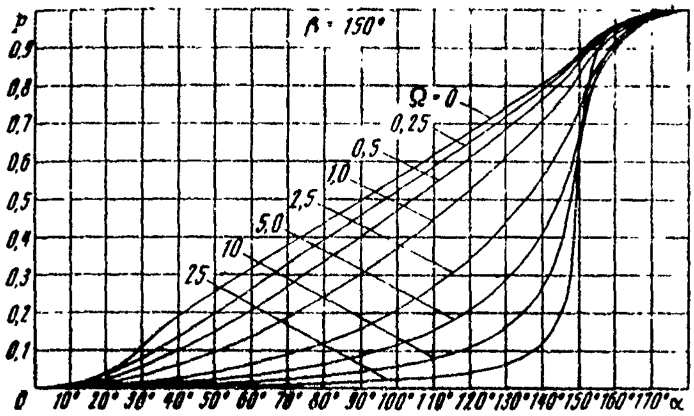

Fig. 6.

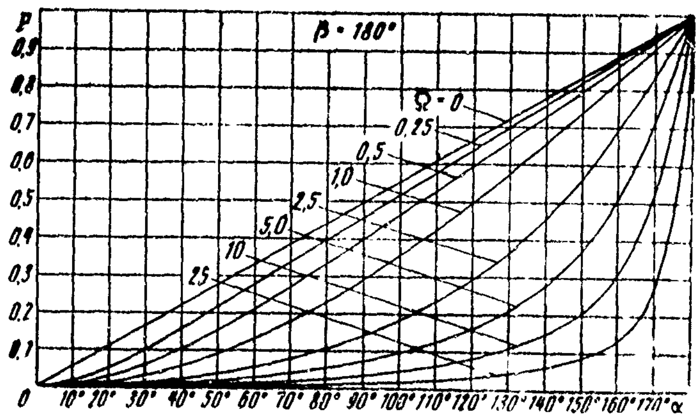

Fig. 7.

Page 54.

If we consider that θ=const (this assumption it is fulfilled with large θ), $\rho=\rho_0 e^{-\lambda H}$, then on the basis [8]

$$V \approx V_0 \exp\left[-\frac{c_x S \rho}{2m\lambda\,|\sin\theta|}\right], \qquad (20)$$

whence it follows that

$$\alpha_m \approx \sqrt{\frac{I\lambda^2 \sin^2\theta}{-2m_z^\alpha \rho S l}}\,\chi(\alpha_0)\exp\left[\frac{\rho S\left(-c_y^\alpha + c_x + \frac{m_z^{\bar{\omega}_z}}{i_z}\right)}{4m\lambda\,|\sin\theta|}\right]. \qquad (21)$$

maximum transverse overload $n_n = \frac{|c_n^\alpha|\,\alpha_m\, qS}{mg_3}$ is determined by the formula

$$n_{n\,max} = \frac{\chi(\alpha_0)}{2^{3/4} e^{3/4}} \frac{c_n^\alpha}{\left(c_x + \frac{c_y^\alpha}{3} - \frac{m_z^{\omega_z}}{3i_3}\right)^{3/4} (-m_z^\alpha)^{1/4}} \frac{V_0^2 \lambda^{1/4} |\sin\theta|^{1/4}}{g_3} \frac{I^{1/4}}{(ml)^{1/4}}. \qquad (22)$$

Here g_3 - terrestrial acceleration of gravity in units of which overload is measured.

The separate groups of factors characterizes the effect of the aerodynamic characteristics of vehicle.

In conclusion let us note that the boundary of the atmosphere H_1, from which begins the noticeable effect of aerodynamic moments on motion about the center of mass, is arrange/located above the boundary of the atmosphere H_2, beginning with which the trajectory of vehicle it differs from Keplerian. It is real/actual, height/altitude

H_2 can be determined with the aid of relationship/ratio (20) from the condition that the velocity decreases in comparison with the rate of entry, for example, by 0.1o/o:

$$\rho(H_2)=\frac{\lambda m|\sin\theta|}{500c_x S}. \qquad (23)$$

Height/altitude H_1 can be determined when the initial value of angle of attack decreases, for example, by 1o/o. In accordance with formula (6) with $\mu=0$ for small α is valid to the formula

$$\alpha=\alpha_0 I_0(x)\approx\alpha_0\left(1-\frac{x^2}{4}\right).$$

Hence

$$\rho(H_1)=\frac{I\lambda^2\sin^2\theta}{50|m_z^\alpha|Sl}; \qquad (24)$$

$$H_1-H_2=\frac{1}{\lambda}\ln\frac{\rho(H_2)}{\rho(H_1)}=\frac{1}{\lambda}\ln\frac{ml|m_z^\alpha|}{10I\lambda|\sin\theta|c_x}. \qquad (25)$$

Difference H_1-H_2 can reach several ten kilometers. Let us note that the angle of entry into the atmosphere θ_0 in formula (18) should be calculated precisely for height/altitude H_1.

The authors express appreciation to A. I. Kur'yanov after aid in the formulation of the problem and valuable observations according to the results of work.

Page 55.

REFERENCES.

1. G. E. Kuzmak, V. A. Yaroshevsky. Application of the asymptotic methods to some problems of the re-entry vehicles dynamics. Proceedings of the XIV International Astronautical Congress, Paris, 1963, p 273-291.

2. G. E. Kuzmak. Asymptotic solutions of some nonlinear differential second order equations with variable coefficients. Work III All-Union math. congress/descent, Vol. 1, the publishing house of the AS USSR, 1956.

3. V. M. Volosov. Differential equations of motion, which contain the parameter of slowness. DAN of the USSR, 1956, Vol. 106, No. 1, page 7-10.

4. G. E. Kuzmak. To a question concerning the spatial motion of axisymmetric solid body about fixed point under the effect of the torque/moments, which are slowly changed in time. DAN, 1960, Vol. 132, No. 3, page 549-552.

5. V. A. Yaroshevskiy. Application/use of an asymptotic method

to some tasks of the dynamics of flight vehicles. Engineering journal, 1962, Vol. 2, No. 2.

6. Kh. Allen. Hypersonic flights and the problem of return. Coll. of the "problem of the motion of the nose cone of long-range", 1958.

7. E. S. Venttsel'. Probability theory. Fizmatgiz, 1958.

8. H. J. Allen, A. T. Eggers. A study of the motion and aerodynamic heating of ballistic missiles entering the earth's atmosphere at high supersonic speeds, NACA Report 1381, 1958.

The manuscript entered 8/VII 1969.

STUDY OF TRAJECTORIES OF THE SPACECRAFT LAUNCHED FROM THE SURFACE OF THE MOON AND REENTERING THE ATMOSPHERE OF THE EARTH.

V. V. Demishkin, V. A. Il'in.

Page 56.

The study of trajectories space equipment, that starts from the surface of the moon and returning in the atmosphere of the Earth, is conducted with the aid of the approximation method by which they disregard the size/dimensions of the sphere of influence of the moon in comparison with distance an Earth-moon during the calculation of geocentric section, they replace the proper motion of the moon by motion along circular Keplerian orbit, is not considered a change in the vector of the orbital speed of the moon for the time of the selenospherical motion of vehicle and the extent of active section with start from the surface of the moon.

Is briefly examined the schematic of performance calculation of the geocentric and selenospherical section of vehicle. Are establish/installed the properties of the invariance of the parameters of trajectory with respect to the replacement of nonapogean geocentric flight/passage of moon-Earth, apogean and vice versa, also, to the representation of trajectory relative to the plane lunar orbit. Are given the results of the calculations of the required rates at the end of the active section and areas on the surface of the moons, from which is feasible the output to the assigned/prescribed flight trajectory to the Earth. Are given the estimations of geographic latitudes of landing spot during approach from the side of the North Pole for trajectories with single immersion into the atmosphere.

§1. Formulation of the problem. Basic assumptions. Set-up of the solution of problem.

Let us examine following task. Space vehicle (Fig. 1), which is located in the given point on the surface of the moon (point O), starts and completes passive flight/passage to the sphere of influence of the moon (point 1). After leaving the sphere of influence of the moon, vehicle completes passive flight/passage to the Earth so that the perigee of the orbit of return (conditional perigee) is arrange/located in the dense layers of the Earth's atmosphere on the assigned/prescribed distance from the surface of the Earth (point 2).

The trajectory of flight/passage moon-Earth must satisfy a series of the limitations, basic from which they are: the assigned/prescribed inclination of the plane of flight/passage to equatorial plane i; the selected latitude of conditional perigee φ_{κ}; assigned/prescribed power engineering of booster stages of vehicle - rate V_{c0} at the end of the active section with start from the surface of the moon, limitation from above the duration of flight/passage moon-Earth t_{62}; the realization of time/temporary rating, i.e., the selection of this torque/moment of start from the surface of the moon and such duration of flight/passage moon-Earth, with which the return to the Earth would be realize/accomplished at the moment of time, convenient for landing/fitting of vehicle at the given point of the surface of the Earth.

Page 67.

Stated problem represents by itself the very complex two-point boundary-value problem whose numerical solution by the procedure of spheres of influence [1], [2] or by more precise methods is connected with the overcoming of the considerable difficulties, caused in essence by the need for knowing certain solution of problem, sufficiently close to unknown. For approximate solution of task, let us assume:

- the effect of the moon on vehicle it is limited to the limits of its sphere of influence;

- during the calculation of the geocentric trajectory phase it is possible all the geocentric and selenospherical parameters on the sphere of influence of the moon to replace by the appropriate parameters, calculated in the center of attracting moon;

- the moon moves on circular Keplerian orbit; the vector of the orbital speed of moon $\vec{V}_{\pi}$ for the time of the motion of vehicle in selenosphere is considered constant/invariable;

- the extent of active section with the start of vehicle from the surface of the moon can be disregarded.

Comparing given formulation of the problem with the formulation of the problem in [3], we note that the problem under consideration can be solved in accordance with the scheme presented in [3] and with the use of the results obtained there:

- regardless of the seleno centric motion according to the procedure [4], [5] are determined attitude sensing of the plane of geocentric flight/passage moon-Earth and the parameters of this flight/passage from the condition of tangential return in the atmosphere of the Earth, as a result of which is located the vector of selenospherical speed of vehicle $\vec{V}_{c1}$ in exit point on selenosphere;

... is determined according to the procedure of work [3] the selenospherical hyperbola of vehicle, passing through the given point on the surface of the moon and which ensures on selenosphere to vehicle rate $\vec{V}_{c1}$.

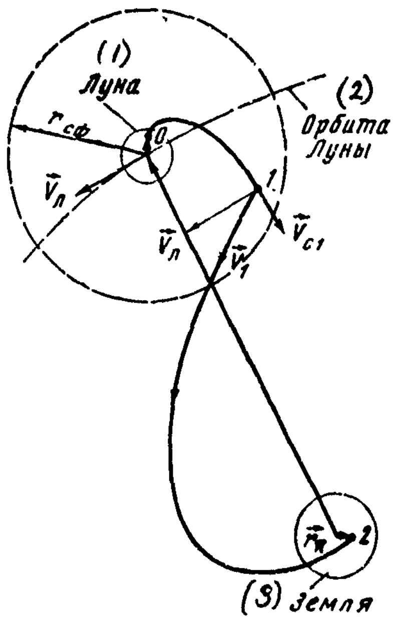

Fig. 1.

Key: (1). Moon. (2). Orbit of moon. (3). Earth.

Page 58.

With the synthesis of trajectories moon-Earth are considered all the formulated above limitations with the exception/elimination of the requirement of time/temporary mating. Let us note that, as in [5], a question concerning time/temporary mating here is not examined, since, in the first place, for its account is required the more precise trajectory calculation and, in the second place, this mating does not in practice affect the characteristics of the trajectories of flight/passage moon-Earth.

Taking into account the uniform character of stated problem and task of the synthesis of the trajectories of the flight around of the moon [4], and also the first three assumptions, it is possible on the basis of the given in [4], [5] results of comparative trajectory calculations of the flight around of the moon employing the approximate procedure and the procedure of spheres of influence (radius of the sphere of influence of moon $r_{c\phi}$ is final) to confirm that in the task in question the parameters of approximate solution must be coordinated well with the parameters of the corresponding solution, obtained according to the procedure of spheres of influence. As concerns last/latter assumption, on the basis of the numerous calculations of the powered flight trajectories of rockets it is possible to confirm that the disregard of their extent does not lead to any noticeable error.

§2. Geocentric and selenospherical the trajectory phases.

For determining the orientation of the plane of flight/passage, moon-Earth and the positions of the radius-vector of vehicle in this plane are assigned the inclination of the plane of the orbit of the moon to equatorial plane $i_{Л}$, the argument of the latitude of the moon $u_{Л}$, i, angular stage distance moon-Earth $\Delta\eta_{12}$ and direction of the motion of vehicle during approach to the Earth with respect to the hemispheres of the Earth. As a result are located the arguments of the latitude of vehicle u_1 and u_2 at points 1 and 2; angle α_1 between the plane of the orbit of the moon and the plane of flight passage moon-Earth $\alpha_1 > 0$, if the shortest rotation from the transversal component of the vector of the geocentric speed of vehicle $\vec{V}_{1t}$ in point 1 to $\vec{V}_{\pi}$ is visible in direction from the Earth to the moon that occur counterclockwise, and also φ_{κ}.

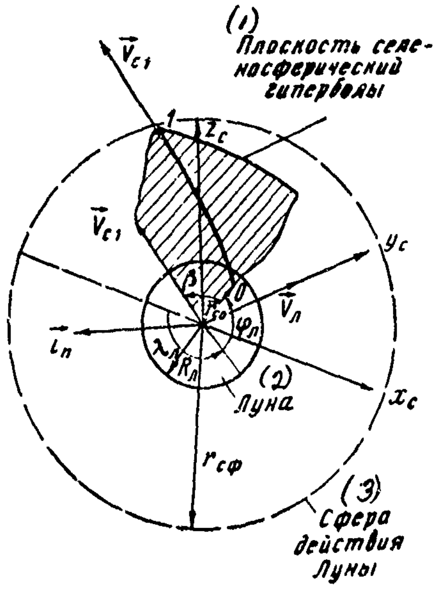

Fig. 2.

Key: (1). Plane selenospherical hyper-oxen. (2). Moon. (3). Sphere of influence of moon.

Page 59.

The direction of the action of vehicle with respect to the hemispheres of the Earth is characterized by parameter sgncos u_1: with sgncos u_1=+1 flight/passage moon-Earth occurs through the Northern Hemisphere, and with sgncos u_1=-1 - through the Southern Hemisphere. During the calculation of the dynamic parameters, the trajectory of flight/passage moon-Earth is considered as arc of conic section in the specific above plane with perigee radius-vector $\vec{r}_\pi$, passing through the radius-vector of moon $\vec{r}_Л(\vec{r}_к, \vec{r}_Л)=\Delta\eta_{12}$. Assigning values $r_к, r_Л$ and $\Delta\eta_{12}$, we determine all parameters of this flight/passage. The results of the calculations of the parameters of the geocentric section of flight/passage moon-Earth are given in [5].

Let us introduce the rectangular right system of selenocentric coordinates $x_c\, y_c\, z_c$ (Fig. 2): axis $+x_c$ is the continuation of vector $\vec{r}_Л$, axis $+y_c$ it coincides with vector $\vec{V}_Л$. Let us introduce also the spherical selenocentric system of coordinates $r_c, \lambda_c, \varphi_c$ (r_c— selenocentric radial distance, longitude $+\lambda_c$ is counted off in plane $x_c y_c$ from line an Earth-moon counterclockwise, if we look from axle/axis $+z_c$; latitude $+\varphi_c$— from plane $x_c y_c$ to the side $z_c>0$). When λ_c, φ_c is determined the position of point on the surface of the moon, we designate them through $\lambda_Л, \varphi_Л$.

The position of vehicle on the surface of the moon (point 0) is assigned by vector $\vec{r}_{c0}=\{-R_Л\cos\varphi_Л\cos\lambda_Л, -R\cos\varphi_Л\sin\lambda_Л, R_Л\sin\varphi_Л\}$, where $R_Л$— the mean radius of the moon.

On selenosphere $|\vec{r}_c|=r_{cф}$ is assigned/prescribed freely moved on it vector $\vec{V}_{c1}=\vec{V}_1-\vec{V}_Л$, where $\vec{V}_1$— the vector of the geocentric speed of vehicle in point 1. In projections on axle/axis x_c, y_c, z_c $\vec{V}_{c1}$ it has the components

$$\vec{V}_{c1}=\{V_{1r}, V_{1t}\cos\alpha_1-V_Л; V_{1t}\sin\alpha_1\}. \quad (1)$$

Here always $V_{1t}>0$, But radial component of geocentric rate $V_{1r}<0$ for the geocentric route A, which does not contain apogee ($\Delta\eta_{12}<180°$); $V_{1r}>0$ for the geocentric route C, which contains apogee ($\Delta\eta_{12}>180°$); $V_{1r}=0$ for geocentric Hohmann flight/passage ($\Delta\eta_{12}=180°$).

The task of the calculation of selenospherical motion is reduced to the construction of selenospherical motion it is reduced to the construction of the selenospherical hyperbola, passing through vector $\vec{r}_{c0}$ and by that ensuring to vehicle on selenosphere the achievement of vector $\vec{V}_{c1}$. Let us introduce the unit vector

$$\vec{i}_n=\frac{[\vec{r}_{c0}, \vec{V}_{c1}]}{|[\vec{r}_{c0}, \vec{V}_{c1}]|}, \quad (2)$$

normal to the plane of hyperbola. From the side of unit vector $\vec{i}_n$ the rotation from $\vec{r}_{c0}$ and $\vec{V}_{c1}$ to the shortest angle β is visible that occur counterclockwise:

$$\cos\beta=\frac{(\vec{r}_{c0}, \vec{V}_{c1})}{R_{Л} V_{c1}}. \quad (3)$$

Page 60.

In [3], it is shown, that if we consider $\vec{V}_{c1}$ directed along the asymptote of hyperbola, then with an accuracy to small $\left(\frac{r_{\pi c}}{r_{c\Phi}}\right)^2$, where $r_{\pi c}\leqslant R_{Л}$ — selenocentric distance of the pericenter of hyperbola, we have:

the focal parameter of the hyperbola

$$p_c = R_л \left[\sqrt{\frac{1}{4}\frac{R_л}{a_c}\sin^2\beta + 1 - \cos\beta} + \frac{1}{2}\sqrt{\frac{R_л}{a_c}\sin\beta} \right]^2, \quad (4)$$

eccentricity of the hyperbola

$$e_c = \sqrt{\frac{p_c}{a_c} + 1}. \quad (5)$$

Here $a_c = \dfrac{1}{\dfrac{V_{c1}^2}{K_л} - \dfrac{2}{r_{cф}}}$ – the assigned/prescribed real semi-axis of hyperbola; $K_л$ – the gravitational constant of the moon. the orientation of hyperbola is assigned by unit vector (2) and by the directed to pericenter unit vector

$$\vec{l}_к = \mu \frac{\vec{r}_{c0}}{r_{c0}} + \nu \frac{\vec{V}_{c1}}{V_{c1}},$$

where $$\mu = \frac{\cos\eta_{c0} + \dfrac{1}{e_c}\cos\beta}{\sin^2\beta}, \quad \nu = -\frac{\dfrac{1}{e_c} + \cos\beta\cos\eta_{c0}}{\sin^2\beta}.$$

Here η_{c0} — the true anomaly of point of start on the surface of the moon in the plane of hyperbola. Angle β varies within the limits $0 \leqslant \beta \leqslant \bar{\beta} < \pi$, where

$$\cos\bar{\beta} = -\frac{1}{1+\frac{R_Л}{a_c}}. \qquad (6)$$

With $\beta=\bar{\beta}$ the launching point from the surface of the moon is pericenter of hyperbola, with $\beta=0$ we have vertical climb in selenosphere.

In connection with flight/passages moon-Earth with start from the surface of the moon let us establish/install the properties of the invariance of the characteristics of selenospherical motion, analogous to the properties of the trajectories of the flight around of the moon [5] and of the start with orbit of ISL [3].

During the replacement of the nonapogean route A by apogean C or vice versa in $\vec{V}_{c1}$ [see (1)] reverses the sign 1st component V_{1r}. Let us change the coordinates of launching point $\vec{r}_{c0}$ so that relative to the new launching points and vector $\vec{V}_{c1}$ motion along hyperbola would remain constant/invariable. For this is sufficient invariability cos β. But then from (3) it follows that in $\vec{r}_{c0}$ must change sign the 1st component. Vectors $\vec{i}_x$ and $\vec{i}_n$ are replaced on

$\vec{i}_к(-++)$, $\vec{i}_п(+--)$; here, also, subsequently by sign "+" are designated the constant/invariable cell/elements of vectors, and by sign "-" the cell/elements, which change sign. Thus, of vectors $\vec{r}_{c0}$ and $\vec{i}_к$ longitudes $\lambda_Л, \lambda_{кс}$ are replaced on $\pi-\lambda_Л, \pi-\lambda_{кс}$, of vector $\vec{i}_п$ longitude $\lambda_{пс}$ is replaced on $2\pi-\lambda_{пс}$, and latitude $\varphi_{пс}$ — on $-\varphi_{пс}$.

Page 81.

With the representation of geocentric trajectory relative to the plane of the orbit of the moon, which is equivalent to change signcos u_1, $y\vec{V}_{c1}$ [see (1)], reverses the sign 3rd component $V_1, \sin\alpha_1$. Analogously it is possible to show that the motion of vehicle in the plane of hyperbola will remain constant, if we replace $\vec{r}_{c0}$ by $\vec{r}_{c0}(++-)$, $\vec{i}_к$ by $\vec{i}_r(++-)$ and $\vec{i}_п$ by $\vec{i}_п(--+)$, vectors r_{c0} and $\vec{i}_к$ $\varphi_Л$ and $\varphi_к$ they are replaced on $-\varphi_Л, -\varphi_{кс}$, and in vector. $\vec{i}_п$ $\lambda_{пс}$ it is replaced on $\pi+\lambda_{пс}$.

§3. Results of calculations of trajectory of surface moon-atmosphere of the Earth.

Calculation was performed for the following initial data: $r_Л=r_{Л\,ср}=384\,394,8$ km, $i_Л=28°$ (1969-1972), $r_к=6421$ km, i=90°, the mean radius km of 6371 Earth, the gravitational constant

$K_{\oplus}=398580$ Earth km³/s², $R_Л=1738$ km, $K_Л=4889$ km³/s², $r_{сф}=66000$ km. The basic varied parameters they were $u_Л$, $\Delta\eta_{12}$, β and $\lambda_Л$. Are taken into account the following special feature/peculiarities of the motion of vehicle in the setting in question (see [3], [5] and §2):

1) the parity of all values on $u_Л$ relative to value $u_Л=180°$;

2. "rule of recalculation" [5] and invariance of characteristics of the selenospherical motion of vehicle, in accordance with which during change sgncosu, (for $i_Л<i<\pi-i_Л$) $u_Л$ it is replaced on $u_Л+180°$, α_1, φ_* and $\varphi_Л$ they reverse signs; parameters of hyperbola in its plane are not changed.

3) the symmetry of selenospherical characteristics on $\Delta\tau_{12}$ relative to value $\Delta\tau_{12}=180°$, in accordance with which during transition that of route A to route C and vice versa $\lambda_Л$ is replaced on $180°-\lambda_Л$, and $\varphi_Л$ and all parameters of hyperbola in its plane remain constant/invariable.

Velocity at the end of active section V_{c0} does not depend on the location of launching point on the surface of the moon. Since $V_{1t}\ll V_Л$, from (1) follows very weak dependence V_{c1}, V_{c0} and the parameters of selenospherical motion on $i_Л$, $u_Л$ and i (Fig. 3). Thus, the parameters of selenospherical action are determined in by basic value $\Delta\eta_{12}$ and by the coordinates of launching point $\lambda_л, \varphi_л$. It is virtually important that V_{c0} unlike V_{c1} weakly depends also on $\Delta\eta_{12}$. As a result, disposing of small supply in the momentum/impulse/pulse of velocity 300-400 m/s in comparison with min min $V_{c0} \approx 2510$ m/s, it is possible, changing orientation $\vec{V}_{c0}$, to realize start to the Earth from different points of the surface of the moon along essentially different trajectories moon-Earth.

In the case of vertical climb in selenosphere, vectors $\vec{r}_{c0}$ and $\vec{V}_{c1}$ are collinear, whence taking into account $V_{1t} \ll V_л$ we obtain:

$$\operatorname{tg} \lambda_{л\,верт} \approx -\frac{V_л}{V_{1r}}, \quad \max \operatorname{tg} |\varphi_л|_{верт} \approx \frac{V_{1t}}{V_л},$$
$$\operatorname{sgn} \varphi_{л\,верт} = \operatorname{sgn} \cos u_1.$$

Hence it follows that the trajectories moon-Earth with vertical climb in selenosphere can be realized from very narrow area on the surface of the moon when $0 < \lambda_л < \pi$, $|\varphi_л| \leqslant 10^\circ,5$.

Page 62.

In order to rate/estimate the maximum sizes of area on the surface of the moon, from which is feasible the output to the predetermined trajectory of flight/passage moon-Earth, let us examine trajectories with tangent to surface the moon by start at limiting values $\beta=\bar{\beta}$. From given to Fig. 4 dependences $\beta=\bar{\beta}(i_Л, u_Л, i, \Delta\eta_{12})$, calculated on (6) it is apparent that with increase V_{c1} $\bar{\beta}$ it decreases.

When $V_{c1}\to\infty$ $\bar{\beta}\to\frac{\pi}{2}$; $\max_{\{u_Л, \Delta\eta_{12}\}}\bar{\beta}(i_Л=28°, i=90°)\approx 142°$.

The locus of start with $\beta=\bar{\beta}$ represents the intersection of plane with normal vector $\vec{V}_{c1}$ with the sphere of radius $R_Л$; the results of the calculation of boundary curves are given to Fig. 5 (change $\lambda_Л$ during transition from route A to C is taken into account by the marking of axle/axis). From geometric considerations it is clear that

$$\varphi_{Л\,max}=-\varphi_{Л\,верт}+(\pi-\bar{\beta}),\quad \varphi_{Л\,min}=-\varphi_{Л\,верт}-(\pi-\bar{\beta}),$$
$$\lambda_{Л\,max}\approx\lambda_{Л\,верт}-\bar{\beta},\quad \lambda_{Л\,min}\approx\lambda_{Л\,верт}+\bar{\beta}.$$

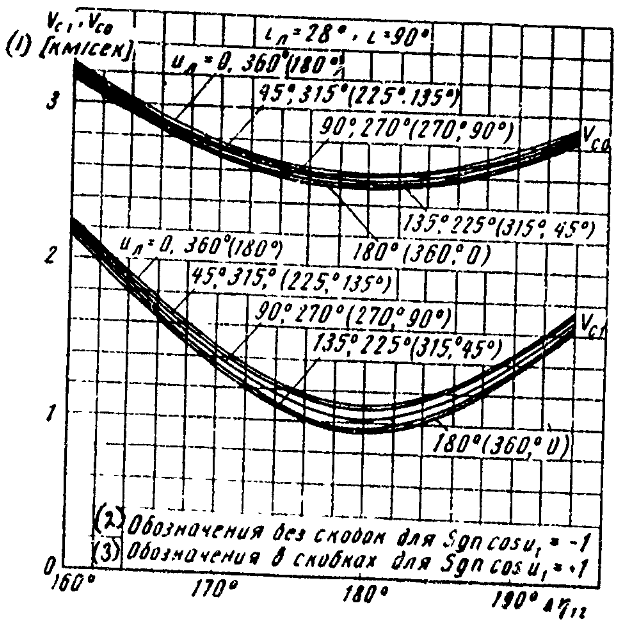

Fig. 3.

Key: (1). [km/s]. (2). Designations without brackets for sgn cos u_1=1. (3). Designations in brackets for sgn cos u_1=1.

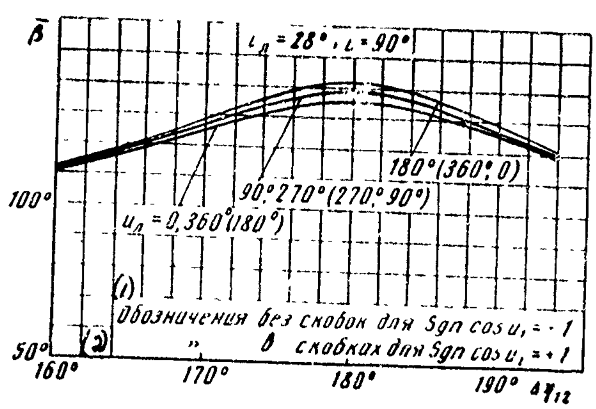

Fig. 4.

Key: (1). Designations without brackets for sgn cos u_1=1. (2). Designations in brackets for sgn cos u_1=1.

Page 63.

From the points of lunar surface, which fall inside ovals Fig. 5, the start to the Earth with given ones $i_Л$, $u_Л$, i, $\Delta\eta_{12}$ and sgncos u_2 is impossible. With increase V_{c0} the area of possible launching points from the surface of the moon decreases and is confined to vector $\vec{V}_{c1}$. With $V_{c0} \leqslant 3250$ m/s is always feasible the start to the Earth for any $\varphi_Л$ when $43° < \lambda_Л < 137°$, for any $\lambda_Л$ when $\varphi_Л > 73°$, $\varphi_Л < -65$ in the case sgn cos u_1=-1; $\varphi_Л > 65°$; $\varphi_Л < -73°$ in the case sgn cos u_1=1. Thus, the use of trajectories with inclined lift in selenosphere significantly expands the area on lunar surface, whence is feasible output to assigned/prescribed trajectory of flight to the Earth.

During the approach of vehicle to the Earth from the side of the North Pole and realization of the trajectory of landing/fitting vehicle with single immersion into the atmosphere, they can be of interest of the value of geographic latitudes of the points of landing/fitting $\varphi_\oplus$. Range angle from the point of conditional perigee to the point of landing/fitting vehicle which with i=90° is equal to a difference in geographic latitudes of the point of landing/fitting and conditional perigee $\Delta\phi$, depends on the value of the maximum overload of vehicle n_Σ. In the case of the ballistic trajectories of descent at values $n_\Sigma \leqslant 20$ dependence $\Delta\varphi = \Delta\varphi(n_\Sigma)$ can be obtained with the aid of data given in [6]. At values $n_\Sigma \gg 10$, but such, that still it is possible to set/assume $\sin\theta_{вх} \approx \theta_{вх}$, where $\theta_{вх}$ — the angle of the entry into atmosphere, from relationship/ratios $\Delta\varphi \approx 2\theta_{вх}$ [6] and $n_\Sigma = 340\theta_{вх}$ [7] we will obtain $\Delta\varphi \approx \frac{n_\Sigma}{170}$ [rad]. Utilizing dependences $\varphi_к(i_Н, u_Н, l, \text{sgn}\cos u_1 = 1, \Delta\eta_{(1)})$ from [5] and $\Delta\varphi(n_\Sigma)$, it is possible to obtain the dependence of the latitude of the point of landing/fitting $\varphi_\oplus$ on V_{c0} and n_Σ with given ones $i_Н$, $u_Н$, l. The example of this dependence is given to Fig. 6.

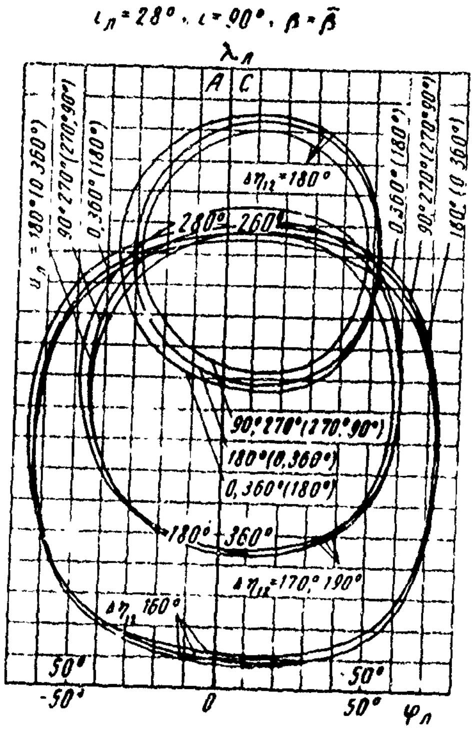

Fig. 5.

Page 64.

Transition from trajectories the surface of the moon - the Earth's atmosphere to trajectories orbit of ISZ [ИСЗ - artificial earth satellite] - the surface of the moon corresponds to the rotation of motion along trajectory. In this case, $\vec{V}_{c1}$ is replaced on - $\vec{V}_{c1}$, and β - on $\pi-\beta$; cos β reverses the sign. With the constant/invariable vector of the point of landing/fitting $\vec{r}_{c0}\,\vec{i}_k$ it remains constant/invariable, $\vec{i}_n$ reverses the sign, the parameters of hyperbola and the location of landing spot on the surface of the moon remain constant/invariable. Although the trajectories orbit of ISZ - the surface of the moon differ in principle from trajectories the surface of the moon - Earth's atmosphere, the vectors of geocentric speeds on sphere of influence in both cases, as show calculations, not very strongly they differ from each other [5]. Therefore the given above results can be used for the qualitative analysis of the properties of the selenospherical motion of flight/passages orbit of ISZ - surface of the moon.

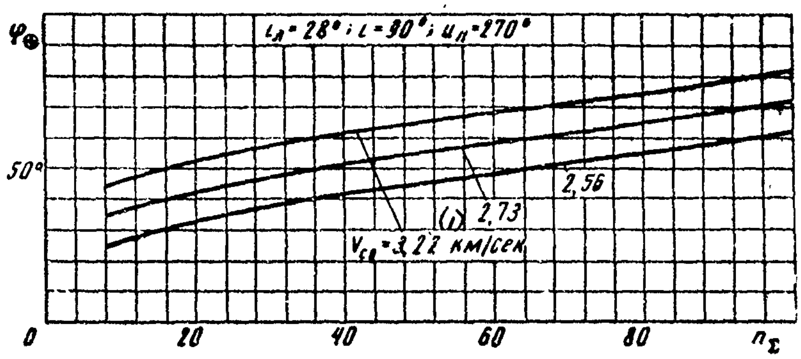

Fig. 6.

Key: (1). km/s.

* * *

REFERENCES

1. V. A. Yegorov. about the trajectories of return from the moon to the Earth. "space research," Vol. 5, iss. 4, 1967.

2. V. A. Yegorov. On the effect of the spread of the initial data on the trajectory of return from the moon to the Earth. "space investigations", Vol. 7, iss. 1, 1969.

3. V. A. Il'in, N. A. Istomin. Approximate synthesis of optimum trajectories Earth-moon-Earth with injection into orbit of the artificial satellite of the moon. The scientific notes of TsAGI, Vol. 1, No, 1, 1970.

4. V. A. Il'in. Synthesis of the trajectories of the close flight around of the moon with reentry into the atmosphere of the Earth, Journal will calculate. material and math. physics, Vol. 7, No 2, 1967.

5. V. A. Il'in, V. V. Demeshkina, N. A. Istomin. Study of the trajectories of the close flight around of the moon with reentry into the atmosphere of the Earth. "space research," of Vol. 8, No 1, 1970.

6. D R Chapman. An analysis of the corridor and guidance requirements for supercircular entry into planetary atmospheres, NASA TR, 1959, NR-55.

7. A T Allen, A T Eggers. A study of the motion and aerodynamic heating of ballistic missiles entering the earth's atmosphere at high supersonic speeds. NASA Rep., 1958, No 1381.

Received 1/VII 1969.

Page 65.

SCIENTIFIC RESULTS OF THE FLIGHT OF AUTOMATIC IONOSPHERIC LABORATORIES "ANTAR'".

L. A. Artsimovich, G. L. Grodzovskiy, Yu. I. Danilov, V. M. Zakharov, N. F. Kravtsev, R. N. Kuz'min, M. Ya. Marov, P. M. Morozov, V. Ye. Nikitin, A. N. Petunin, V. V. Utkin, V. M. Chulev, Ye. G. Shvidkovskiy.

With the aid of geophysical rockets was produced the starting/launching to height/altitudes by 100-400 km of automatic ionospheric laboratories "ANTAR" with gas plasma-ionic engines for the investigation of the prospects for controlled flight in upper air. The obtained telemetry data about the functioning of on-board systems and scientific instruments of high-altitude laboratories made it possible to study the condition of the work of gas ion-plasma jet engine in the ionosphere taking into account meteorological conditions and to obtain the data of direct measurements of the parameters of neutral atmosphere. Is carried out the study of complex interaction of gas ionic jet and neutralizer (electron emitter) with the plasma of the ionosphere. Given data of scientific processing of the results of the experiments conducted.

Automatic ionospheric laboratories "ANTAR". Automatic laboratories "ANTAR" with gas plasma-ionic engine are started to height/altitudes by 100-400 km with the aid of sounding rockets for the study of the prospects for controlled flight in upper air. The basic properties of upper air and the principles of the use of upper air for the controlled flight of orbital vehicles were described in works [1], [2]. Main in this problem is the use of air of upper air for economical engine systems. In this case, the necessary for air-breathing orbital vehicles jet velocity into ten kilometers per second can be realized for a gas working medium/propellant only in ion-plasma jet engines [3].

Essential stage in the study of the prospects for controlled flight in upper air is the direct/straight study of the special feature/peculiarities of the conditions of the work of gas ion-plasma jet engine (ERD) in upper air, that also was carried out in flight of automatic ionospheric laboratories "ANTAR".

For the first time testing electroreactive plasma engines under real space flight condition was carried out at Soviet automatic station "Probe" -2 in, 1964, where the electroreactive plasma engines were utilized as controls for an orientation system. One should note also the interesting investigations of work in space of mercury and cesium ion engines, carried out during the years 1964-1965 in the USA.

Page 86.

The basic goal of the flight of automatic ionospheric laboratories "ANTAR" was the study of interaction of exhaust jet of gas plasma-ionic engine with flight vehicle under conditions of flight in the ionosphere.

To Fig. 1, is given the photograph of laboratory. On Fig. 2, is given the schematic of the laboratory: 4 - gas plasma-ionic engine, 5 - control unit of the operation of engine and measuring complex, 6 - on-board power supplies, by 7 - telemetering equipment, 3 - ion traps, 8 - electrostatic fluxmeters, 1, 2 - ionization gauges, 9 - antenna.

In works [1], [2] they were presented are the results of the flight of laboratory "Antar'" with gas ERD, working on argon. In this article are set forth the results of the flight of automatic ionospheric laboratory "ANTAR" with the gas plasma-ionic engine, working on nitrogen. This engine contained gas plasma source, the electrostatic accelerator of ionic nitrogen exhaust jet and the system of neutralizers - electron emitters. Besides the thermionic-emitting neutralizers which were used during the study of engine on argon, were utilized effective plasma neutralizers.

In flight were measured and with the aid of telemetering equipment were transferred on ground receiving office the basic electrical parameters of engine, the value of the ambient pressure in the range of installation of motor, and also the value of the electric intensity and ion current from the ionosphere on the surface of vehicle. These data characterize interaction of exhaust jet (ion beam) with ionospheric plasma and they make it possible to rate/estimate the potential ϕ_0, which acquires vehicle in the process of the generation of ionic exhaust jet. The study of the value of the potential of vehicle has important value, since is determined the efficiency of the process of neutralizing ionic exhaust jet.

For determining the potential which acquires flight vehicle in the process of the generation of ionic exhaust jet, was utilized that described in [1], [2] the method, instituted on value measurement of intensity/strength $E = \varphi_r$ of electric field and density I of ion current from the ionosphere on the surface of vehicle.

Fig. 1

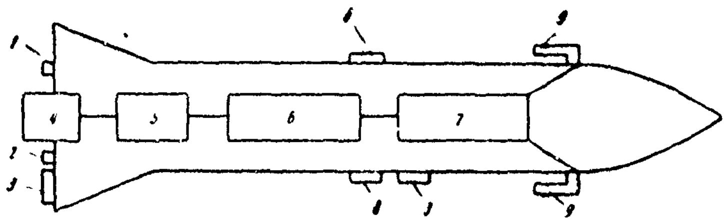

Fig. 2.

Page 67.

Intensity/strength E of electric field of the housing of laboratory "ANTAR" in flight was determined with the aid of two electrostatic fluxmeters, described in [1], [2]. Density I of ion current from the ionosphere to the surface of laboratory was measured by two types of the instruments: with the aid of the collector/receptacles of the electrostatic fluxmeters which accept the ion flow of all energies, which come in upon surface from the ionosphere, and with the aid of the collector/receptacles of the ion traps which record ion flow with the energies, exceeding 52 eV. The schematic of the used four-electrode ion trap is given to Fig. 3: 1 - screen grid for the elimination of the effect of the positive potential of grid 2, 3 - suppressor grid, 4 - collector, 5 - cathode follower, 6 - radiotelemetry system.

System of the neutralization of gas ionic exhaust jet, plasma neutralizer. Neutralizer in electroreactive plasma-ionic engine is intended for the exception/elimination of the accumulation of charge on the housing of vehicle and prevention of the loss of reactive thrust/rod. The effectiveness of the process of neutralization as a result of the large extent of the region of neutralization virtually can be investigated only in flight experiment, and measurements must be carried out at different height/altitudes in order to rate/estimate the contribution of the charged particles of upper atmosphere.

Basic requirements for neutralizer - life, compactness, small consumption of energy and substance. Long operating time is provided by the location of neutralizers outside the boundaries of the beam of the accelerated ions, which makes it possible to avoid its erosive destruction by fast ions. During the use of a hot cathode as neutralizer, ion current from emitter is limited to space charge, which leads to the increase of the potential of flight vehicle and reduction the energy efficiency of engine. Negative space charge near emitter can be compensated for by the small consumption of cesium ions, obtained as a result of the surface ionization of cesium atoms. On the same emitter it is possible to obtain the necessary electron stream low energy during a sufficient removal/distance from ion beam. So work plasma neutralizers with surface ionization.

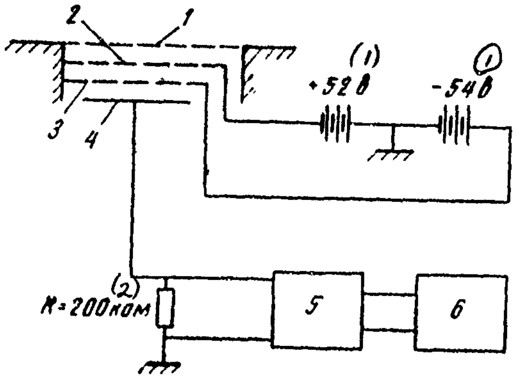

Fig. 3.

Key: (1). V. (2). kiloohm.

Page 68.

In the used plasma neutralizer of emission of electrons and ions of cesium, it was provided by the tungsten emitter, heated to temperature of 2500°K. The medium energy of electrons, which determines the value of the potential of bundle, depends on the filament voltage, temperature of emitter and from the flow of neutral atoms of cesium. As showed experiments, for obtaining electronic current I_e is required the ion current of cesium

$$I_i \approx 4 \sqrt{\frac{m_e}{M_{Cs}}} I_e.$$

It render/showed more convenient to apply as work substance not metallic cesium, but its alloys. In the used version of plasma neutralizer, the emitter is made and tungsten fusion with rhenium.

The schematic of plasma neutralizer is shown on Fig. 4. Cesium chloride was placed in cavity 1 of housing 2; the pairs of salt entered the region of the location of emitter 3 through the microgap between pin 4 and the housing. Cesium chloride dissociated on the incandescent surface of emitter, then occurred the partial ionization of cesium atoms. The necessary flow pair was obtained at the temperature of cesium chloride of 650-670°C.

Before the setting up to laboratory "Antar" plasma neutralizers underwent preliminary testings: neutralizer was establish/installed perpendicularly to the boundary of the beam of the accelerated ions at a distance of 1-2 cm from it, the compensated ion beam was headed for the "floating" collector/receptacle whose potential was close to the potential of ion beam, in this case, was provided stable electronic current I_e.

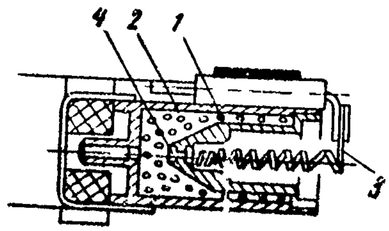

Fig. 4.

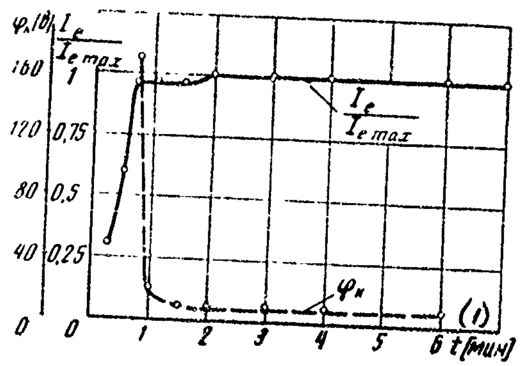

Fig. 5.

Fig. 5.

Key: (1). t [min].

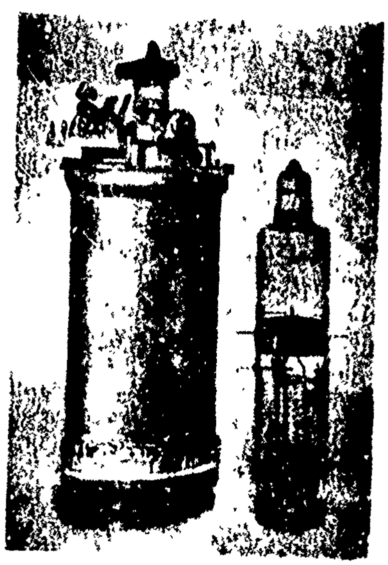

Fig. 6.

Page 69.

The dependence of a change in current $I_e/I_{e\,max}$ on time is shown on Fig. 5; there is shown change the potential of collector φ_k, which took the stationary value equal to $\varphi_k \approx 5-10$ V during the achievement of the saturation of electronic current from neutralizer. Testings showed the reliable work of neutralizer during multiplying and the stability of its parameters.

Measurements of pressure in the region of the motor installation into the flight of automatic laboratory "Antay" with the aid of the ionization gauges. The measurement of external pressure in the zone of installation of the motor of automatic ionospheric laboratory "amber" is realize/accomplished with the aid of two ionization gauges (1 and 2, see Fig. 2), which were establish/installed in the end-type part of the laboratory near plasma-ionic engine. Measurement began after the function of the automatic divide/marking off device and opening in flight of the bulb/flasks of manometers (Fig. 6).

To Fig. 7, is given the circuit diagram of ionization gauge 1 into telemetric system 2.

The used ionization gauges together with amplifier equipment make it possible to conduct the measurements of pressure in the range from 10^{-4} to 10^{-8} mm Hg. In connection with the fact that on the operation of plasma-ionic engine the decrease of pressure from 10^{-5}-10^{-6} mm Hg and is not exerted a substantial influence below, the lower value of the range of pressure measurement was of limited by the value 10^{-6} mm Hg.

To Fig. 8, the reduced pressure in the region of plasma-ionic engine in the stage of the descent of automatic ionospheric laboratory "Antar". There for a comparison are given the values of pressures at these height/altitudes on meteorological measurements. Some fluctuations of pressure in the region of installation of plasma-ionic motor on automatic laboratory "Antar", apparently, are connected with the precession of vehicle in flight.

Results of the flight of automatic ionospheric laboratory "Antar" with plasma-ionic engine on nitrogen.

In accordance with the flight program, given by the control unit of 5 (see Fig. 2), plasma-ionic engine was preliminarily included at the height/altitude approximately 160 km without the feed of the high (accelerating) stress u for preliminary warm-up and degassing. The complete firing of plasma-ionic engine on nitrogen with accelerating voltage u≈2100-2200 V was produced according to program at the height/altitude of 250 km. Was fixed the stable operation of engine prior to the atmospheric entry to the height/altitudes approximately 110 km. Maximum altitude in this flight was 325 km.

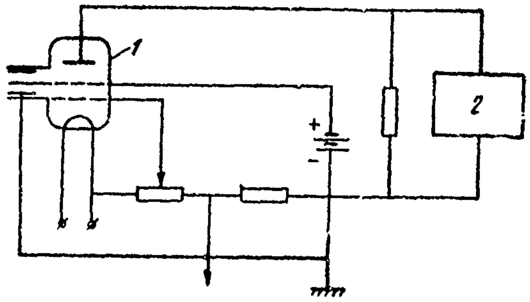

Fig. 3.

Page 70.

Plasma-ionic engine on nitrogen in flight worked with accelerating voltage of the ionic jet u≈2100-2200 V how was provided the rate of exhaust ionic jet v≈120 km/s. Table gives some results of the in-flight studies of laboratories "Antar" with the plasma-ionic engines, which worked on argon and on nitrogen.

The average values of the quantities of intensity/strength E_1 of electric field and potentials ϕ_{01} of vehicles in the work of thermionic-emitting neutralizers in order of values are close. Work with plasma neutralizer leads to a considerable reduction in strength E_2 of field to level 2-3 V/cm and the achievement of the low value of the potential ϕ_{02} of housing, which does not exceed 10 V. The measured current distribution in engine system shows that the relationship/ratio between the ion current, compensated for by electrons from neutralizers, and by total ion current is 97o/o; 3o/o comprise leakage currents to accelerating electrode and the housing of laboratory.

Consequently, under conditions of flight in the ionosphere of laboratory "amber" with plasma-ionic engine on nitrogen was realize/accomplished the effective neutralization of ionic exhaust jet both in the sense of the compensation ion current by electronic current from neutralizers and the compensations the positive space charge of ions by electrons. With the achieved/reached in flight value of the potential of flight vehicle relative to the boundary ionospheric plasma (in the work of plasma neutralizer) within limits to 10 V on the process of neutralization is expend/consumed less than 0.5o/o energy of exhaust jet.

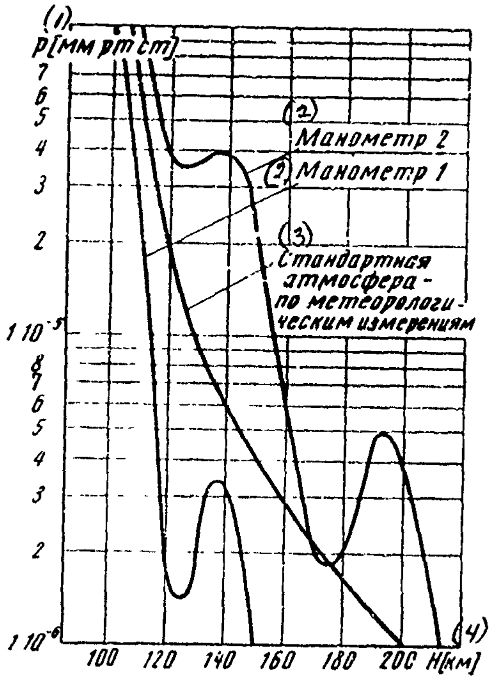

(5) Параметры	(6) Двигатель на аргоне	(7) Двигатель на азоте
(8) u [в]	~300	2100—2200
v [км/сек] (9)	~40	120
(10) Термоэмиссионный нейтрализатор		
(11) E_1 [в/см]	15	10
φ_{01} [в] (8)	50—70	100—200
(12) Плазменный нейтрализатор		
(11) E_2 [в/см]	—	2—3
φ_{02} [в] (8)	—	5—10

Fig. 8.

Key: (1). [mm Hg]. (2). Manometer. (3). Standard atmosphere for meteorological measurements. (4). H [km]. (5). Parameters. (6). Engine on argon. (7). Engine on nitrogen. (8). [V]. (9). [km/s]. (10). Thermionic-emitting neutralizer. (11). [V/cm]. (12). Plasma neutralizer.

Page 71.

Testings of automatic ionospheric laboratories conducted "Antar" showed efficiency of gas ERD in the ionosphere during considerable changes in the external pressure at height/altitudes 100-400 km. Is reached the effective neutralization of nitrogen ionic exhaust jet at the jet exhaust velocity to 120 km/s.

REFERENCES

1. G. L. Grodzovskiy, A. N. Dyukalov, N. F. Kravtsev, M. Ya. Marov, V. Ye. Nikitin, A. N. Petunin, L. A. Simonov, V. V. Utkin. On the scientific results of the flight of automatic ionospheric laboratory "Antar-1". Proc. XIX Congress IAF, New York, October, 1968.

2. G. L. Grodzovskiy, A. N. Dyukalov, N. F. Kravtsev, M. Ya. Marov, V. Ye. Nikitin, A. N. Petunin, L. A. Simonov, V. V. Utkin. Scientific results of the flight of automatic ionospheric laboratory "Antar'-1". "Space investigations", Vol. VI, iss. 6, 1968.

3. G. L. Grodzovskiy, S. N. Ivanov, V. V. Tokarev. Mechanics of space low-thrust mission. M., "science", 1966.

Received 3/XI 1969.

Page 72.

SOLUTION OF THE PROBLEM OF THE OSCILLATIONS OF LIQUID IN THE CAVITIES OF ROTATION BY THE METHOD OF STRAIGHT LINES.

I. V. Kolin, V. N. Sukhov.

Is given the solution of the problem of the oscillations of liquid in the cavities of rotation by the method of straight lines. Is given estimation of the accuracy/precision of method and its convergence. Is given the comparison of the results of calculation according to the method of straight lines with the results of calculation by variational method.

The study of the oscillations of liquid in cavities is necessary for the analysis of the stability of the disturbed motion of the flight vehicles, which have on board the large masses of liquid propellant [1], [2]. For the solution of this problem in the case of the arbitrary cavities, partially filled by liquid, widely are utilized variational methods [3] - [5]. Rate of convergence and, therefore, the accuracy/precision of the solution of problem are determined by the rational selection of the system of coordinate functions, in a series along which is expanded the solution. For each form of cavity, this task must be solved especially.

"As a rule, the best results it is possible to expect from the system of harmonic functions, satisfying besides because of completeness to a maximum quantity of boundary conditions. Therefore the requirement of universality and maximum standardization of the algorithm of count they are located in known contradiction with the requirement of the maximum account of the individual properties of cavity" [1].

FOOTNOTE [1]. G. N. Mikishev, B. I. Rabinovich. Dynamics of solids with the cavities, partially filled by liquid. M., "Machine-building", 1968, page 182. ENDFOOTNOTE.

In the present work for the solution of the problem of the oscillations of liquid, it is utilized by one of the varieties of finite-difference method - method of straight lines. The advantage of this method in comparison with variation is the direct satisfaction of boundary conditions on free and hydrophilic surfaces. Therefore the proposed method is universal, suitable for the arbitrary smooth cavities of rotation and cavities of rotation, divided by continuous partition/baffles.

The numerical realization of the algorithm of finite-difference method by ETsVM [digital computer] also considerably is simplified, since the equation of frequencies is record/written in an explicit form. The comparison of the results of calculation by the method of straight lines with the results of calculation by other methods shows the high accuracy/precision of the proposed method.

Page 73.

§ 1. Determination of potentials of velocities and frequencies of oscillations of liquid.

The task of the natural oscillations of liquid in the cavity of rotation is formulated as follows [3]:

$$r^2\frac{\partial^2\varphi}{\partial r^2}+r\frac{\partial\varphi}{\partial r}+\frac{\partial^2\varphi}{\partial\eta^2}+r^2\frac{\partial^2\varphi}{\partial x^2}=0 \quad \text{в}^{(1)}\ \tau; \qquad (1.1)$$

$$j\frac{\partial\varphi}{\partial x}-\omega^2\varphi=0 \quad \text{на}^{(2)}\ \Sigma; \qquad (1.2)$$

$$\frac{\partial\varphi}{\partial n}=0 \quad \text{на}^{(2)}\ S, \qquad (1.3)$$

Key: (1). in (2) on

where $\varphi=\varphi(r, \eta, x)$ - velocity potential of liquid;

r, η, x – the cylindrical coordinates (see figure);

τ – volume, occupied with liquid;

Σ – undisturbed free surface of liquid;

S – hydrophilic surface of cavity;

ω – the natural frequency of oscillation of liquid;

j – strength of the field of mass forces;

$\bar{n}$ – unit vector of standard to the hydrophilic surface of cavity.

For the cavities of rotation potential φ can be searched for in the form

$$\varphi(r, \eta, x) = \cos m\eta \, \Phi(r, x), \tag{1.4}$$

where m takes values m=0, 1, 2, ..., equal to the number of waves in circumference during the oscillations of liquid.

The equation of Laplace (1.1) for function $\Phi(r, x)$ takes the form

$$r^2 \frac{\partial^2 \Phi}{\partial r^2} + r \frac{\partial \Phi}{\partial r} + m^2 \Phi + r^2 \frac{\partial^2 \Phi}{\partial x^2} = 0. \quad (1.5)$$

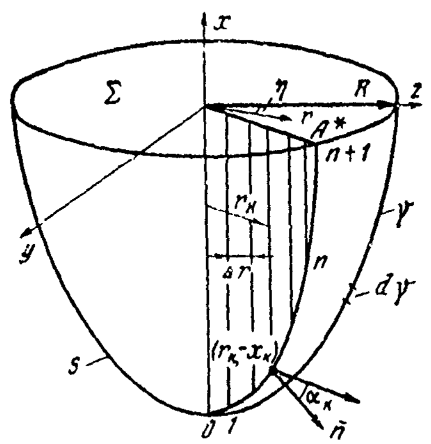

Fig. 1.

Page 74.

Conditions on Σ and S are converted as follows:

$$j\frac{\partial\Phi}{\partial x}-\omega^2\Phi=0 \qquad \overset{(1)}{\text{при}}\ x=0; \qquad (1.6)$$

$$\frac{\partial\Phi}{\partial r}\cos\alpha-\frac{\partial\Phi}{\partial x}\sin\alpha=0 \qquad \overset{(2)}{\text{на}}\ \gamma, \qquad (1.7)$$

Key: (1). when. (2). on.

where γ - forming cavities.

α - angle between directions r and $\bar{n}$.

For approximate solution of task (1.5), (1.6), (1.7) let us use the method of straight lines. Let us examine section γ by the vertical plane, passing through axle/axis Ox. R=OA - radius of the maximum cross section of cavity with liquid. Let us divide R into n+1 of equal cutting by length Δr=R/n+1. Through points $r_k=k\Delta r$, 0 let us conduct the vertical direct/straight, parallel axle/axes Ox. These straight lines intersect generatrix γ at points $(r_k, -x_k)$. The value of velocity potential along the k straight line let us designate $\Phi_k=\Phi_k(r_k, x)$, and the angle between the direction r and the standard at point $(r_k, -x_k)$ through α_k. In the equation of Laplace (1.5) derivatives for r of the first and second orders let us replace with the difference relationship/ratios

$$\frac{\partial\Phi}{\partial r}=(\Phi_{k+1}-\Phi_{k-1})(2\,\Delta r)^{-1}; \quad (1.8)$$

$$\frac{\partial^2\Phi}{\partial r^2}=(\Phi_{k+1}-2\,\Phi_k+\Phi_{k-1})(\Delta r)^{-2}. \quad (1.9)$$

Then (1.5) it is converted as follows:

$$\left[r_k^2(\Delta r)^{-2}-\frac{r_k}{2\,\Delta r}\right]\Phi_{k-1}-[m^2+2\,r_k^2(\Delta r)^{-2}]\,\Phi_k+$$
$$+\left[r_k^2(\Delta r)^{-2}+\frac{r_k}{2\,\Delta r}\right]\Phi_{k+1}+r_k^2\ddot{\Phi}_k=0, \quad (1.10)$$

where

$$\ddot{\Phi}_k=\frac{\partial^2\Phi_k}{\partial x^2}. \quad (1.11)$$

Conditions on free and hydrophilic surfaces are replaced by conditions in the discrete number of points

$$j\frac{\partial\Phi_k}{\partial x}-\omega^2\Phi_k=0 \qquad \text{при (1)}\ x=0, \quad (1.12)$$

$$(\Phi_{k+1}-\Phi_{k-1})(2\,\Delta r)^{-1}-\frac{\partial\Phi_k}{\partial x}\operatorname{tg}\alpha_k=0 \quad \text{на (2)}\ \gamma. \quad (1.13)$$

Key: (1). with. (2). on.

Henceforth we will be restricted to the examination of cavities whose floating surface coincides with the maximum transverse size of cavity. Generalization to the case of arbitrary cavity does not represent work, but it is conjugate/combined with cumbersome calculations. Total number of unknowns Φ_k, connected n by equations of type (1.10), are equal n+2.

Page 75.

Excess variables can be excluded, on the basis of following considerations. For the antisymmetric oscillations of liquid in singly connected cavity, which represent the greatest practical interest,

$$\Phi_0(0,\ x)=0. \tag{1.14}$$

At point A of the contact of floating surface with the wall of cavity, must simultaneously be made conditions (1.6) and (1.7) which is equivalent to the condition

$$\frac{\partial\Phi}{\partial r}=\omega^2 j^{-1}\Phi\,\mathrm{tg}\,\alpha_{n+1} \text{ with } \qquad r=R,\quad x=0. \tag{1.15}$$

If in cavity there is a cylindrical insert,

$$\frac{\partial\Phi}{\partial r}=0 \text{ with } \qquad r=R. \tag{1.16}$$

For the replacement of derivative $\frac{\partial\Phi}{\partial r}$ in relationship/ratio (1.15), it is possible to utilize the following finite-difference relationship/ratios:

$$\frac{\partial \Phi}{\partial r}=\frac{\Phi_{n+1}-\Phi_n}{\Delta r}+0(\Delta r), \quad (1.17)$$

$$\frac{\partial \Phi}{\partial r}=\frac{\Phi_{n+1}-\frac{4}{3}\Phi_n-\frac{1}{3}\Phi_{n-1}}{2\Delta r}+0(\Delta r^2). \quad (1.18)$$

For calculations with the increased degree of accuracy, especially during satisfaction of condition (1.16), it is expedient to utilize relationship/ratio (1.18). Taking into account (1.15) and (1.17), we have

$$\Phi_{n+1}=\Phi_n[1-\omega^2 j^{-1}\Delta r \operatorname{tg}\alpha_{n+1}]^{-1}. \quad (1.19)$$

Analogous relationship/ratios can be utilized in the case of doubly connected cavities. Eliminating Φ_0 and Φ_{n+1}, the system of differential equations (1.10) can be written in the following matrix form:

$$A\Phi+B\ddot{\Phi}=0, \quad (1.20)$$

where

$$\Phi=\begin{bmatrix}\Phi_1\\ \Phi_2\\ \vdots\\ \Phi_n\end{bmatrix}, \quad B=VV, \quad (1.21)$$

V - diagonal matrix/die whose cell/elements are equal to r_k;

A - three-diagonal matrix/die:

$$A=\begin{bmatrix} c_1 d_1 & & & & \\ q_1 c_2 d_2 & & & & \\ & q_2 c_3 d_3 & & & \\ & & \vdots & \vdots & \cdot \\ & & & \cdot\ \cdot\ \cdot & \\ & & & & q_{n-1} c_n \end{bmatrix}. \qquad (1.22)$$

Page 76.

Here

$$c_i=-\left[\frac{m^2}{r_i}+2r_i(\Delta r)^{-2}\right],\quad i=1,\ 2,\ldots,(n-1);$$

$$c_n=-\left[\frac{m^2}{r_n}+2r_n(\Delta r)^{-2}\right]+[r_n(\Delta r)^{-2}+(2\,\Delta r)^{-1}]\times$$
$$\times[1-\omega^2 j^{-1}\Delta r\,\mathrm{tg}\,\alpha_{n+1}]^{-1},$$

$$d_i=\frac{r_i^2}{(\Delta r)^2}+\frac{r_i}{2\Delta r};\quad q_i=\frac{r_{i+1}^2}{(\Delta r)^2}-\frac{r_i+1}{2\Delta r}.$$

For the doubly connected cavities

$$c_1=-\left[\frac{m^2}{r_1}+r_1(\Delta r)^{-2}\right]+\left[r_1(\Delta r)^{-2}-\frac{1}{2\Delta r}\right][1+\omega^2 j^{-1}\Delta r\,\mathrm{tg}\,\alpha_{n+1}]^{-1}.$$

Equation (1.20) is convenient to convert to the form

$$A^0\Phi^0+\ddot{\Phi}^0=0, \qquad (1.23)$$

where

$$\Phi^0=V^0\Phi,\quad A^0=(V^0)^{-1}A(V^0)^{-1};$$

V0 - diagonal matrix/die whose cell/elements are equal to $\sqrt{r_k}$.

Particular solution (1.23) let us search for in the form

$$\Phi^0 = Ce^{\lambda x} K^0, \qquad (1.24)$$

where C - arbitrary constant,

λ - unknown value,

K^0 - unknown vector.

Substituting (1.24) in (1.23), we will obtain:

$$(A^0 + \lambda^2 E) CK^0 = 0, \qquad (1.25)$$

where E - unit matrix.

The significant solution of uniform system (1.25) corresponds to those λ_i, which are the roots of the characteristic equation

$$|A^0 + \lambda_i^2 E| = 0. \qquad (1.26)$$

If all the $\lambda_i^2 > 0$, then general solution for Φ^0 can be presented in the form

$$\Phi_k^0 = \sum_{i=1}^{n} [c_i \exp(\lambda_i x) + c_{-i} \exp(-\lambda_i x)] K_{ki}^0, \qquad (1.27)$$

where $K_l^0 = V^0 K_l$.

If there is $\lambda_s^2 < 0$ (for s=1, 2, ..., l), then the general solution representablly as follows:

$$\Phi_k^0 = \sum_{s=1}^{l} [c_s \sin \lambda_s x + c_{-s} \cos \lambda_s x] K_{ks}^0 +$$

$$+ \sum_{l=l}^{n} [c_l \exp(\lambda_l x) + c_{-l} \exp(-\lambda_l x)] K_{kl}^0, \quad (1.28)$$

where

$$\lambda_s = \sqrt{|\lambda_s^2|}, \; K_s^0 = V^0 K_s. \quad (1.29)$$

Page 77.

Relationship/ratio (1.25) is the discrete analog of the equation of Bessel; therefore

$$R\lambda_{l\,\overrightarrow{n\to\infty}}\,\xi_l, \quad K_{l\,\overrightarrow{n\to\infty}} \begin{bmatrix} J_m\left(\xi_l \frac{\Delta r}{R}\right) \\ J_m\left(\xi_l \frac{2\Delta r}{R}\right) \\ \vdots \\ J_m\left(\xi_l \frac{n\Delta r}{R}\right) \end{bmatrix}, \quad (1.30)$$

where $J_m\left(\xi_l \frac{r}{R}\right)$ - a Bessel function of first kind the m order, and ξ_l - roots of the equation

$$\frac{\xi_l J_m'(\xi_l)}{J_m(\xi_l)} = \omega_l^2 \frac{R}{j} \operatorname{tg} \alpha_{n+1}. \quad (1.31)$$

The relationship/ratio between coefficients c_l and c_{-l} can be obtained from the satisfaction of dynamic boundary free-surface conditions (1.11):

$$\left.\begin{aligned} c_l &= \frac{c_{-l}\,\omega^2}{j\lambda_l}; \\ z_l &= \frac{z_l^0\,\omega^3}{j\lambda_l}, \end{aligned}\right\} \qquad (1.32)$$

where $z_l = c_l - c_{-l}$ and $z_l^0 = c_l + c_{-l}$. Boundary conditions on hydrophilic surface (1.12), written in matrix form, they take the following form:

$$NZ^0 - \omega^2 j^{-1} M \Lambda^{-1} Z^0 = 0. \qquad (1.33)$$

Here Λ - diagonal matrix/die with the cell/elements, equal to λ_l, and matrix elements M and N are respectively equal to:

$$m_{kl} = \begin{cases} (K_{k+1\,s} - K_{k-1\,s})(2\Delta r)^{-1}\sin\lambda_s x_k + \lambda_s K_{ks}\,\mathrm{tg}\,\alpha_k \cos\lambda_s x_k \\ \qquad \begin{pmatrix} k = 1, 2, \ldots, n \\ s = 1, 2, \ldots, l \end{pmatrix}; \\ (K_{k+1\,s} - K_{k-1\,i})(2\Delta r)^{-1}\,\mathrm{sh}\,\lambda_i x_k + \lambda_i K_{ki}\,\mathrm{tg}\,\alpha_k\,\mathrm{ch}\,\lambda_i x_k \\ \qquad \begin{pmatrix} i = (l+1), \ldots, n, \\ k = 1, 2, \ldots, n \end{pmatrix}; \end{cases} \qquad (1.34)$$

$$n_{kl} = \begin{cases} (K_{k+1\,s} - K_{k-1\,s})(2\Delta r)^{-1}\cos\lambda_s x_k - \lambda_s k_{ks}\,\mathrm{tg}\,\alpha_k \sin\lambda_s x_k \\ \qquad \begin{pmatrix} s = 1, 2, \ldots, l \\ k = 1, 2, \ldots, n \end{pmatrix}; \\ (K_{k+1\,i} - K_{k-1\,i})(2\Delta r)^{-1}\,\mathrm{ch}\,\lambda_i x_k + \lambda_i K_{ki}\,\mathrm{tg}\,\alpha_k\,\mathrm{ch}\,\lambda_i x_k \\ \qquad \begin{pmatrix} i = (l+1), \ldots, n; \\ k = 1, 2, \ldots, n \end{pmatrix}. \end{cases} \qquad (1.35)$$

Page 78.

From the condition for existence of the significant solution of system (1.33) we obtain the equation of the frequencies:

$$|N-\omega^2 j^{-1} M \Lambda^{-1}|=0. \qquad (1.36)$$

The given above algorithm of solution directly can be utilized only for the cavities which have $a_{n+1}=0$. Otherwise the matrix elements A (1.22) are the functions of the unknown parameter $\frac{\omega^2}{j}$ and for obtaining the solution is utilized the method of successive approximations. For determining the matrix elements A, we are assigned by value $\frac{\omega_0^2}{j}$. Solving equation (1.25), we determine $\lambda_i^{(0)}$ and $K_{ki}^{(0)}$. Utilizing these values, it is possible to comprise the equation of frequencies (1.36), solving which, we find the first approximation $\frac{\omega_{(1)}^2}{j}$. Again we determine matrix elements A and, repeating the process of calculations consecutively, we obtain values $\lambda_i^{(1)}$, $K_{ki}^{(1)}$ and $\frac{\omega_{(2)}^2}{j}$.

If sequence $\frac{\omega_{(k)}^2}{j}$ (with k=0, 1, 2) is convergent, then the limit, to which converges this sequence, there is solution of problem. Numerical examples of the calculation of the cavities of various forms show that the given above method of successive approximations possesses rapid convergence and requires for its realization of virtually of 2-3 approach/approximations.

§ 2. Comparison of method direct/straight and of variational method.

Variational methods at present widely are utilized for the solution of the problem of the oscillations of liquid in cavities [3] - [5]. Therefore is of interest the comparison of the solutions, obtained by the method of straight lines and by variational method. Before passing is direct to comparison, we will obtain the solution of problem by the method which subsequently let us call the modified method of straight lines. For certainty let us examine the cavity which has $\alpha_{n+1}=0$. Let us search for solution in the form:

$$\Phi(r,x)=\sum_{i=1}^{N}J_m\left(\xi_i\frac{r}{R}\right)\left[c_i\exp\left(\xi_i\frac{x}{R}\right)+c_{-i}\exp\left(-\xi_i\frac{x}{R}\right)\right], \quad (2.1)$$

where ξ_i there are roots of equation $J_m'(\xi_i)$.

Constants c_i and c_{-i} we find from the satisfaction of conditions (1.6), (1.7) - dynamic free-surface conditions and the condition of nonpassage on the hydrophilic surface in the discrete number of points with the coordinates $(r_k, -x_k)$, which are utilized in the method of straight lines. Taking into account (1.30), it is possible to confirm that the solutions, obtained by the method of straight lines and by the modified method of straight lines, are close to each other with sufficiently large N.

Page 79.

In variational method the task of the oscillations of fluid (1.1), (1.2), (1.3) is equivalent to the task of the minimum of the functional:

$$U=\frac{1}{2}\int_{\tau}(\nabla\varphi)^2\,d\tau-\frac{\omega^2}{j}\int_{\Sigma}\varphi^2\,dS. \tag{2.2}$$

Expressions for a velocity potential φ let us search for in the form

$$\varphi=\Phi(r,\ x)\cos m\eta, \tag{2.3}$$

where $\Phi(r, x)$ is assigned in the form (2.1).

Utilizing expression (2.3), it is possible to show that the task of the oscillations of liquid is equivalent to the task of the minimum of the functional:

$$U'=\int_{\gamma}\frac{\partial\Phi}{\partial n}\Phi r\,d\gamma+\int_{0}^{R}\Phi(r,\ 0)\,r\left[\left.\frac{\partial\Phi}{\partial x}\right|_{x=0}-\frac{\omega^2}{j}\Phi(r,\ 0)\right]dr, \tag{2.4}$$

where γ - generatrix cavities, and d γ - a differential of the arc of generatrix.

Thus, in variational method and the modified method of straight lines solution searches for in one and the same form. Boundary conditions in the method of straight lines are satisfied in the discrete number of points on the free and hydrophilic surface. In variational method boundary conditions are satisfied on the average with weight Φr on the same surfaces. At the high values of N both solutions they must lead to one and the same results, if we the solution for Φ in variational method search for in the form(2.1).

§ 3. Results of calculation.

For estimating the accuracy/precision of the method of straight lines, were carried out the calculations of the cavities of the various forms whose natural frequencies are sufficiently agreed to by variation and experimental methods. As such cavities were selected spherical, toroidal and conical (with the half-angle of 31°).

Table 1 gives the results of calculating the I eigenvalue $\lambda_1 R$ of matrix/die A^0 (1.25) when $\alpha_{n+1}=0$, when for the exception/elimination of variable Φ_{n+1} is utilized relationship/ratio (1.17). With $n\to\infty$ $\lambda_1 R$ must approach $\xi_1=1{,}841$, i.e., for the root of equation $J_1'(\xi_i)=0$.

More accurate results can be obtained, if we for an exception/elimination Φ_{n+1} utilize formula (1.18). In this case already with n=10 approximate value $\lambda_1 R=\xi_1=1{,}842$.

Table 1.

	(1) Метод прямых									$J_1'(\xi_i)=0$
	$\Phi_{n+1}=\Phi_n$								$\Phi_{n+1}=\frac{4}{3}\Phi_n-\frac{1}{3}\Phi_{n-1}$	
n	4	6	8	10	12	14	16	18	10	
$\lambda_1 R$	2,045	1,983	1,950	1,929	1,915	1,901	1,896	1,893	1,842	1,841

Key: (1). Method of straight lines.

Page 80.

Table 2 gives the comparison of the results of calculation by the method of straight lines and by variational method of frequency in spherical cavity with a radius R_c. Between these realizations good agreement is observed . For $\frac{h}{R_c}=1$ the comparison is conducted with the results of works [6], which are obtained by approximate solution of integral equation.

The results, given in Table 3, 4, 5, characterize the convergence of the process of consecutive approximations for a spherical cavity when $\frac{h}{R_c}=0,5$, for the toroidal cavity (ratio R_2/R_1 of inside and external radii in maximum cross section is equal to 0.364) when $\frac{h}{R}=0,5$ $\left(R=\frac{R_1-R_2}{2}\right)$ and for a conical cavity. Value $\frac{\omega^2 R}{j}$ according to calculation by variational method is equal to 0.078935 for a toroidal cavity even 1.30 for the conical cavity (half-angle is equal to 30°).

Table 2.

$\frac{h}{R_c}$	Вариационный метод, $\frac{\omega^2}{j} R_c$ (1)	Метод последовательных приближений, $\frac{\omega^2}{j} R_c$ (2)		$\frac{h}{R_c}$	Вариационный метод, $\frac{\omega^2}{j} R_c$ (1)	Метод последовательных приближений, $\frac{\omega^2}{j} R_c$ (2)	
		$N=10$	$N=16$			$N=10$	$N=16$
0,1	1,036	1,0361	1,036	0,6	1,262	1,2687	—
0,2	1,072	1,0733	1,073	0,7	1,324	1,3356	—
0,3	1,113	1,1149	1,115	0,8	1,394	1,3586	—
0,4	1,158	1,1607	1,161	0,9	1,470	1,4460	—
0,5	1,208	1,2114	—	1,0	1,565 [6]	1,5832	—

Key (1). Variational method. (2). Method of successive approximations.

Table 3. Sphere, $n=10, \frac{h}{R_c}=0{,}5$.

k	$\frac{\omega^2}{j} R_c$	$\lambda_1 R$
0	1,18015	1,92899
1	1,21122	1,51783
2	1,21145	1,48899
3	1,21143	1,49118
4	1,21143	1,49119

Table 4. Torus, $n=10, \frac{h}{R}=0{,}5$.

k	$\frac{\omega^2 R}{j}$	$\lambda_1 R$
0	0,08336	1,42402
1	0,078091	1,33659
2	0,078443	1,33699
3	0,078420	1,33619
4	0,078420	1,33619

Table 5. Cone $\alpha=31°$, $n=6$.

k	$\frac{\omega^2}{J}R$	$\lambda_1 R$
0	0,94303	1,9229
1	1,23763	1,39807
2	1,30582	1,10009
3	1,31987	1,013803
4	1,32269	0,994829
5	1,323256	0,990973
6	1,323364	0,99020
7	1,323386	0,99005
8	1,323394	0,99001

Page 81.

The given results show that the method of straight lines provides sufficient accuracy/precision of the solution of the problem of the oscillations of liquid in the cavities of rotation.

* * *

REFERENCES.

1. K. S. Kolesnikov. Liquid-propellant rocket as controlled system. M., "Machine-building", using 1968.

2. G. N. Mikishev, B. I. Rabinovich. Dynamics of solid with with

the cavities, partially filled by liquid. M., "Machine-building", 1968.

3. Variational methods in tasks of oscillations of liquid and body with liquid. Coll. of article edited by N. N. Moiseyeva, CC AN USSR, 1962.

4. M. R. Lawerence, C. J. Wang, R. E. Reddy. Variational solution of fuel sloshing models. Jet Propulsion, v 28, No 11, 1958.

5. H. N. Abramson, G. F. Ransleben. Simulation of fuel sloshing characteristics in missile tanks by use of small models. ARS J No 7, 1960.

6. B. Budiansky. Sloshing of liquids in circular canals and spherical tanks. J of the Aerospace Sciences, v 27, 1960, No 3.

7. L. V. Dokuchaev. Solution of the boundary-value problem of the oscillations of liquid in conical cavities. PMM, Vol. XVIII, iss. 1. 1964.

The manuscript entered 8/VII 1969.

Page 82.

BEARING CAPACITY THE TRANSIENT CREEP OF CAISSON DURING FREE TWISTING.

I. I. Pospelov, N.I. Sidorova.

Work [1] examines steady creep of the thin-walled rods of multiply connected cross-section during free twisting.

In this work is given the solution of the problem of bearing capacity and the transient creep of the thin-walled rods of multiply connected cross-section during free twisting by the method of successive approximations [2], [3]. Complete strain is represented in the form of the sum of instantaneous deformation, by nonlinear form voltage-sensitive, and creep strain, nonlinear voltage-sensitive and time. The behavior of material during creep is described by the theory of flow. Solution for the k iteration of voltage/stresses and relative angle of twist is obtained in the form of quadratures. Is carried out the numerical computation of bearing capacity, voltage/stresses and relative angle of twist of caisson on ETsVM [digital computer] M-20.

Let us examine the behavior of the thin-walled rod of multiply connected cross-section, which is found under conditions of creep, under the action of the alternating/variable in time torsional moment, applied to end/faces. It is directed axle/axis Oz along the axis of rod, axle/axis Ox and Oy it is arranged by arbitrary form in cross-sectional flow. Assuming that the cross section of rod is not deformed in its plane, we will obtain following expressions for the components of the displacement vector:

$$u = -\theta zy, \quad v = \theta zx, \quad w = \theta\chi(x, y),$$

while for the strain tensor components:

$$\varepsilon_{yz} = \frac{\theta}{2}\left(\frac{\partial\chi}{\partial y} + x\right), \quad \varepsilon_{xz} = \frac{\theta}{2}\left(\frac{\partial\chi}{\partial x} - y\right), \tag{1}$$

where θ - the linear angle of twist; χ - certain function from x, y.

Let us comprise expression for the circulation of shearing strain on certain closed duct/contour Γ,

which lies within the cross section of rod.

Page 83.

Utilizing (1) and an expression for a shearing strain ε_{zt} in the plane, tangential to duct/contour Γ at certain point

$$\varepsilon_{zt}=\varepsilon_{yz}\frac{dy}{dl}+\varepsilon_{xz}\frac{dx}{dl},$$

where $\frac{dy}{dl}$, $-\frac{dx}{dl}$ - the direction cosines of normal to a curve, we will obtain

$$\oint_{\Gamma}\varepsilon_{zt}\,dt=\theta F, \qquad (2)$$

where F - the area, limited by duct/contour Γ.

We utilize a usual assumption about neglect that comprise of shearing stress along the standard of duct/contour and constancy according to the thickness of the duct/contour that comprise of shearing stress along tangent to duct/contour. Then the stressed and states of strain of thin-walled rod will be described by values σ_{zt} and ε_{zt}. Henceforth let us use to designations $\sigma_{zt}=s$, $\varepsilon_{zt}=\gamma$.

We assume that the complete strain γ is composed of instantaneous that comprise $\gamma^{\text{мг}}$, by nonlinear voltage-sensitive, and creep strain γ^{p}, nonlinear voltage-sensitive and the time:

$$\gamma=\gamma^{\text{мг}}+\gamma^{p}. \qquad (3)$$

The relationship/ratio between the rate of creep strain $\dot{\gamma}^p$, the stress s and the time t is accepted as following:

$$\dot{\gamma}^p = \frac{\sqrt{3}}{2} f(\sqrt{3}\, s). \tag{4}$$

Here differentiation is conducted on the modified time τ, which is the function of the physical time t:

Equation (4) is convenient to present, isolating linear part in the form

$$\dot{\gamma}^p = \frac{3}{2} Ds(1-\eta), \tag{5}$$

where

$$\eta = 1 - \frac{f(\sqrt{3}s)}{D\sqrt{3}s}. \tag{6}$$

For the increase of the velocity of the convergence of the sequence of approach/approximations, one should select

$$D = \frac{f(\sqrt{3}s_{max})}{s_{max}}.$$

Communication/connection of instantaneous deformation with stress let us accept in the form

$$\gamma^{\text{MF}} = \frac{s}{2\mu} + \frac{\sqrt{3}}{2} B(\sqrt{3}s)^m = \frac{s}{2\mu} + \frac{\sqrt{3}}{2}\left(\frac{\sqrt{3}}{\sigma^0} s\right)^m, \tag{7}$$

where μ - shear modulus; m, B, $\sigma^0 = (B)^{-\frac{1}{m}}$ - constants of material.

Page 84.

Isolating linear part, equation let us present as

$$\gamma^{\text{иг}} = \frac{s}{2\mu_1}\left[1+\omega\left(\sqrt{3}s\right)\right], \tag{8}$$

where

$$\omega = \frac{\mu_1-\mu}{\mu} + \frac{3\mu_1}{\sigma^0}\left(\frac{\sqrt{3}s}{\sigma^0}\right)^{m-1}, \tag{9}$$

$$\mu_1 = \frac{1}{\frac{1}{\mu} + \frac{3}{\sigma^0}\left(\frac{\sqrt{3}s_{max}}{\sigma^0}\right)^{m-1}}, \tag{10}$$

that it corresponds to secant module/modulus on the diagram of the intensities of stress and strain for $\sqrt{3}s_{max}$. Conditional value s_{max} can be selected during solution by method by spaces as maximum value of the stresses, calculated on the preceding/previous space.

From equations (3), (5), (8) we will obtain the equations, which describe the behavior of material with transient creep and the nonlinear elasticity:

$$\gamma = L(s) + \varphi(s), \tag{11}$$

where

$$L(s) = \frac{s}{2\mu_1} + \frac{3}{2}Ds \tag{12}$$

[$A(s)$ - linear operator];

$$\varphi(s)=\frac{1}{2\mu_1}\frac{d}{d\tau}(s\omega)-\frac{3}{2}Ds\eta. \quad (13)$$

At differentiated equation (2) for τ and after substituting in it the velocity of shearing strain, determined (11), we will obtain Bredt's generalized formula:

$$L\oint_{\Gamma} s\,dl+\oint_{\Gamma}\varphi(s)\,dl=\dot{\theta}F. \quad (14)$$

Let us examine the rod whose cross section is represented in Fig. 1; $\bar{s}_{nn}, \bar{l}_{nn}, \bar{\delta}_{nn}$; $s_{n-1,n}, l_{n-1,n}, \delta_{n-1,n}$; $s_{nn}, l_{nn}, \delta_{nn}$; $s_{n,n+1}, l_{n,n+1}, \delta_{n,n+1}$ — respectively stress, length and the thickness of cell/elements $A_nA_{n-1}, A_{n-1}B_{n-1}, B_{n-1}B_n, B_nA_n$ of the n cell;

From the equations of equilibrium of forces in node/units $B_0, A_0, B_1, \ldots, A_{n-1}, B_n$ all stresses are expressed as $s_{11}, s_{22}, \ldots, s_{nn}$ as follows:

$$\left.\begin{array}{l} s_{01}=-\frac{\delta_{11}}{\delta_{01}}s_{11},\quad \bar{s}_{11}=\frac{\delta_{11}}{\bar{\delta}_{11}}s_{11},\quad s_{12}=\frac{\delta_{11}}{\delta_{12}}s_{11}-\frac{\delta_{22}}{\delta_{12}}s_{22};\\ \ldots\ldots\ldots\ldots\ldots\ldots\ldots\ldots\ldots\ldots\\ \bar{s}_{kk}=\frac{\bar{\delta}_{kk}}{\delta_{kk}}s_{kk},\quad s_{k,k+1}=\frac{\delta_{kk}}{\delta_{k,k+1}}s_{kk}-\frac{\delta_{k+1,k+1}}{\delta_{k,k+1}}s_{k+1,k+1},\end{array}\right\} \quad (15)$$

where k=1, 2, ..., n, moreover $\delta_{n+1,n+1}=0$, $\delta_{00}=0$.

Page 85.

The equation of the moment balance of internal and external forces will take the form

$$M = 2\sum_{i=1}^{n} s_{ii}\delta_i F_i. \qquad (16)$$

After using Bredt's generalized formula (14) to the duct/contour of each cell and after connecting equation (16), we will obtain system of equations with n+1 by unknown functions $s_{11}, s_{22}, \ldots, s_{nn}, \theta$:

$$\left.\begin{aligned}
&a_{11} L(s_{11}) + a_{12} L(s_{22}) = \dot{\theta} F_1 + f_1;\\
&a_{21} L(s_{11}) + a_{22} L(s_{22}) + a_{23} L(s_{33}) = \dot{\theta} F_2 + f_2;\\
&a_{32} L(s_{22}) + a_{33} L(s_{33}) + a_{34} L(s_{44}) = \dot{\theta} F_3 + f_3;\\
&\cdots\cdots\cdots\cdots\cdots\cdots\cdots\cdots\cdots\cdots\\
&a_{k,k-1} L(s_{k-1,k-1}) + a_{kk} L(s_{kk}) + a_{k,k+1} L(s_{k+1,k+1}) = \dot{\theta} F_k + f_k;\\
&\cdots\cdots\cdots\cdots\cdots\cdots\cdots\cdots\cdots\cdots\\
&a_{n,n-1} L(s_{n-1,n-1}) + a_{nn} L(s_{nn}) = \dot{\theta} F_n + f_n;\\
&s_{11}\delta_{11} F_1 + s_{22}\delta_{22} F_2 + \ldots + s_{nn}\delta_{nn} F_n = \frac{M}{2},
\end{aligned}\right\} \qquad (17)$$

where

$$\left.\begin{aligned}
&a_{k,k-1} = -\delta_{k-1,k-1}\frac{l_{k-1,k}}{\delta_{k-1,k}};\\
&a_{kk} = \delta_{kk}\left(\frac{\bar{l}_{kk}}{\bar{\delta}_{kk}} + \frac{l_{k-1,k}}{\delta_{k-1,k}} + \frac{l_{kk}}{\delta_{kk}} + \frac{l_{k,k+1}}{\delta_{k,k+1}}\right);\\
&a_{k,k+1} = -\delta_{k+1,k+1}\frac{l_{k,k+1}}{\delta_{k,k+1}},\\
&f_k = -\varphi(\bar{s}_{kk})\bar{l}_{kk} + \varphi(s_{k-1,k})\, l_{k-1,k} - \varphi(s_{k,k})\, l_{kk} - \varphi(s_{k,k+1})\, l_{k,k+1};
\end{aligned}\right\} \qquad (18)$$

θ - the relative angle of twist, common for all cells.

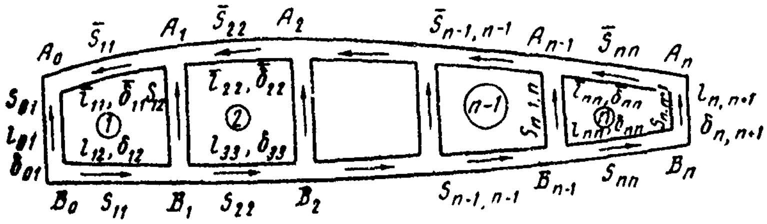

Fig. 1.

Page 86.

After excluding from equations (17) θ and after using reverse/inverse to the linear operator L operator L^{-1}, which has the form

$$L^{-1}z = e^{-3\mu_1 D(\tau-\tau_0)}\{L^{-1}[z(\tau_0)] + 2\mu_1 \int_{\tau_0}^{\tau} z e^{3\mu_1 D(\xi-\tau_0)} d\xi\}, \qquad (19)$$

we will obtain

$$\left.\begin{aligned}
&(a_{11}F_2-a_{21}F_1)s_{11}+(a_{12}F_2-a_{22}F_1)s_{22}-a_{23}F_1s_{33}=\\
&=L^{-1}(f_1F_2-f_2F_1);\\
&a_{21}F_3s_{11}+(a_{22}F_3-a_{32}F_2)s_{22}+(a_{23}F_3-a_{33}F_2)s_{33}-\\
&-a_{34}F_2s_{44}=L^{-1}(f_2F_3-f_3F_2);\\
&\cdots\cdots\cdots\cdots\cdots\cdots\cdots\cdots\\
&a_{k,k-1}F_{k+1}s_{k-1,k-1}+(a_{kk}F_{k+1}-a_{k+1,k}F_k)s_{kk}+\\
&+(a_{k,k+1}F_{k+1}-a_{k+1,k+1}F_k)s_{k+1,k+1}-a_{k+1,k+2}F_ks_{k+2,k+2}=\\
&=L^{-1}(f_kF_{k+1}-f_{k+1}F_k);\\
&\cdots\cdots\cdots\cdots\cdots\cdots\cdots\cdots\\
&a_{n-1,n-2}F_ns_{n-2,n-2}+(a_{n-1,n-1}F_n-a_{n,n-1}F_{n-1})s_{n-1,n-1}+\\
&+(a_{n-1,n}F_n-a_{nn}F_{n-1})s_{nn}=L^{-1}(f_{n-1}F_n-f_nF_{n-1});\\
&\delta_{11}F_1s_{11}+\delta_{22}F_2s_{22}+\ldots+\delta_{nn}F_ns_{nn}=\frac{M}{2}.
\end{aligned}\right\}\quad(20)$$

System (20) determines the stressed state in rod at the any moment of time. Initial conditions are determined from the solution of elasto-plastic problem. The procedure of calculation by the method of successive approximations consists of following. In the 1st approach/approximation we set/assume $\eta=\omega=0$, then $\phi=0$ and $f_k=0$. System (20) will be linear. After solving it, let us find the first approximation for $s_{11}^{(1)}, s_{22}^{(1)}, \ldots, s_{nn}^{(1)}$ and from any equation of system (17) the first approximation for θ. Then on formulas (13), (18), (19) we determine $\varphi(s)$, f_k, $L^{-1}(f_kF_{k+1}-f_{k+1}F_k)$ and for the determination of the second approach/approximation we solve the system of linear equations (20) with the converted right sides, etc. This process is continued before the achievement of the required accuracy/precision of results.

Page 87.

For the caisson whose cross section has two axes of symmetry and consists of four cells from equations (20) for the k iteration we will obtain:

$$\left.\begin{aligned} s_{11}^{(k)} &= -\frac{b_2}{4\delta_{22}F_2 b}M + \frac{1}{b}L^{-1}\Phi^{k-1}; \\ s_{22}^{(k)} &= \frac{\frac{M}{4} - \delta_{11}F_1 s_{11}^k}{\delta_{22}F_2}, \end{aligned}\right\} \quad (21)$$

where

$$b = b_1 - \frac{\delta_{11}F_1}{\delta_{22}F_2}b_2;\; b_1 = a_{11}F_2 - a_{21}F_1;\; b_2 = a_{12}F_2 - (a_{22} + a_{23})F_1;$$

$$\Phi = f_1F_2 - f_2F_1;\; L^{-1}\Phi - e^{-3\mu_1 D(\tau-\tau_0)}\left[bs_{11}(\tau_0) + \frac{b_2}{4\delta_{22}F_2}M(\tau_0) + 2\mu_1\int_{\tau_0}^{\tau}\Phi e^{3\mu_1 D(\xi-\tau_0)}d\xi\right];$$

$$\theta^k(\tau) = \theta(\tau) + \frac{a_{11}}{2\mu_1 F_1}[s_{11}^k - s_{11}(\tau_0)] + \frac{3}{2}\frac{Da_{11}}{F_1}\int_{\tau_0}^{\tau}s_{11}^n d\xi + \frac{a_{12}}{2\mu_1 F_1}[s_{22}^k - s_{22}(\tau_0)] + \frac{3}{2}\frac{Da_{12}}{F_1}\int_{\tau_0}^{\tau}s_{22}^k d\xi - \frac{1}{F_1}\int_{\tau_0}^{\tau}f_1^{k-1}d\xi. \quad (22)$$

Equations (21)-(22) can be used for determining the bearing capacity of caisson and in the absence of creep. In this case, one should assume $f(\sqrt{3}s) = 0$.

Example of numerical computation. Numerical computation was conducted for the caisson, prepared from the material D16A-T whose cross section has two axes of symmetry and consists of four cells, on formulas (21) and (22). In this case, it was accepted $l_{11}=\bar{l}_{11}=l_{22}=$ $=\bar{l}_{22}=300$ мм; $\delta_{11}=\delta_{22}=\bar{\delta}_{11}=\bar{\delta}_{22}=3$ мм; $F_1=F_2=0{,}45\cdot10^5$ мм^2; $l_{01}=l_{12}=l_{23}=150$ мм; $\delta_{01}=\delta_{12}=\delta_{23}=1{,}5$ мм.

Was utilized the power law of creep $\dot{\gamma}^p=\frac{\sqrt{3}}{2}A(\sqrt{3}s)^n$ [here $A=0.16\cdot10^{-8}$ (daN/mm^2)$^{-n}$ 1/min, n=3.1]; the modified time $\tau=\tau(t)$ was assigned by table.

t	0	1	2	3	4	5	10	25	50
τ	0	8	14	17	19,5	22	30	45	70

For describing the instantaneous deformation of material, the real diagram $s\sim\gamma$ was approximated by the dependence

$$\gamma^{\text{мг}}=\frac{s}{2\mu}+\frac{\sqrt{3}}{2}B(\sqrt{3}s)^m=\frac{s}{2\mu}+\frac{\sqrt{3}}{2}\left(\frac{\sqrt{3}s}{\sigma^0}\right)^m$$

(μ=2133 daN/mm^2, σ^0=46 daN/mm^2, m=9).

The calculation of the stressed and state of strain of caisson, which is found under conditions of transient creep, was conducted both for a constant and variable in time external torsional moment.

Page 88.

During calculation entire time interval in question was divide/marked off into the cuts, in each of which they were calculated $s_{11}(\tau)$, $s_{22}(\tau)$, $\theta(\tau)$ with the initial conditions, calculated in the preceding/previous cut, and during the first stage initial conditions were determined from the solution of elasto-plastic problem. For an improvement in the convergence of approach/approximations D and μ_1, it was computed on each cut on the formulas

$$D=A(\sqrt{3}s_{max})^{n-1},\ \mu_1=\frac{1}{\frac{1}{\mu}+\frac{3}{\sigma^0}\left(\frac{\sqrt{3}s_{max}}{\sigma^0}\right)^{m-1}},$$

where $s_{max}=s_{01}$ - the maximum value of the stress in caisson, calculated on the preceding/previous interval of time.

From the solution of elasto-plastic problem which was obtained according to equations (21), (22) and it is represented in Fig. 2, was determined the bearing capacity of caisson $M_{\text{пред}}=1\cdot10^7$ daN•мм. In this case, it was set/assumed A=0, i.e., was eliminated creep, $\eta=1-\left(\frac{s}{s_{max}}\right)^{n-1}$, and a change in the external torsional moment was described by equation $M=M_0+N\tau$, where M_0 was selected in such a way that entire/all construction would be deformed in elastic range. Since s=s(γ) it is increasing function, for the bearing capacity of caisson conditionally was accepted this value of the external torsional moment by which the intensity of strain, determined in the this problem as $\frac{2\gamma}{\sqrt{3}}$, in the most stressed filament reaches 1o/o.

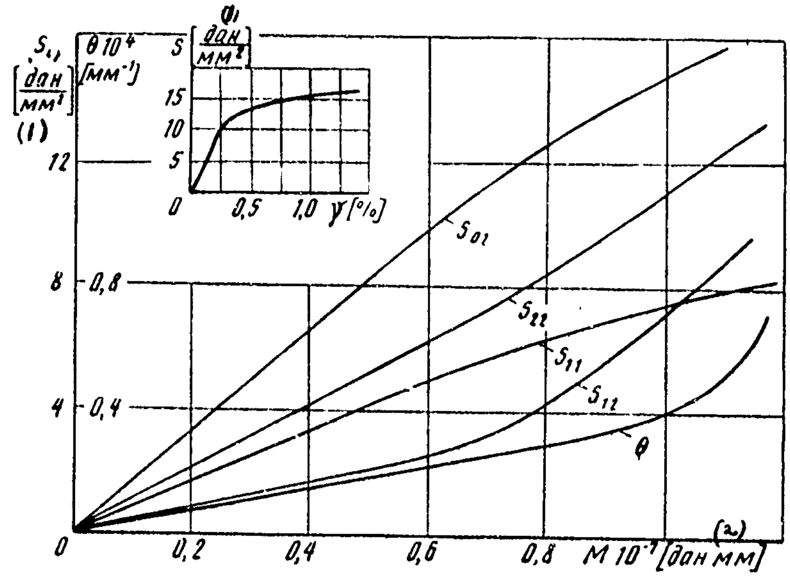

Fig. 2.

Key: (1). daN/mm². (2). daN·mm.

Page 89.

Fig. 3 and 4, give the picture of the redistribution of stresses between the separate cell/elements of caisson and a change in the relative angle of twist in the course of time with the constant in time torsional moment, which comprises $0{,}75\,M_{\text{пред}}$ and the torque/moment, which is changed according to the law $M = M_0 + N\tau(t)$, where $M_0 = 0.424 \cdot 10^7$ DaN·мм, $N = 0.1 \cdot 10^7$ daN·mm/min.

Dotted curves correspond to the calculation, carried out without the account of the plastic properties of material, i.e., B=0 in formula (7). The results of calculation show that upon consideration of the plastic properties of material in construction occurs a more intense increase in the relative angle of twist.

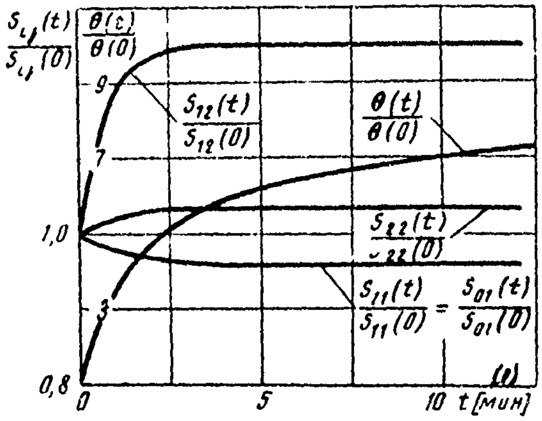

Fig. 3.

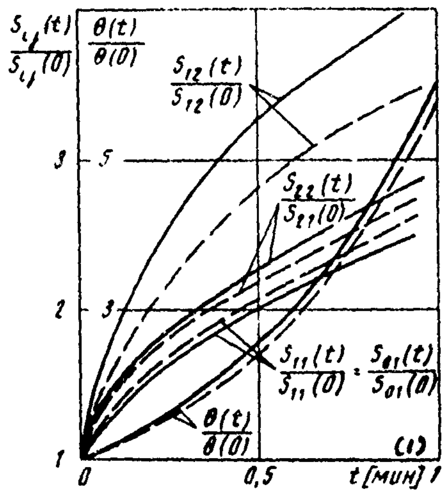

Fig 4.

Key: (1). min.

Fig. 4.

Key: (1). min.

Page 90.

Fig. 5, gives the picture of the redistribution of stresses and a change in the relative angle of twist in the course of time with the cyclically changing external torsional moment. During the decrease of external torsional moment, was accepted linear communication/connection between s and γ, i.e., in formula (7) was accepted B=0.

The obtained results of numerical computation testify to the high velocity of the convergence of successive approximations. So, the disagreement between the stress levels, which correspond to the second and third approach/approximations, they are observed in the third sign.

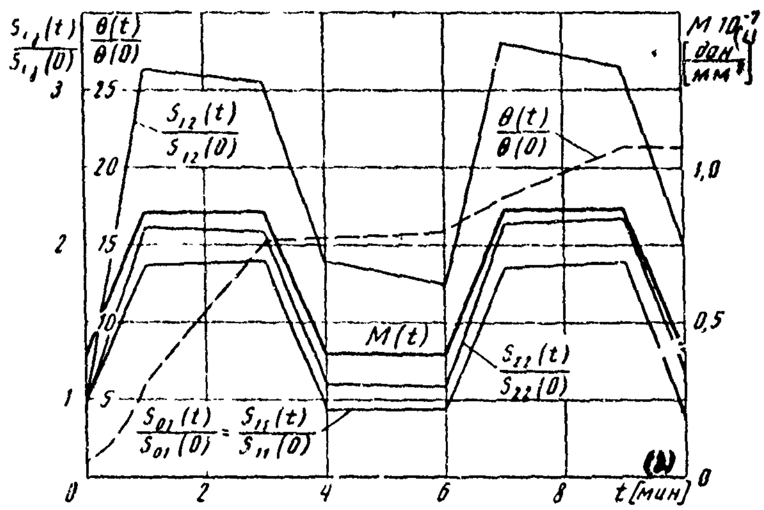

Fig. 5.

Key: (1). daN/mm². (2). min.

REFERENCES.

1. Yu. N. Rabotnov. Creep of the elements of constructions. M., "science", 1966.

2. A. A. Il'yushin, I. I. Pospelov. On the method of successive approximations in the task of transient creep. Engineering journal, Vol. IV, iss. 4, 1964.

3. I. I. Pospelov. Method of successive approximations in the

task of transient creep and nonlinear elasticity. "Scientific notes of TsAGI", No2, 1970.

The manuscript entered 26/VI 1969.

Page 11.

THEORY OF CRITICAL BEHAVIOR OF GAS EJECTOR WITH LARGE PRESSURE DIFFERENTIALS.

V. N. Gusev.

Within the framework of the dynamics of perfect gas, is investigated the critical mode of operation of gas ejector with the cylindrical mixing chamber with large pressure differentials. For the calculation of flow in the jet, overexpanded relative to the static pressure low-pressure gas, is utilized the theory of the hypersonic compressed layer. The calculations conducted confirm the established/installed previously experimentally fact (G. L. Grodzovskiy, Bull. of the AS USSR MZhG, 1968, No 3) which with large pressure differentials attainable compression ratios in ejectors exceed maximum computed values, given by theories developed for the case of the moderate pressure differentials.

The phenomenon of closing in supersonic gas ejector was studied for the first time by M. D. Millionshchikov and G. I. Ryabinkov [1].

In subsequent reports by G. I. Taganova, I. I. Mezhirov, N. A. Nikol'skiy, V. I. Shustov, S. N. Vasil'yev and V. T. Kharitonov [2], [3] the theory of critical behavior it underwent essential refinement. At the moderate pressure differentials, the basic parameters of gas ejector obtained by calculation, were located in good agreement with the results of experiment. Taking into account the mixing of the ejection and ejected flows, critical behavior of the work of gas ejector was examined in works [4] - [6]. Below within the framework of the theory of the flow of perfect gas it is investigated critical operating modes of gas ejector with large pressure differentials.

Let us examine gas ejector with the cylindrical camera/chamber to mixings worker in critical behavior (Fig. 1). Section 1 corresponds to the mixing chamber inlet, section 3 - to an output from it, section 2 is the section of the closing in which in work in critical behaviors the rate of the ejected gas becomes equal to the speed of sound. It is assumed that at the end of the mixing chamber it is realize/accomplished the complete mixing of gases. Let us introduce following designations. p_0' - total pressure high-pressure gas; p_{01} - the total pressure low-pressure gas; p_0'' - total pressure of the mixture, which emerges from ejector; $k_* = \frac{G_1}{G'}$ - critical coefficient of ejection, equal to the ratio of the mass flow rate G_1 of the ejected gas to the mass flow rate G' of the ejection gas under the conditions of closing. The geometric dimensions of ejector are determined by radius r' of the jet of high-pressure gas in section 1 and by radius r" the mixing chamber. Mach number of high-pressure gas in section 1 let us designate through M_1'.

Let us pause at the special feature/peculiarities of the discharge of high-pressure gas jet with large pressure differentials. Since the static pressure high-pressure gas in section 1 is greater static pressure low-pressure gas in this same section, the expansion of gas occurs out of nozzle and is spread in flow on centered on nozzle discharge edge rarefaction wave. Considerable zone of flow in jet proves to be overexpanded relative to the static pressure low-pressure gas. Flow in this region will approach flow from certain equivalent source whose intensity changes during transition from one ray/beam to another [7].

Page 92.

The degree of increase in flow in jet will be determined by the system of those limit of overexpansion zone of flow of the shock waves. The gas, passed through the suspended shock wave I (see Fig. 1), forms the adjacent the jump compressed layer, which concentrates in itself the large part of high-pressure gas [7]. Thus, the flow of gas in the high-pressure jet of gas ejector will be not only heterogeneous, but also it will consist, generally speaking, of two-qualitatively different flows. It is obvious that this flow cannot be described within the framework of hydraulic theories.

At sufficiently high values $\bar{p}'_0 = \frac{p'_0}{p_{01}}$ for the duct/contour of the compressed layer it is possible to write [17]:

$$\frac{d^2 f}{d\varphi^2} = f + \frac{2}{f}\left(\frac{df}{d\varphi}\right)^2 - \frac{2\pi r'^2 p'_0}{QU_m}\sin\varphi\left[f^2 + \left(\frac{df}{d\varphi}\right)^2\right]^{\frac{3}{2}} \times$$
$$\times\left[\frac{p}{p'_0} - \frac{2\gamma}{\gamma+1}M'^2\sin^2\varepsilon\left(\frac{\gamma-1}{2}M'^2\right)^{-\frac{\gamma}{\gamma-1}}\right], \qquad (1)$$

where

$$\varepsilon = \mu - (\varphi - \theta'),\ \mu = \operatorname{arctg}\left(-f \Big/ \frac{df}{d\varphi}\right).$$

Here r, φ - polar coordinates with pole at point O (see Fig. 1), $f(\varphi) = \frac{r}{r'}$ - a duct/contour of shock,

ε - angle of the slope of jump to the direction of the incident flow,

μ - the angle, formed by the direction of radius-vector r and by the direction of tangent to the duct/contour of jump, Q - a total gas flow through the compressed layer,

U_m - maximum speed,

M and θ - a Mach number and the angle of the slope of velocity vector before the shock layer in high-pressure gas,

p - variable pressure on the outer edge of the compressed layer,

γ - specific heat ratio in high-pressure gas.

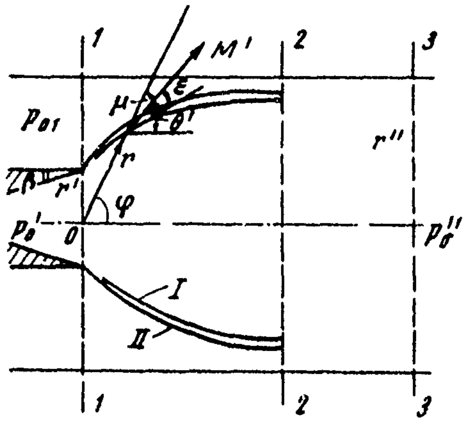

Fig. 1.

Page 13.

Assuming the flow of low-pressure gas one-dimensional, for pressure on the outer edge of compressed layer II (see Fig. 1) we have:

$$p = p_{01}\left(1+\frac{\varkappa-1}{2}M^2\right)^{-\frac{\varkappa}{\varkappa-1}};\qquad(2)$$

M it is determined from the flow equation:

$$M\left(1+\frac{\varkappa-1}{2}M^2\right)^{-\frac{\varkappa+1}{2(\varkappa-1)}}=$$

$$=M_1\left(1+\frac{\varkappa-1}{2}M_1^2\right)^{-\frac{\varkappa+1}{2(\varkappa-1)}}\left[\left(\frac{r''}{r'}\right)^2-1\right]\left[\left(\frac{r''}{r'}\right)^2-(f\sin\varphi)^2\right]^{-1}.$$

Here M_1 - Mach number of low-pressure gas in cross section 1,

$\varkappa$ - specific heat ratio in low-pressure gas.

Substituting (2) in equation (1), for the duct/contour of high-pressure jet, finally we will obtain:

$$\frac{d^2 f}{d\varphi^2} = f + \frac{2}{f}\left(\frac{df}{d\varphi}\right)^2 - \frac{2\pi r'^2 p_0'}{QU_m}\sin\varphi\left[f^2 + \left(\frac{df}{d\varphi}\right)^2\right]^{\frac{3}{2}} \times$$
$$\times\left[\left(\frac{p_{01}}{p_0'}\right)\left(1 + \frac{\varkappa - 1}{2}M_1^2\right)^{-\frac{\varkappa}{\varkappa-1}} - \frac{2\gamma}{\gamma + 1}M'^2\sin^2\varepsilon\left(\frac{\gamma - 1}{2}M'^2\right)^{-\frac{\gamma}{\gamma-1}}\right]. \quad (3)$$

The entering the equation values Q, M' and θ' are the functions of the polar coordinates and parameters M_a', β, γ. With f >> 1 for them, are valid the asymptotic dependences, given in [7]. These functions were determined numerically by method of characteristics from the program, comprised on the basis of the procedure for of calculation and formulas, presented in [8]. The boundary conditions of task take form [7]:

$$f = 1,\ \frac{df}{d\varphi} = f'_{*1}\ \text{при}\ \varphi = \frac{\pi}{2}, \qquad (4)$$

Key: (1). with.

Where

$$f'_{*1} = \frac{-M_{*1}^2 \sin 2\theta_{*1} + [M_{*1}^4 \sin^2 2\theta_{*1} - 4(M_{*1}^2 \cos^2\theta_{*1} - 1)(M_{*1}^2 \sin^2\theta_{*1} - 1)]^{\frac{1}{2}}}{2(M_{*1}^2 \cos^2\theta_{*1} - 1)};$$

$$\theta_{*1} = \beta + \left\{\left(\frac{\gamma+1}{\gamma-1}\right)^{\frac{1}{2}} \operatorname{arctg}\left[\left(\frac{\gamma-1}{\gamma+1}\right)^{\frac{1}{2}} \sqrt{M_{*1}^2 - 1}\right] - \operatorname{arctg}\sqrt{M_{*1}^2 - 1}\right\} - \left\{\left(\frac{\gamma+1}{\gamma-1}\right)^{\frac{1}{2}} \operatorname{arctg}\left[\left(\frac{\gamma-1}{\gamma+1}\right)^{\frac{1}{2}} \sqrt{M_1'^2 - 1}\right] - \operatorname{arctg}\sqrt{M_1'^2 - 1}\right\};$$

$$M_{*1} = \sqrt{\frac{2}{\gamma-1}\left[\bar{p}_0'^{\frac{\gamma-1}{\gamma}}\left(1 + \frac{\varkappa-1}{2} M_1^2\right)^{\frac{\varkappa(\gamma-1)}{\gamma(\varkappa-1)}} - 1\right]}.$$

With the assigned/prescribed jump/drop p'_0 and the geometry of ejector $\frac{r''}{r'}$ the integration of equation (3) was conducted at several values M_1, thus far in section 2 when $\mu = 0$ mach number of low-pressure gas did not reach the speed of sound.

After the determination of M_1 for the critical coefficient of ejection, it is possible to write

$$k_* = \frac{q(\lambda_1)}{\alpha\theta\, \bar{p}_0'\, q(\lambda_1')}. \qquad (5)$$

Adding to equation (5) the known equations of the ejection

$$\left.\begin{aligned}\bar{p}_0^{\prime\prime} &= \frac{q(\lambda_1)+a\bar{p}_0^{\prime}q(\lambda_1^{\prime})}{(1+a)q(\lambda^{\prime\prime})}\sqrt{1+k^{*}\vartheta\frac{z(\vartheta)-2}{(1+k_{*}\vartheta)^2}}\,;\\ z(\lambda^{\prime\prime}) &= \frac{q(\lambda_1)z(\lambda_1)+a\bar{p}_0^{\prime}q(\lambda_1^{\prime})z(\lambda_1^{\prime})}{q(\lambda_1)+a\bar{p}_0^{\prime}q(\lambda_1^{\prime})}\left[1+k_{*}\vartheta\frac{z(\vartheta)-2}{(1+k_{*}\vartheta)^2}\right]^{-\frac{1}{2}},\end{aligned}\right\}\quad(6)$$

we will obtain the complete system of equations, which determines the parameters of the ejector, working in critical behavior.

Page 94.

In last/latter relationship/ratios it is accepted: λ - derived rate, ϑ - relation of the critical speeds of ejection and ejected gases, $q(\lambda)$, of $z(\lambda)$ - gas-dynamic functions, $\bar{p}_0^{\prime\prime}=\frac{p_0^{\prime\prime}}{p_{01}}$ - compression ratio of ejector, $a=\left[\left(\frac{r^{\prime\prime}}{r^{\prime}}\right)^2-1\right]$.

Fig. 2, depicts the dependences $\bar{p}_0^{\prime\prime}$ on $\bar{p}_0^{\prime}$ at different values k_* and $(r^{\prime\prime}/r^{\prime})^2\geqslant 20$ with $\gamma=\varkappa=1{,}4,\ M_1^{\prime}=1,\ \vartheta=1$ and β = 0 (unbroken curves).

At smaller values $\left(\frac{r^{\prime\prime}}{r^{\prime}}\right)^2$ the calculations were not performed, since here are disrupted applicability conditions of the theory of the hypersonic compressed layer. For a comparison on this same figure at the same values k_* are given the experimental data, borrowed from work [6] (dotted curves), and calculated - according to the theory of critical behavior [2] (dot-dash curves).

As it follows from Fig. 2, the calculations conducted confirm established/installed previously experimentally fact [6] that with large jump/drops in pressure $\bar{p}_0'$ attainable compression ratios in ejectors exceed maximum computed values according to theory [2]. In this case, maximum compression ratio of ejector will be realized with greater than according to theory [2], values $\bar{p}_0'$.

Let us pause at the case $k_* = 0,$ determining maximum compression ratio of ejector with the assigned/prescribed jump/drop in the pressure $\bar{p}_0'$. In this case the Mach number of low-pressure gas at the mixing chamber inlet M_1 = 0, and critical behavior of the work of ejector in the setting accepted will be determined from the natural condition of expansion of jet of high-pressure gas to the transverse size/dimension of the chamber of mixing r*. In this case the total pressure low-pressure gas p_0' will be equal to the external to pressure in space, where escapes jet. At high values of the pressure gradient $\bar{p}_0' = \frac{p_0'}{p_{01}}$ the discharge of such jets into space with constant pressure was examined in work [7]. In specific heat ratio in high-pressure gas $\gamma = 1.4$ $M_1' = 1$ and $\theta = 1$ these data (unbroken curve), together with experimental (triangles), borrowed from work [9], represented in Fig. 3 in the form of dependence on a jump/drop in the pressure $p_0' = \frac{p_0'}{p_{01}}$ the maximum removal/distance $\frac{r''}{r'}$ of suspended shock wave from the axle/axis of jet on the assumption that the thickness of the adjacent the jump compressed layer is negligible. Here corrected values $\frac{r''}{r'}$ for the series of the sonic ejectors, working in critical behavior when $k_* = 0$ (small circles - experiment [6], dotted curve - theory of critical behavior [2]).

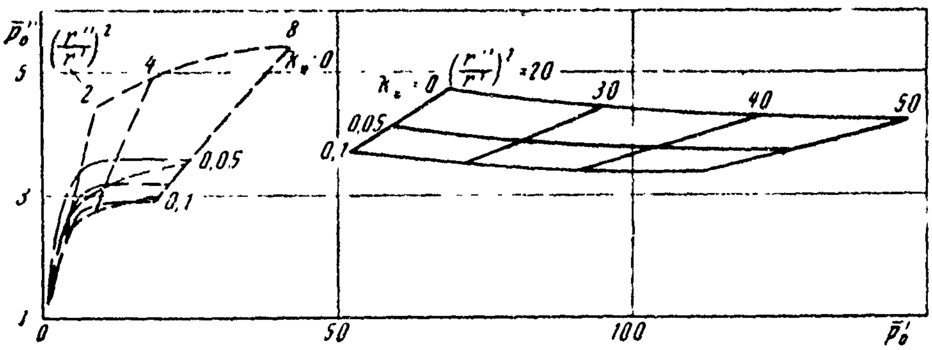

Fig. 2.

Page 95.

Comparison shows that with an increase in the jump/drop in the pressure p_0' the experimental values $\frac{r''}{r'}$ will move away from theoretical dependence [2], approaching values $\frac{r''}{r'}$, by that determined in the maximum removal/distance of suspended shock wave from the axle/axis of jet with its flow into space with constant pressure.

When $k_* = 0$ system (6) for the calculation of compression ratio of ejector is converted to the form

$$\left.\begin{aligned} \bar{p}_0 &= \frac{\alpha \bar{p}_0' q(\lambda_1')}{(1+\alpha) q(\lambda'')}; \\ z(\lambda'') &= z(\lambda_1') + \frac{\left(\frac{\gamma+1}{2}\right)^{\frac{1}{\gamma-1}}}{\alpha p_0' q(\lambda_1')}. \end{aligned}\right\} \quad (7)$$

In the case of the sonic ejector ($M_1' = 1$) when $\gamma = 1.4$ results of the calculations of maximum compression ratic of ejector depending on $\bar{p}_0'$ when $k_* = 0$ are given tc Fig. 2. From the comparison of findings with the experimental [6] it follows that the dependence $\bar{p}_0''(\bar{p}_0')$ when $k_* = 0$ has a maximum at finite value $\bar{p}_0'$ and $\bar{p}_0' \to \infty$ approaching a constant value.

Let us determine the limiting values of compression ratio of ejector when $k_* = 0$ in the case of infinite jump/drops in the pressure $\bar{p}_0'$. For entering the equations ejection (7) of value $\frac{r''}{r'}$, determined here for the maximum removal/distance of suspended shock wave from the axle/axis of jet during its discharge in space with constant pressure, from work [7] it follows:

$$\left(\frac{r''}{r'}\right)^2 = \xi(\gamma, \beta, M_1')\,\bar{p}_0'. \quad (8)$$

When $\bar{p}_0' \gg 1$

$$\alpha=\left[\left(\frac{r''}{r'}\right)^2-1\right]^{-1}\approx\left(\frac{r''}{r'}\right)^{-2}=\frac{1}{\xi(\gamma,\ \beta,\ M_1')\,\bar{p}_0'}\,.$$

and the equations of ejection (7) taking into account (8) are converted to the form, which does not depend on $\bar{p}_0'$:

$$\left.\begin{aligned}\bar{p}_0''&=\frac{q(\lambda_1')}{\xi(\gamma,\ \beta,\ M_1')\,q(\lambda'')};\\ z(\lambda'')&=z(\lambda_1')\quad\frac{\left(\frac{\gamma+1}{2}\right)^{\frac{1}{\gamma-1}}\xi(\gamma,\ \beta,\ M_1')}{q(\lambda_1')}\,.\end{aligned}\right\}\qquad(9)$$

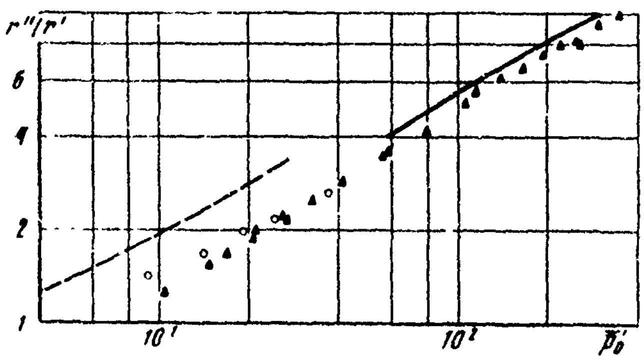

Fig. 3.

Page 96.

In the case $\gamma = 1.4$ and $\beta = 0$ at the values of number $M_1'=1$ and 3, for which those entering in (9) values $\xi(\gamma, \beta, M_1')$ were determined in work [7], the limiting values of compression ratio of ejector when $k_*=0$ were given in the table:

M_1'	ξ	$\bar{p}_0^*$
1	0,37	3,76
3	0,033	10,5

Comparison shows that when $p_0' \gg 1$ the transition from the sonic ejector to supersonic leads to an essential increase in compression ratio of ejector.

In conclusion the author thanks to T. V. Klimov for aid in conducting of the necessary calculations.

REFERENCES

1. G. N. Abramovich. Applied gas dynamics. M., the State Technical Press, 1953.

2. Yu. N. Vasiliev. Theory of supersonic ejector with the cylindrical mixing chamber. Coll. "rotodynamic machines and jet apparatuses", iss. 2. M., "Mashinostroyeniye", 1967.

3. V. T. Kharitonov. Investigation of the effectiveness of gas ejector with the cylindrical mixing chamber. Thermal-power engineering, No 4, 1958.

4. W. L. Chow, A. L. Addy. Interaction between primary and secondary streams of supersonic ejector systems and their performance characteristics. AIAA J, v 2, No 4, 1964.

5. Yu. K. Arkadov. Gas ejector with the nozzle, perforate/punched by the longitudinal slots. Izv. of the AS USSR,

MZhG, No 2, 1968.

6. G. L. Grodzovskiy. To the theory of the gas ejector of high compression ratio with the cylindrical mixing chamber. Izv. of the AS USSR, MZhG, No 3, 1968.

7. V. N. Gusev, T. V. Klimova. Flow in escaping from those underexpanded it puffed jets. Bull. of the AS USSR MZhG, No 4, 1968.

8. O. N. Katskova, I. N. Naumova, Yu. D. Shmyglevskiy, N. P. Shulina. Experiment in the calculation of the plane and axisymmetrical supersonic flows of gas by method of characteristics of the CC of the AS USSR, 1961.

9. K. Bier, B. Schmidt. Zur form der Verdichtungsstove in Frei expandierenden Gasstrahlen. Z fur angewandte Physik, HF 11, 1961.

Received 30/VII 1969.

Page 97.

KINETIC THEORY OF BOUNDARY LAYER BETWEEN PLASMA AND A MAGNETIC FIELD.

N. G. Korshakov.

On the basis of kinetic equations and the equations of Maxwell, they are derive/concluded and are solved by ETsVM [ЭЦВМ - digital computer] of the equation of the boundary layer between the plasma and the magnetic field during the Maxwellian function of particle distribution in the undisturbed plasma. Is obtained the distribution of the basic values, which characterize transition layer in its entire width.

Basic results in boundary-layer theory between the plasma and the magnetic field were obtained by the authors, imposing following limitations for the formulation of the problem: the simplified form of the function of particle distribution in the flow, encountering for magnetic field [1] - [3], the absence of electric fields and polarization of plasma [4] - [5] or construction of the functions of distribution across the boundary layer, giving possibility to obtain simple analytical formulas for the values, characterizing the structure of layer [6].

The first attempt to remove/take some of these limitations was undertaken by Yu. S. Sigov, who solved in [5], [7] - [9] the problem of reflection by the magnetic wall of the plasma ion flow and electrons. Striving to get rid of the infinite values of density and current at the turning point of particles, that appear in the case of monoenergetic flow, it replaced them with step functions. By the following space in the trend of development of boundary-layer theory between the plasma and the magnetic field is the examination of "natural" Maxwellian function of particle distribution in the undisturbed plasma and appearing between them and the magnetic field of interlayer. In article will be solved the task of the structure of two-dimensional boundary layer during the Maxwellian function of particle distribution in the undisturbed plasma.

In work [4] was derived integrodifferential equation for a vektor potential (case only of magnetic boundary layer) and is obtained the distribution of magnetic field. As it will be evident, this case is in a sense maximum for a common/general/total task. Therefore in article is first obtained a simpler differential equation for vector potential, which makes it possible to obtain the distribution of the remaining characteristic values of layer.

Simplification in the equation in comparison with that given in work [4] is achieved because of use as the initial position for the derivation not of the equation of the balance of pressures in boundary layer, but the equation of Maxwell, or as a result of the fact that the ranges of integration in phase space are examined in the alternating/variable particle speed, and not energy and generalized momentum. In the formulation of the problem of any simplifying assumptions in comparison with those accepted in work [4] made.

Page 18.

MAGNETIC BOUNDARY LAYER.

The adopted system of coordinates is given to Fig. 1. The formulation of the problem is well known from [4]. The rarefied plasma (to the left of interlayer) is given into contact with magnetic field. Due to the absence of the collisions through some time interval all processes in interlayer can be considered as being steady. Task is one-dimensional, i.e., all values depend only on one coordinate x. Plasma when $x \to -\infty$ is described by the Maxwellian distribution function for ions and electrons. There are no seized particles within layer.

As examples it is possible to give two cases of the realization of the picture indicated: either negative and positive particles have an equal mass, identical Larmorov radii; therefore there is no separation of charges and electric field does not appear or electrons possess such values of the parameters and are distributed so that the separation of charges can be disregarded. The possibility of the realization of this case will be examined below.

The structure of layer is described by equation with self-consistent field for functioning particle distribution and the equation of Maxwell:

$$u\frac{\partial f}{\partial x}+\frac{e}{Mc}[\vec{v}H]\frac{\partial f}{\partial\vec{v}}=0, \qquad (1)$$

$$\Delta A=\frac{4\pi}{c}j. \qquad (2)$$

Here u - composing particle speed along axle/axis x, $H=[\nabla A]$.

Density and current are expressed by the appropriate torque/moments from the distribution function:

$$j=e\int vf(x,\vec{v})\,d\vec{v},\quad n=\int f(x,\vec{v})\,d\vec{v}. \qquad (3)$$

and $A'(+\infty) = H_0$.

The distribution function of ions when $x \to -\infty$

$$f(x, v) = n_0 \frac{M}{2\pi T} \exp\left[-\frac{M(u^2+v^2)}{2T}\right].$$

(subsequently by the index "0" are noted the values of variables when $x \to -\infty$).

That composing particle speed along the axis z can be without the limitation of generality placed equal to zero. Equation (1) has three integrals and solution (1) will be random function from these integrals.

Let us introduce the dimensionless variables

$$\bar{u} = u\sqrt{\frac{M}{2T}}, \quad \bar{v} = v\sqrt{\frac{M}{2T}}, \quad a = \frac{eA}{c\sqrt{MT}}, \quad x_0 = \left(\frac{Mc^2}{4\pi n_0 e^2}\right)^{\frac{1}{2}},$$

$$\bar{x} = \frac{x}{x_0}, \quad \bar{j} = \frac{j}{en_0}\sqrt{\frac{M}{2T}}$$

and let us replace of variables in expressions (3) for density and current $(u, v) \to (u_0 v_0)$. Then the arbitrary function of distribution f(u, v) passes into known $f(u_0, v_0)$, that depend on constants of motion of particle. Integration limits in expression (3) $u^2 \geqslant 0$ $u_0^2 \geqslant 0$ will pass in $u_0^2 \geqslant u^2 - 2v_0 u$, $u_0^2 \geqslant 0$

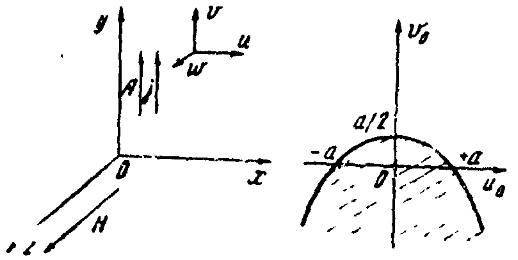

Fig. 1.

Page 99.

The region of integration is shown in Fig. 1. Point x of boundary layer, reach the particles with phase coordinates, which are located out of the limits of the shaded range, limited by parabola. Calculating torque/moments from (3) and introducing function $Z_\nu = \exp\left(-\frac{x^2}{4}\right) D_\nu(x)$ [10], we will obtain equation for a vektor potential (Fig. 2):

$$a'' = \frac{2^{-3/4}}{\sqrt{\pi}} \sqrt{a}\, Z_{-\frac{1}{2}}\left(\frac{a}{\sqrt{2}}\right). \qquad (4)$$

where $D_\nu(x)$ – function of parabolic cylinder.

Respectively

$$\frac{n}{n_0} = 1 - \frac{2^{-\frac{1}{4}}}{\sqrt{\pi}} \int_0^a \frac{Z_{\frac{1}{2}}\left(\frac{a}{\sqrt{2}}\right)}{\sqrt{a}}\, da. \qquad (5)$$

Equation (4) has the integral:

$$a'^2+n+\frac{2^{-\frac{1}{4}}}{\sqrt{\pi}}\sqrt{a}\,Z_{-\frac{3}{2}}\left(\frac{a}{\sqrt{2}}\right)=1.$$

Function $Z_{-\frac{1}{2}}(x)$ does not have zeros with real x; therefore vektor potential increases monotonically and parabola in Fig. 1 does not have sections of backward action.

Boundary conditions take the form $a(-\infty)=0$ (this always can be obtained from the condition of gauge invariance) and $a'(+\infty)=1$ (it is obtained from the condition of equality pressures plasma and magnetic on both sides of boundary).

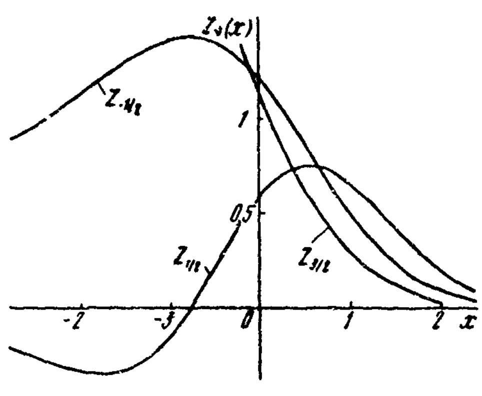

Fig. 2.

Page 100.

Utilizing an asymptotic representation of function $Z_{-\frac{1}{2}}'(x)$ at the low values of the argument, we will obtain when $x \to -\infty$ expression for a vektor potential $a = \frac{1}{576\Gamma\left(\frac{3}{4}\right)^2}(x - x_0)^4$, from which evident that boundary condition is satisfied with final x_0, i.e. there exists the interface between the plasma and the magnetic field. Accepting $x_0 = 0$, we will obtain the following asymptotic formulas:

$$a' = \frac{1}{144\Gamma\left(\frac{3}{4}\right)^2} x^3, \quad j = \frac{1}{24\Gamma\left(\frac{3}{4}\right)} x^2, \quad n = 1 - \frac{1}{12\Gamma\left(\frac{1}{4}\right)\Gamma\left(\frac{3}{4}\right)} x^3.$$

Let us note that the given in work [4] asymptotic dependence of magnetic field on coordinate is inaccurate due to the stealing in in calculations error.

In the point of section, all basic values and their first-order derivatives are continuous.

Equation (4) with conditions $a(0) = 0,\ a'(+\infty) = 1$ was integrated by ETsVM. Results are given to Fig. 3. It is easy to establish that

$R_{\Pi_i} = x_0$ in the case in question and the width of boundary layer is 8-10 Larmorov ionic radii.

Let us now move on to more common/general/total task.

POLARIZED BOUNDARY LAYER.

Coordinate system, accepted for this task, given to Fig. 4. Let us again introduce the condition of the rarefaction of the plasma (mean free paths of particles considerably exceed their Larmorov radii). This allows for the time intervals greater than the set-up time of all values, which characterize the structure of interlayer, but less than the characteristic time of the collisions of particles, to consider task as stationary. Task one-dimensional, i.e., a change in all values occurs only along the axis x.

When $x \to -\infty$ there is two-component, nonpolarized plasma with the Maxwellian distribution function of ions and electrons and characterized by the values of the parameters $\mu = \frac{m_e}{m_i}$ (where m_e - a mass of electron, and m_i - a mass of ion) and $\lambda = \frac{T_e}{T_i}$, i.e. by the relation of electronic and ionic temperatures. There are no seized particles in transition layer. All particles, entering the boundary layer, emerge it. Task let us examine in nonrelativistic setting.

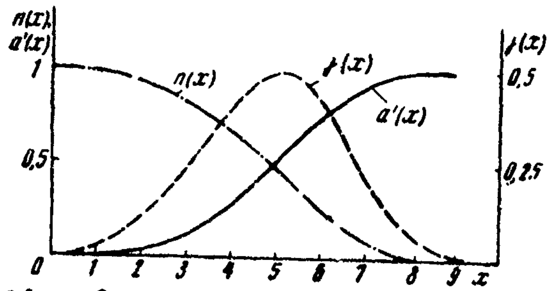

Fig. 2.

Page 101.

Let us write the equations of Boltzmann without account the collision of particles and equations of Maxwell for ions and electrons, that describe a change of the basic parameters of plasma in the transition layer:

$$u\,\frac{\partial f_{ie}}{\partial x}+\frac{e_{ie}}{m_{ie}}\left(\vec{E}+\frac{1}{c}\,[\vec{v}\vec{H}]\,\frac{\partial f_{ie}}{\partial \vec{v}}\right)=0; \qquad (6)$$

$$\left.\begin{aligned}&\Delta\Phi(x)=-4\pi e\,(n_i-n_e);\\&\Delta A(x)=\frac{4\pi}{c}\,(j_e+j_i);\\&E=-\nabla\Phi,\ H=[\nabla A].\end{aligned}\right\} \qquad (7)$$

Equations (6) have all of six integrals, which express the laws of conservation of energy and generalized momentum for the system of particles - the field:

$$\left.\begin{aligned}&u^2+v^2+w^2+\frac{2e_{ie}\Phi}{m_{ie}}=(c_1^{ie})^2;\\&v+\frac{e_{ie}A}{m_{ie}c}=c_2^{ie};\\&w=c_3^{ie}.\end{aligned}\right\} \qquad (8)$$

Subsequently without the limitation of generality, let us assume that $c_3^{ir}=0$. Furthermore, if we require, in order to $\Phi, a \to 0$ when $x \to -\infty$, then c_1^2 and c_2 will represent the kinetic energy and the y-th component of the velocity of the particle, respectively.

The solution of equations (6) will be a random function of integrals (8). Let us substitute them in the moments for density and current:

$$\left.\begin{aligned} j_{el} &= e\int v_{el} f_{el}(x, \vec{v})\, d\vec{v}; \\ n_{el} &= \int f_{el}(x, \vec{v})\, d\vec{v}. \end{aligned}\right\} \quad (9)$$

Integration in (9) takes place with respect to all particles reaching point x of the boundary layer.

The systems of equations (7) is of the fourth order and four boundary conditions are necessary for it. Two of them ($A \to 0$, $\Phi' \to 0$) with $x \to -\infty$, As the third condition we take: $\Phi' \to 0$ when $x \to +\infty$. The fourth boundary condition will be the requirement of that, so that the magnetic field when $x \to +\infty$ would have a value, ensuring the equilibrium of boundary layer as a whole (equality pressure in the plasma when $x \to -\infty$ and of magnetic field when $x \to +\infty$):

$$\frac{A'^2(+\infty)}{8\pi} = \langle p_{xx}(-\infty)\rangle. \quad (10)$$

Let us introduce the dimensionless variables:

$$\bar{\Phi} = \frac{e\Phi}{m_e c_{T_e}^2}, \quad a = \frac{eA}{m_e c c_{T_e}}, \quad \bar{x} = \frac{x}{x_0},$$

$$x_0 = \left(\frac{m_e c^2}{4\pi n_0 e^2}\right)^{\frac{1}{2}}, \quad \bar{u} = \frac{u}{c_{T_e}}, \quad \bar{v} = \frac{v}{c_{T_e}}.$$

where $c_{T_e} = \sqrt{\frac{2T_e}{m_e}}$ - characteristic thermal electronic rate,

n_0 - an electron density or ions when $x \to -\infty$

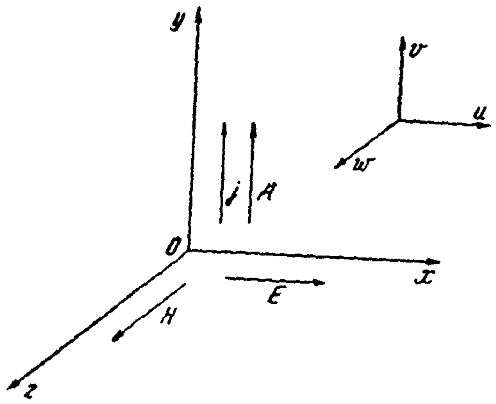

Fig. 4.

Page 102.

Then (10) it is rewritten in the form

$$a_{\infty}^{'2} = 1 + \frac{T_i}{T_e} = 1 + \varkappa^{-1}. \qquad (10')$$

The conditions of integration in (9) take the form (for example, for electrons) $u^2 \geqslant 0,\ u_0^2 \geqslant 0$ or, utilizing the appropriate integrals, $u_0^2 \geqslant 0,\ u_0^2 \geqslant -2\Phi + a^2 + 2av_0$.

(Here and subsequently let us drop/omit marks about dimensionless variables).

Let us pass in formulas (9) from the plane of variables (u, v) to (u_0, v_0). Range of integration is the exterior of parabola (Fig. 5a). Within the phase space, next by parabola, are located all those particles which turned conversely towards plasma, ahaving reached point x of boundary layer. With motion to the side positive x the parabola is opened, and its apex/vertex moves down along the axis of ordinates (of what it is possible to be convinced after concrete/specific/actual calculations by ETsVM). Analogous position exists for the ions (see Fig. 5b).

After expressing the torque/moments of distribution function and after leading them to dimensionless form, we will obtain the system of the fourth order for the vector and magnetic potentials:

$$a'' = \frac{2^{-\frac{3}{4}}}{\sqrt{\pi}} \sqrt{a} \left\{ Z_{-\frac{1}{2}}(\alpha) + \lambda^{-\frac{1}{4}} \mu^{\frac{3}{4}} Z_{-\frac{1}{2}}(\beta) \right\}, \quad (11)$$

$$\frac{1}{\tau} \Phi'' = n_e - n_i, \quad (12)$$

where

$$n_e = \exp(2\Phi) - \frac{2^{-\frac{1}{4}}}{\sqrt{\pi}} \int_0^a \frac{Z_{\frac{1}{2}}(\alpha)}{\sqrt{a}} da; \quad (13)$$

$$n_i = \exp(-2\lambda\Phi) - (\lambda\mu)^{\frac{1}{4}} \frac{2^{-\frac{1}{4}}}{\sqrt{\pi}} \int_0^a \frac{Z_{\frac{1}{2}}(\beta)}{\sqrt{a}} da; \quad (14)$$

$$\left.\begin{aligned} \alpha &= \sqrt{2}\left(\frac{a}{2} - \frac{\Phi}{a}\right); \\ \beta &= \sqrt{2\mu\lambda}\left(\frac{a}{2} + \frac{1}{\mu}\frac{\Phi}{a}\right). \end{aligned}\right\} \quad (15)$$

Let us draw some conclusions from these equations. Function $Z_{-\frac{1}{2}}(x)$ is strict positive on an entire range of change real variable x; therefore vektor potential and magnetic field increase strictly monotonically.

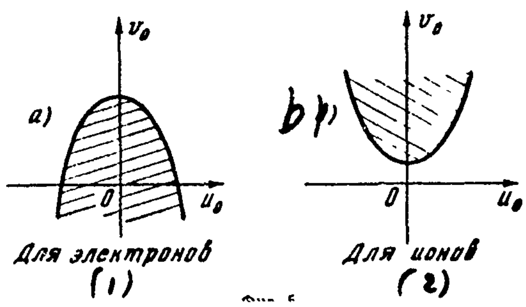

Fig. 5.

Key: (1). For electrons. (2). For ions.

Page 103.

Potential Φ is limited; therefore when $x \to +\infty$ α, $\beta \to +\infty$ and, therefore, the currents of electrons and ions vanish. When $x \to -\infty$ $\alpha \to 0$ and therefore on the basis of limitedness $Z_{-\frac{1}{2}}(x)$ ion and electronic current when $x \to -\infty$ vanishes.

In equation (12) the parameter $\tau = \frac{c^2}{c_{T_e}^2}$ or $\tau^{-1} = 4E \cdot 10^{-6}$ (E - in electron volts) is sufficiently low. Therefore equation (12) - equation with the low parameter at higher derivative at the energies, distant from the relativistic.

One of conditions has form $n_e'(+\infty) = n_i'(+\infty) = 0$. By the unique value of the potential Φ_∞, that satisfying this condition, on the basis of (13)-(14), as showed experiment in machines, it is $\Phi_\infty = 0$.

One of the special feature/peculiarities of equations (11)-(12) is the fact that into the argument of the functions, which stand in the right side of the equations, enters the relation $\gamma = \frac{\Phi}{a}$. When $x \to -\infty$ and $a \to 0$, $\Phi \to 0$ and this sense becomes not defined. Let us calculate it when $x \to -\infty$ according to l'Hospital's rule

$$\gamma = \lim \frac{\Phi}{a} = \lim \frac{\Phi'}{a'} = \lim \frac{\Phi''}{a''}$$

and let us substitute within last/latter limit the right sides of equations (11)-(12). We will obtain transcendental equation for γ:

$$f(\gamma) = (\lambda\mu)^{\frac{1}{4}} Z_{\frac{1}{2}}\left(\sqrt{2\frac{\lambda}{\mu}}\gamma\right) - Z_{\frac{1}{2}}(-\gamma\sqrt{2}) - \\ - \frac{\gamma}{2\tau\sqrt{2}}\left[Z_{-\frac{1}{2}}(-\gamma\sqrt{2}) + \lambda^{-\frac{1}{4}}\mu^{\frac{3}{4}} Z_{-\frac{1}{2}}\left(2\sqrt{\frac{\lambda}{\mu}}\gamma\right)\right] = 0. \qquad (16)$$

The roots of equation (16) can be determined by ETsVM. As became clear, equation (16) has three roots $\left(\mu = \frac{1}{1836}\right.$ subsequently):

1. $\gamma \approx -\sqrt{\tau}$;
2. $\gamma \approx +\sqrt{\tau}$;
3. $\gamma \approx -0{,}54$.

All three roots very weakly depend on the parameter λ.

The asymptotic solutions of equations (11)-(12) when $x \to -\infty$ take the form

$$a = k_1 (x - x_0)^4; \quad \Phi = k_2 (x - x_0)^4. \qquad (17)$$

It is evident that the boundary conditions are realized with final x_0 Let us accept $x_0 = 0$.

Integration in the machine of equations (11)-(12) with the conditions at left end/lead, which are obtained, if we take roots of 1 or 2, it showed that the solutions do not satisfy right boundary conditions, the ionic density or electrons increases exponentially. In this case let us examine the third root:

$$a = 0{,}1625 \cdot 10^{-2} x^4; \quad \Phi = 0{,}877 \cdot 10^{-3} x^4;$$
$$a' = 0{,}65 \cdot 10^{-2} x^3; \quad \Phi' = 0{,}35 \cdot 10^{-2} x^3.$$

In one case of equation (11)-(12) are solved simply: this the case when $\lambda=\mu^{-1}$. In this case, Larmorov radii of particles are equal, the separations of particles do not appear, $j_i \approx \mu j_e$, and the picture of the behavior of values with an accuracy down to the terms of order μ coincides with that depicted on Fig. 3.

The practice of count by ETsVM of system (11)-(12) showed that the count was unstable, solution with conditions at left end/lead, characterized by the third root, is rapidly shot down to the solutions, characterized by the first or second root; therefore equations (11)-(12) were replaced by system (11)-(12'), where

$$n_e = n_i. \quad (12)'.$$

Page 104.

It is possible to note that the instability of the count of system (11)-(12) appears when is already valid replacement (12'), in therefore as boundary conditions for (12') it is possible to take either solution (11)-(12) at the point when it still not is stable, or asymptotic solution (11)-(12) at the point where the substitution of (12') is already valid, which was done. The conditions for (11)-(12') they were undertaken in the form $n(0)=0$, $\Phi(0)=0$. Remaining conditions (11)-(12), as it was explained from calculations, they are satisfied.

As it follows from the overall theory of differential equations, this approach/approximation is correct on an entire range of interlayer, with the exception/elimination of narrow sublayer near boundary. In our case this sublayer is realized near x= 0, where act asymptotic laws.

In the case when $\frac{\lambda-\mu^{-1}}{\lambda} \ll 1$, equations can be approximately replaced with following (out of the range of narrow sublayer near x = 0):

$$a'' = \frac{2^{-\frac{3}{4}}}{\sqrt{\pi}} \sqrt{a} \left[Z_{-\frac{1}{2}} \left(\frac{a}{\sqrt{2}} \right) + \lambda^{-\frac{1}{4}} \mu^{\frac{3}{4}} Z_{-\frac{1}{2}} \left(\sqrt{\frac{\lambda\mu}{2}}\, a \right) \right];$$

$$\Phi = \frac{2^{-\frac{9}{2}}}{\sqrt{\pi}} \frac{\lambda-\mu^{-1}}{\lambda\mu^{-1}} Z_{\frac{1}{2}} \left(\frac{a}{\sqrt{2}} \right) \sqrt{a}.$$

The low parameter of expansion is actually the smallness of electric forces in comparison with magnetic in interlayer (with the exception/elimination of left end/lead). This when Larmorov radii of particles converge, the picture of value change approaches a similar pattern in the case of magnetic boundary layer. Density change is described by the appropriate formula.

As an example of general solution, let us examine the case $\lambda = 1$ (isothermal plasma, Fig. 6). Width of boundary layer approximately $4\sqrt{R_i r_i}$ where R_i, r_i — ionic and electronic Larmorov radius respectively. Magnetic field rapidly increases because of electronic current, then slowly it emerges at its value in $+\infty$ because of ionic. Ions are run up/turned first in essence by the negative electric field (to the point of its maximum turns the half of particles), then, after losing its energy, by magnetic field. Appears the dual charged layer. Electrons, after obtaining high energy in the range of negative electric field, weakly "feel" into further magnetic field; therefore their current in the range of positive electric field is low in comparison with ionic. With an increase in the parameter λ, Larmorov radii of ions and electrons converge and the value of the electric field, which attempts to draw together the turning points of ions and electrons, it decreases. It is possible to note that range with the sharp gradient of electric field and small width (order of Debye screening distance), examined, for example, in [9], it does not appear.

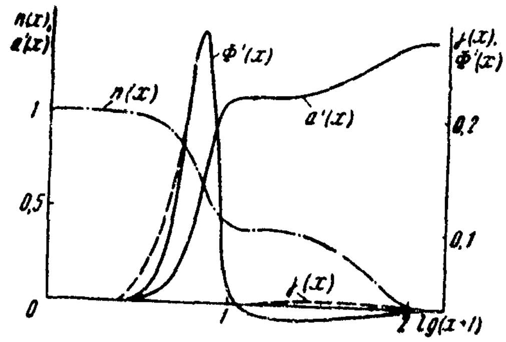

Fig. 6.

Page 105.

REFERENCES

1. V. C. Ferraro. Theory of a plane model. J of Geophys. Res, 1952, 57, No 1.

2. V. P. Shabanskiy. Structure of the transition layer between the plasma and the magnetic field. ZhETF, 1961, Vol. 40, No 4.

3. A. N. Morozov, L. S. Solov'yev. Kinetic examination of some plasma configurations. ZhETF, 1961, Vol. 40, No 5.

4. H. Grad. Boundary layer between plasma and a magnetic field. Phys. of Fluids, 1961, v 4, No 11.

5. Yu. S. Sigov, B. A. Tver. On the structure of the boundary layer between the magnetic field and the plasma flow. "geomagnetism and aeronomy", 1963, Vol. 4, No 6.

6. H.Sestero. Structure of plasma sheaths. Phys. of Fluids, 1964, v 7, No 1.

7. Yu. S. Sigov. To kinetic boundary-layer theory between the rarefied plasma and the magnetic field. Journal of Comp. matem. and matem. physics, 1964, Vol. 4, No 6.

8. Yu. S. Sigov. On interaction of the flows of the rarefied plasma with magnetic fields of space objects. "space investigations", 1964, Vol. 11, No 6.

9. Yu. S. Sigov. Structure of the boundary layer between the rarefied plasma and the magnetic field. JPMTP, 1965, No 2.

10. G. Beytmen, A. Erdey. Highestest transcendental functions, Vol. 1, 2. M., publishing house "science", 1966.
Received 15/V 1969.

Page 106.

MIXING OF THE GAS JETS CF DIFFERENT DENSITY.

V. M. Slavnov.

Conducted experimental investigation cf the mixing of the gas jets of different density. Was investigated the mixing of two ccaxial, axisymmetric subsonic jets, ensuing frcm the becoming narrow nozzles with large compression. As the working gas of internal jet, were utilized argon and nitrogen, and external jet was created by airflow. It is shown, that the criterion of mixing under these conditions was the ratic of the velocities cf the mixed flows.

The turbulent mixing of gas flows with different density was investigated in a series cf works [1] - [5]. The foundation studies cf the mixing of flows at high rates were carried out by A. Ferri. To them it was advanced and is experimentally tested important hypothesis about the fact that under conditicns of developed turbulence the criterion of the mixing of the ccntacted gas flows with different density is the relaticn of the products of density and the rate in these flows. The develcped by A. Ferrii theory was well confirmed by the experimental study of the mixing of a subsonic jet cf hydrogen, escape/ensuing into cccurrent air flow [4], [5]. The schematic of the utilized in these experiments experimental installation is given to Fig. 1. The long cylindrical tube, which supplies gas of central jet, was the source of sufficiently thick boundary layer in the beginning of the zone of the mixing of flows with different density.

Was of interest the study of the process of the mixing of the gas jets of different density with the reduced thickness of initial boundary layer in nozzle edge. It was possible to expect that the criterion, determining the mixing of flow, in this case will be the ratio of the velocities of the mixed flows and that with equality rates (with small initial turbulence) the turbulent mixing will virtually no. The target/purpose of this work was the experimental investigation of the gas jets of different density, escaping behind nozzles with the high degree of compression.

The schematic of the utilized experimental installation is given to Fig. 2.

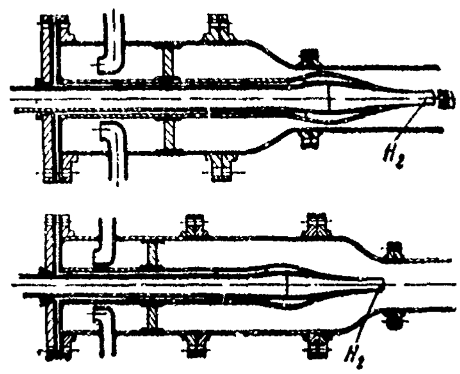

Fig. 1.

Page 107.

The coaxial mixed gas jets of different density were created by the system of two coaxial becoming narrow nozzles with the large compression of nozzles - area of the output section was less than the initial nozzle section by 16 times. In addition in input channels were establish/installed those level the flow of grid. Testings were conducted during the discharge of jets in the atmosphere. To internal nozzle was fed compressed nitrogen or argon, while to external nozzle - the compressed air with temperatures of stagnation $T_0 \approx 288°K$. The total pressure applied compressed air $p_н$ and gas of internal jet p_a was measured with the aid of the nozzles of the total pressure, establish/installed in the channels in front of nozzles. Fig. 3, gives the value of gas density to nozzle edge $\rho/\rho_н$ (was referred to air density under standard conditions $\rho_н$) depending on the given rate λ.

The parameters of the mixed jets were measured with the aid of the comb/rack of the nozzles of the total pressure, which it was establish/installed on different distance from nozzle edge (Fig. 4).

Page 108.

To Fig. 5 given typical distribution of the total pressure p_0 in the section, distant to five boxes from the section/shear of internal nozzle $\frac{l}{d}=5$ during the discharge of nitrogen to air flow (it is referred to atmospheric pressure p_h). The measurement of the parameters of the shift of flows with different density was conducted at distances by 15 and 20 bores from the section/shear of the internal nozzle where was measured complete axle load p_{00} and was calculated its relation to the total pressure gas of internal jet p_a. At the low speeds of external flow $u_в$ the relation $\frac{p_{00}}{p_a}$ as a result of the turbulent mixing of jets was less than unity, with an increase in the velocity of external flow, the zone of mixing was attenuated and relation $\frac{p_{00}}{p_a}$ grew/rose. The results of the measurements conducted are represented in Fig. 6 and 7.

Fig. 6, gives the dependence of relation $\frac{p_{00}}{p_a}$ on the ratio of the velocities of the mixed jets $\frac{u_в}{u_a}$, while in Fig. 7 - dependence on relation $\frac{\rho_в u_в}{\rho_a u_a}$. The data Fig. 6 and 7 show that under conditions of the experiment conducted the criterion of the mixing of the gas jets of different density is the ratio of the velocities of the mixed flows $\frac{u_в}{u_a}$, and not the relation of the products of density and rate

$\frac{\rho_{\text{в}} u_{\text{в}}}{\rho_a u_a}$. This, apparently, is connected with the reduced turbulence level and small initial boundary layer thickness in nozzle edge.

The author expresses appreciation to G. I. Grodzovskiy for valuable councils, and also A. M. Meshcheryakova and N. N. Safonova after aid in experimentation.

REFERENCES

1. G. N. Abramovich. applied gas dynamics. M., "science", 1969.

2. L. A. Vulis, V. P. Kashkarov. Theory of the jets of viscous fluid. M., "science", 1965.

3. A. S. Ginevskiy. Theory of turbelant and Trails, M, "Mashinostroyeniye", 1969.

4 Ferri A, Libby P, Zakkav V Theoretical and experimental investigation of supersonic combustion „Polytechnic Institute of Brooklyn", 1962

5 Ferri A Supersonic combustion progress „Astronaut and Aeronaut", 1964, № 8.

The manuscript entered 4/VI 1969.

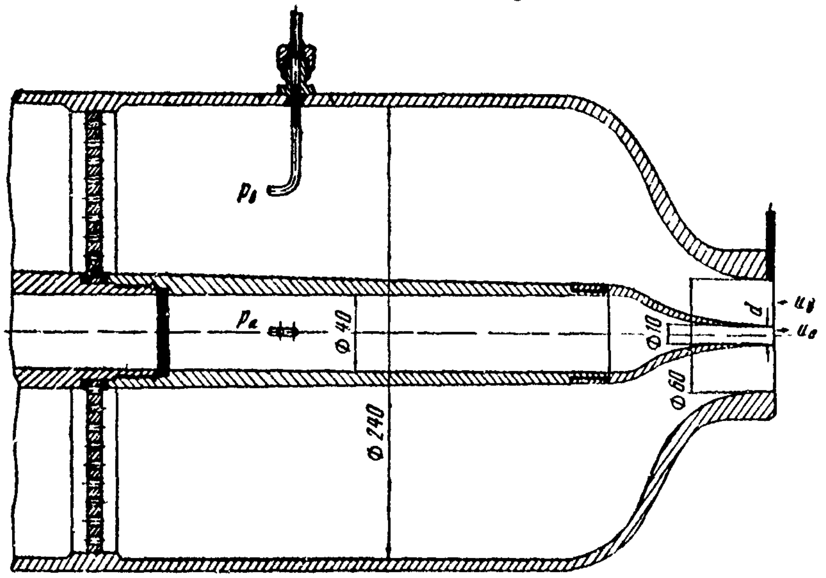

Fig. 2.

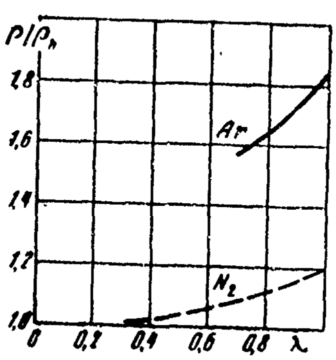

Fig. 3.

Fig. 4.

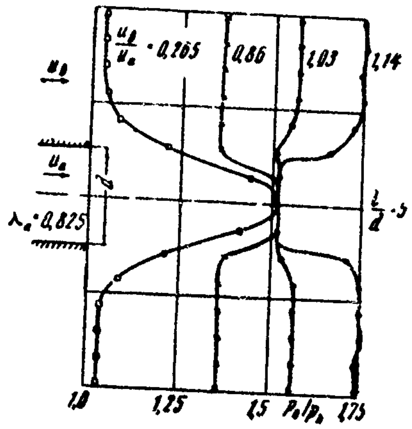

Fig. 5.

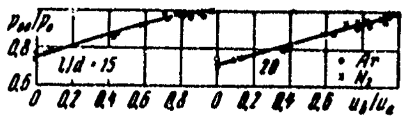

Fig. 6.

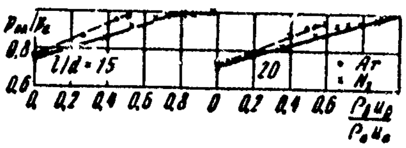

Fig. 7.

Page 109.

Separation of binary gas mixture in a free jet, which escapes into a vacuum.

L. S. Borovkov, V. M. Sankovich.

Work depicts the results of the experimental study of the separation of binary gas mixture or the axle/axis of free jet and is carried out the comparison of these results with F. Sherman's theory.

1. To number previously carried out works on experimental analysis of separation of binary gas mixture, which escapes into vacuum, are related works of Becker's group [1], [2] and Waterman and Stern [3], [4], where it is shown, that nucleus of free jet proves to be substantially enriched heavy component in comparison with initial mixture. According to Becker the separation in free jet is determined by barodiffusion, while according to Waterman and Stern, - by a difference in the thermal velocities of the heavy and light/lung molecules of blending agents.

The results of works [1] - [4] are placed in the doubt of work [5], according to which the separation of mixture is that seeming and is observed only in such a case, when before the entrance into nozzle, that selects mixture for analysis, is shock wave.

The quantitative analysis of the process of separation in free jet is carried out in Sherman's work [6]. Is here proposed the hydrodynamic theory of diffusion separation and are calculated static molar concentrations and the partial flows of heavy component on the axle/axis of binary almost inviscid jet.

The results, obtained by Sherman, it will not agree with the results of works [1] - [4] and [5].

Thus, after the appearance of work [6] arose the need for the new more thorough and more correct experimental analysis of the separation of binary mixture. The attempt to conduct this investigation is made in the present work.

It should be noted that the need for conducting of the investigation indicated is determined not only by scientific, but with carbon trap 7 - it is not above $5 \cdot 10^{-8}$ mm Hg. The measurement of partial concentrations in the camera/chamber of analysis 4 was conducted by mass spectrometer-omegatron RMC-4S 9, by the being analyzer of instrument IPDO-1 [8].

Page 110.

The special coordinate spacer apparatus of 10 described devices makes it possible to derive/conclude nozzle 1 from the jet being investigated and to produce the replacement of it by nozzle with 1A, designed by pressurized/sealed connection to sonic nozzle 11, moreover for both these process/operation coordinate spacer apparatus makes it possible to satisfy in the process of experiment. This makes it possible to consider the effect of residual gas in the camera/chamber after nozzle on the measured partial flows of blending agents, to check the absence of the shock wave before nozzle 1, and also it is constant to determine the initial composition of mixture, i.e., composition in the precombustion chamber in front of the nozzle.

With the aid of the described above device can be defined both composition of the jet, which falls into nozzle 1 and the separation ratio S:

$$S = \frac{\Phi}{\varphi} \bigg/ \frac{N_0}{n_0} = \frac{N - N^*}{n - n^*} \bigg/ \frac{\bar{N}}{\bar{n}}.$$

In this relationship/ratio, obtained from the condition of the preservation/retention/maintaining of the number of molecules in camera/chambers 2 and 4, Φ and φ - partial flows of the heavy and light/lung of components at the point being investigated, N_0 and n_0 - partial concentrations of these components in initial mixture, N and n, N* and n*, $\bar{N}$ and $\bar{n}$ - concentration of the heavy and light/lung of components in the camera/chamber of analysis 4 respectively in the position of nozzle 1 at the point being investigated and out of jet and with the connection of attachment 1A to sonic nozzle.

The accuracy/precision of this determination of separation ratio can be led to 5-7o/o.

3. Experimental investigation of separation was carried out on axle/axis of free jet for mixtures argon - helium and nitrogen - helium at constant temperature T_0 in precombustion chamber (295-300°K), at different initial compositions N_0/n_0(0.1-1), pressures in precombustion chamber p_0 (1-100 mm Hg), diameters D_0 of critical section of sonic nozzle (0.63-7 mm) and with different

distances of x from nozzle edge (X/D_0 = 0.2-20).

The conducted investigation showed that the separation on the axle/axis of jet is described well by Sherman's theory, if:

- Re number which figures as in this theory, is determined not by the geometric D_0 or effective $D_{эф}$ and true diameter D_1 of the sonic part of the flow in nozzle throat:

$$Re = \frac{\rho_0 a_0 D_1}{\mu_0};$$

- Re number exceeds certain value, called below critical Reynolds number $Re_{кр}$

The conducted investigation showed besides the fact that diameter D can be determined in the first approximation, from the relationship/ratio

$$\frac{D_1}{D_0} = \sqrt{3\left(\frac{D^2_{эф}}{D_0^2} - 0,25\right)} - 0,5.$$

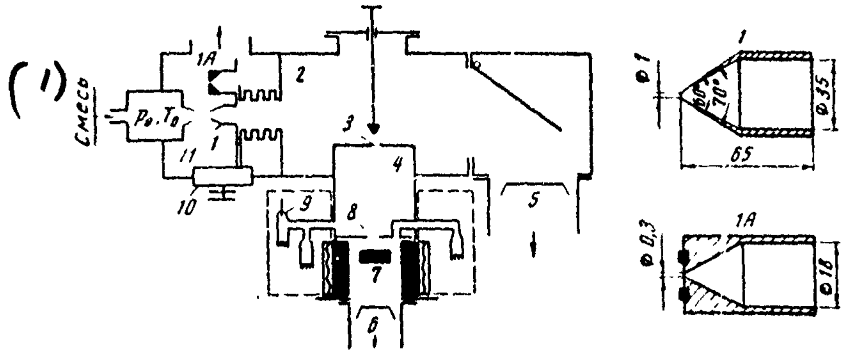

Fig. 1.

Page 111.

This relationship/ratio, as can easily be seen that it occurs, if flow in nozzle throat can be divided into boundary layer and inviscid nucleus, slip on nozzle liners is absent, Mach number in flow core in critical, section is equal to one and the dependence mass rate of discharge in the boundary layer of this flow on a radius is linear.

4. For illustration of formulated above derivations Fig. 2-4, gives results of analysis of separation of mixture argon - helium with initial composition $K_0/n_0 = 0.2$, that escapes behind nozzle by diameter $D_0 = 7$ mm.

Fig. 2, gives the comparison of the experimental and obtained in accordance with Sherman's work theoretical dependences of the separation ratio S on the relative distance x/D of different characteristic diameters D: D_0 (Fig. 2a), $D_{эф}$ (Fig. 2b) and D_1 (Fig. 2c).

Diameter $D_{эф}$ is here determined experimentally according to the consumption of the mixture through the nozzle at different pressures in precombustion chamber. Diameter D_1 is calculated on the given above relationship/ratio between the diameter D_1 and $D_{эф}$.

It is interesting to note that the relationship $\frac{D_{эф}}{D_0}$ for all analyses by us of nozzles and mixtures was determined exclusively by number $Re = \frac{\rho_0 a_0 D_0}{\mu_0}$ and it was described well by the formula

$$\frac{D_{эф}}{D_0} = 1 - \frac{1.5}{\sqrt{Re_0}}.$$

From given Fig. 2, it follows that during the determination of number $Re > Re_{кр}$ from diameters D_0 and $D_{эф}$ the average difference between the experimental and theoretical dependences S(x/D) comprises for those examine/considered a mixture and a nozzle with respect 20 and 10o/o and noticeably exceeds that error (approximately 6o/o), from which coefficient s was determined experimentally. During the determination of number $Re > Re_{кр}$ from the diameter of the sonic part of the flow in nozzle throat the experimental and theoretical dependences $S(x/D_1)$ virtually coincide with each other.

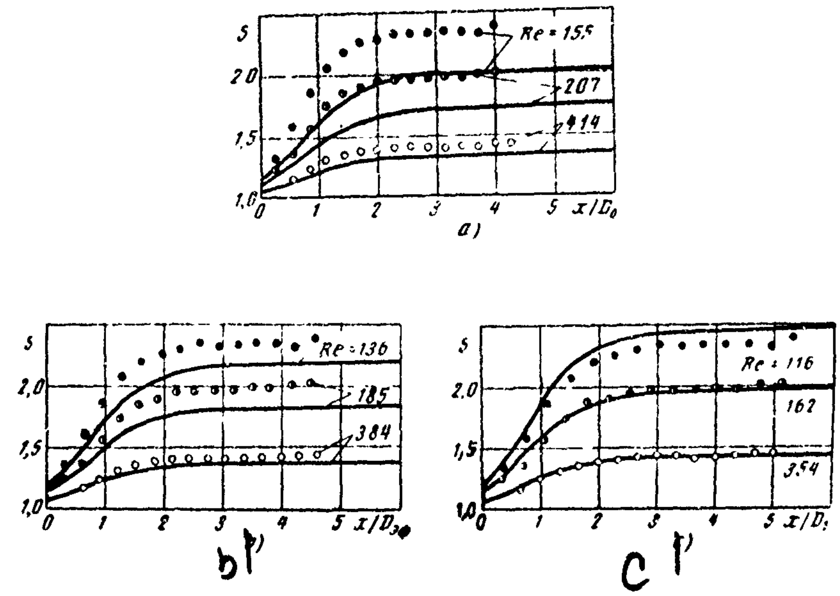

Fig. 2.

Page 112.

Fig. 3, gives the comparison of the described above experimental and theoretical results for diameter D_1 in the following designations of work [6]:

Φ - partial flow of argon at the point being investigated on the axle/axis of jet;

C - constant the linear dependence of the coefficient of viscosity on temperature $\frac{\mu}{\mu_0} = C\frac{T}{T_0}$, which must give the correct values of the coefficients of the viscosity of the gases in question in transonic zone of flow;

$$E = \frac{f_0(1-f_0)}{Sm_0}\left[\frac{m_1 - m_2}{m_0}\left(\frac{\varkappa}{\varkappa - 1}\right) - a_0\right],$$

where

f_0 - the initial molar concentration of argon,

Sm_0 - number of Schmidt in initial mixture,

m_1 and m_2 - molecular masses of argon and helium,

$m_0 = f_0 m_1 + (1-f_0) m_2$ - neutral molecular weight of initial mixture,

$\varkappa = \frac{5}{3}$ - relation of heat capacities for argon and helium,

Φ_0 - thermal-diffusion sense in initial mixture.

Fig. 4, gives the dependence of coefficient S on number $Re = \frac{\rho_0 a_0 D_1}{\mu_0}$ the jet in question for $\frac{x}{D_1} = 5$, i.e. for the case, when coefficient S in this jet is in effect maximum.

As it follows from Fig. 4, critical number $Re_{кр}$ for overall efficiency of S here of the mixture in question is equal approximately to 70.

Analogous results were obtained for other initial compositions of mixture argon helium, other sonic nozzles, and also during the analysis of mixture nitrogen - helium.

The value of number $Re_{кр}$ in particular, for the maximum separation ratio of mixture remained constant and equal in our experiments approximately 70.

5. Need for determination of Re number, which figures as for Sherman's theory with use of diameter of sonic part of flow in nozzle throat, i.e., taking into account boundary layer, is connected, apparently, with the fact that precisely in this part of flow with its expansion in vacuum appear those longitudinal and radial gradients, which produce separation of mixture.

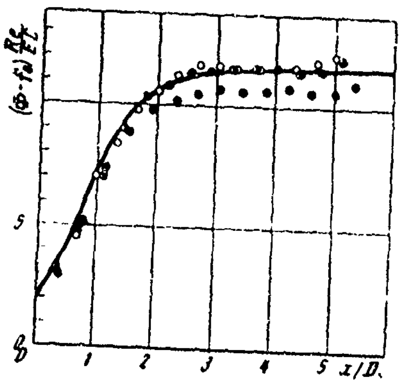

Fig. 3.

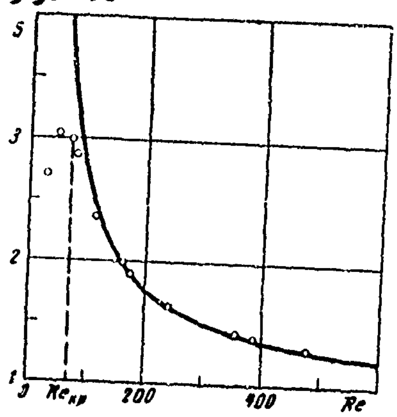

Fig. 4.

Page 113.

In connection with this it is interesting to note that, in evidence of the authors of works [9], experimental and obtained by method of characteristics in work [10] the calculated dependences M (X/D), which they play important role in Sherman's theory, will agree well between themselves with the low numbers Re_0 only in such a case, when as characteristic is utilized diameter, noticeably smaller than diameter $D_{эф}$. [in the work [6] dependence $M(x/D_0)$ is determined experimentally with sufficiently large numbers Re_0 = 2400-7300].

During the discussion of another derivation of present article - derivation about the existence of number $Re_{кр}$ - it is necessary to bear in mind, that Sherman's theory is constructed on basis of equations for a nonviscous gas, wrong with the small Re numbers.

Thus, the process of the separation of the binary gas mixture, which escapes into vacuum, it is realized in actuality and the laws governing this process when $Re > Re_{кр}$ are described by Sherman's theory. As concerns the values of separation ratios, obtained in works [1] - [4] and [5], which, obviously, in the first of them these values are strongly overstated as a result of the inadequacy of the systems of analysis, and in the latter are understated as a result of the small sensitivity of metering equipment.

From Sherman's theory whose validity is here confirmed experimentally, and also from the fact of the existence of the critical Re number, after achievement of which the separation ratio begins to decrease together with Re, can be made two derivations:

- effect of separation in practice cannot be used during obtaining of the superscnic rarefied flows in the underexpanded nozzles;

- effect of separation can not be taken into attention during obtaining of the superscnic rarefied airflow.

In conclusion it is necessary to note that during the execution of this work appeared work [11], where are also given the results of determining the partial flows of argon and helium on the axle/axis of free jet. From indicated work it does not follow, which diameter as characteristic must be selected for determining the Re number in Sherman's theory, however, its results will agree well with the results, obtained in the present work. Fig. 5 gives the comparison of the results of work [11] and of this work with $D = D_0$, which relate to the maximum separation ratios of mixture argon - helium, that escapes behind sonic nozzle.

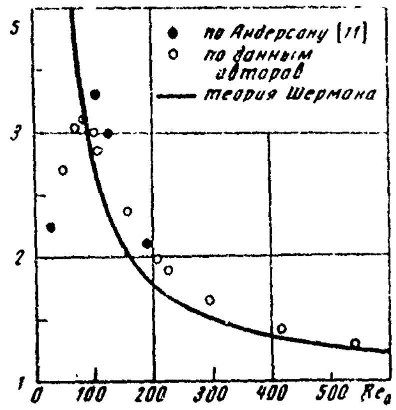

Fig. 5.

Key: (1). according to Anderson. (2). on authors's data. (3). Sherman's theory.

Page 114.

REFERENCES.

1 Becker E. W., Beyrich W., Bier K., Burghoff H., Zigan F. Das Trenndüsenverfahren. Z. Naturforsch., B. 12a, 1957.

2 Becker E. W., Schutte R. Das Trenndüsenverfahren. Z. Naturforsch., B. 15a, 1960.

3 Waterman P., Stern S. Separation of gas mixtures in a supersonic jet, I. J Chem Phys., v. 31, 1959.

4 Stern S., Waterman P., Sinclair T. Separation of gas mixtures in a supersonic jet, II. J Chem Phys., v. 33, 1960.

5 Reis V., Fenn J. Separation of gas mixtures in supersonic jets. J Chem Phys., v. 39, 1963.

6. Sherman F. Hydrodynamical theory of diffusive separation of mixture in a free jet. Phys. of Fluids, v. 8, № 5, 1965.

7. I. S. Borovkov, I. D. Vershini, E. P. Pavlov, V. M. Sankovich. To the method of determining the partial intensities of the components of the molecular flow. Journal is the butt. of material and tech.

physics, No 5, 1968.

8. A. P. Averin, L. N. Linnik, G. I. Nikitin. Mass spectrometers for measuring the partial pressures in vacuum systems. Journal "Instruments and tech. experim.", No 4, 1965.

9 Anderson J., Andres R., Fenn J, Maise G. Studies of low density supersonic jets. Rarefied gas dynamics, v. II, 1966

10. Owen P, Thornhill C The flow in an axiallysymmetric supersonic jet from a nearly sonic orifice into vacuum ARC, R & M, 1948.

11. Anderson J. Separation of gas mixtures in free jets. AIChE J November, 1967

Received 4/VI 1969.

DISTRIBUTION LIST

DISTRIBUTION DIRECT TO RECIPIENT

ORGANIZATION		MICROFICHE
A205	DMATC	1
A210	DMAAC	2
B344	DIA/RDS-3C	9
C043	USAMIIA	1
C509	BALLISTIC RES LABS	1
C510	AIR MOBILITY R&D LAB/FIO	1
C513	PICATINNY ARSENAL	1
C535	AVIATION SYS COMD	1
C591	FSTC	5
C619	MIA REDSTONE	1
D008	NISC	1
H300	USAICE (USAREUR)	1
P005	ERDA	1
P005	CIA/CRS/ADD/SD	1
NAVORDSTA (50L)		1
NASA/KSI		1
AFIT/LD		1

ORGANIZATION		MICROFICHE
E053	AF/INAKA	1
E017	AF/RDXTR-W	1
E403	AFSC/INA	1
E404	AEDC	1
E408	AFWL	1
E410	ADTC	1
E413	ESD	2
	FTD	
	CCN	1
	ASD/FTD/NICD	3
	NIA/PHS	1
	NICD	2